UNIVERSITY OF CALIFORNIA SAN DIEGO

Characterization of FGFR Signaling in Prostate Cancer Stem Cells and Inhibition via TKI treatment

A dissertation submitted in partial satisfaction of the requirements

for the degree

Doctor of Philosophy

in

Chemistry

by

Juyeon Ko

Committee in Charge:

Professor Daniel J. Donoghue, Chair
Professor Ulrich F. Muller
Professor David D. Schlaepfer
Professor Michael J. Tauber
Professor Navtej S. Toor

2021

The dissertation of Juyeon Ko is approved, and it is acceptable in quality and form for publication on microfilm and electronically:

Chair

University of California San Diego

2021

DEDICATION

This dissertation is dedicated to my mom and to the loving memory of Carol Hartman. They are the two most important women in my life that made me who I am today.

Had it not been for the endless support from my mom encouraging me to pursue my curiosity in learning, exploring and to endure any challenges growing up, I would have not been able to aspire to be a scientist and come to the United States to pursue my Ph.D. degree in chemistry. Her long-held belief in me that I would be benefited from higher education and have a career which would contribute to the world has influenced my core values and my pursuing a career in cancer research that I wish to play a part in advancing medical treatments.

Carol was my biggest supporter next to my mom, showed me the way around in the Unites States and taught me so many small things I will cherish forever. I had the privilege to know Carol since 2011 and she showed me the meaning of a family in a whole different way as she treated me like her daughter, and I have learned the value of kindness and openness from her. Her love for me taught me important aspects in life as I was maturing into the person I am today, not only as a scientist but also as a woman following her footsteps. I'm so lucky to have known her in my life and she will always be in my heart.

TABLE OF CONTENTS

LIST OF ABBRIVIATIONS

3D	three-dimensional
ADT	androgen deprivation therapy
ALDH	aldehyde dehydrogenase
AR	androgen receptor
CD	cluster of differentiation
c-KIT	proto-oncogene receptor tyrosine kinase
CRPC	castration resistant prostate cancer
CSC	cancer stem cell
CTC	circulating tumor cell
DFG	Asp-Phe-Gly
DHT	dihydrotestosterone
DNA	deoxyribonucleic acid
ECM	extracellular matrix
EGF	epidermal growth factor
EMT	epithelial-to-mesenchymal transition
FACS	fluorescence activated cell sorting
FGF	fibroblast growth factor
FLT3	fms-like tyrosine kinase 3
IGF	insulin-like growth factor
iPSC	induced pluripotent stem cell
LBD	ligand-binding domain
MAPK	RAS-mitogen activated protein kinase
MEF	Mouse embryonic fibroblast
MET	mesenchymal-epithelial transition
MTT	3-(4,5-dimethylthiazol-2-yl)-2,5-diphenyltetrazolium bromide
NADH	nicotinamideadenine dinucleotide hydrogen
PDGF	platelet-derived growth factor

PDX	patient derived xenograft
PE	phycoerythrin
PI	propidium iodide
PI3K	phosphatidylinositol-3 kinase
PIN	prostatic intraepithelial neoplasia
PIP2	phosphatidylinositol-4,5-bisphosphate
PIP3	phosphatidylinositol-3,4,5-trisphosphate
PLCγ	phospholipase Cγ
PolyHEMA	poly 2-hydroxyethyl methacrylate
PSA	prostate-specific antigen
PTEN	phosphatase and tensin homolog
qPCR	quantitative polymerase chain reaction
R	receptor
RTK	receptor tyrosine kinase
SR	serum replacement
STAT	signal transducer and activator of transcription
TGF	transforming growth factor
TIC	tumor-initiating cell
TKI	tyrosine kinase inhibitor
VEGF	vascular endothelial growth factor

LIST OF FIGURES AND TABLES

ACKNOWLEDGEMENTS

First and foremost, I would like to acknowledge Dr. Daniel Donoghue for his support as the chair of my committee. With his support, I was given an opportunity to join his research group expanding my scientific knowledge and have learned research skills. I would also like to thank April Meyer for her supervision, training, and discussions in the lab throughout the whole research.

I would especially like to thank Dr. Ulrich Muller and Dr. Navtej Toor for taking the time to serve as members of my thesis committee and for providing me invaluable advice. I would like to thank my colleagues Nicole Peiris, Leandro Gallo, Katelyn Nelson, Anna Seck, Fangda Li, and Erika Assoun for their encouragement and friendship in getting through the program.

Chapter 1, in full, is a reprint of the review article as it appears in Cell Cycle. Gallo LH, Ko J, Donoghue DJ. The importance of regulatory ubiquitination in cancer and metastasis. Cell Cycle. 2017;16(7):634–648. doi:10.1080/15384101.2017.1288326. The dissertation author was a co-author of this review but did not perform the research described by the review. The dissertation author was responsible for the following specific subsections of this review in its entirety; E3 ubiquitin ligases in pluripotent cancer stem cells, SMURF1 in head and neck cancer stem cells, Skp2 in nasopharyngeal and prostate cancer stem cells, ITCH in lung cancer stem cells, FBXW7 in colonic and leukemia cancer stem cell maintenance, The misregulated expression of DUBs in metastatic cancers, USP7 promotes APL, aggressive prostate cancer, and NSCLC metastasis, USP4 and USP9X support oncogenic signaling in various tumors, UCH-L1 plays a contradicting role in different tumors, OTUB1 contributes to drug resistance and promotes metastasis. The dissertation author also assisted with other figures, tables, and other sections as well. Co-authors include Leandro H Gallo and Daniel J Donoghue.

Chapter 2, in part, contains material published in the following. Ko J., Meyer A. N., Haas M., Donoghue D. J. Characterization of FGFR signaling in prostate cancer stem cells and inhibition via TKI treatment. Oncotarget. 2021; 12: 22-36. The dissertation author was the primary investigator and first author of this material, being responsible for designing and performing entire experiments and the manuscript writing.

VITA

2014	Bachelor of Science, Chung-Ang University, Seoul, Korea
2015-2020	Teaching Assistant, University of California San Diego, USA
2016	Master of Science, University of California San Diego, USA
2021	Doctor of Philosophy, University of California San Diego, USA

PUBLICATIONS

Ko J, Meyer AN, Haas M, Donoghue DJ. Characterization of FGFR signaling in prostate cancer stem cells and inhibition via TKI treatment. Oncotarget. 2021; 12: 22-36.
Retrieved from https://www.oncotarget.com/article/27859/

Meyer AN, Gallo LH, Ko J, *et al.* Oncogenic mutations in IKKβ function through global changes induced by K63-linked ubiquitination and result in autocrine stimulation. PLoS One. 2018;13(10):e0206014. Published 2018 Oct 18. doi:10.1371/journal.pone.0206014

Gallo LH, Ko J, Donoghue DJ. The importance of regulatory ubiquitination in cancer and metastasis. Cell Cycle. 2017;16(7):634–648. doi:10.1080/15384101.2017.1288326.

ABSTRACT OF THE DISSERTATION

Characterization of FGFR Signaling in Prostate Cancer Stem Cells and Inhibition via TKI treatment

By

Juyeon Ko

Doctor of Philosophy in Chemistry

University of California San Diego, 2021

Professor Daniel J. Donoghue, Chair

Cancer stem cells have been extensively studied in numerous cancers, however, there is no clear identification of this rare subpopulation and a means for an effective therapy targeting these cells although they are implicated in tumor initiation, drug resistance, reoccurrence and metastasis. The review article in Chapter 1 emphasizes how the cancer stem cells exploit a ubiquitination modification in human cancers and metastasis. Ubiquitination is a type of post-translational modification that extends the function of proteins such as stabilizing oncogenic signals and recruiting signaling proteins that favors the cancer progression beyond our current discoveries and knowledge. The studies of cancer stem cells may help us better understand the heterogeneous disease collectively termed cancer.

One type of cancer in which the cancer stem cell theory may lead to alternative therapeutic options is prostate cancer. Chapter 2 presents research hypothesizing that prostate cancer stem cells (CSCs) take advantage of Fibroblast Growth Factor Receptor (FGFR) signaling for survival and proliferation among the bulk tumor and possess the ability to survive the current therapy of androgen deprivation but can be targeted by FGFR inhibitors. As tyrosine kinase inhibitors (TKIs) have shown great effectiveness for some cancers, they have shown only modest outcome in prostate cancer treatment. The research presented here focuses on studying the FGFR signaling in the rare subpopulation shown as 3-dimensional spheroids compared to a bulk tumor represented as monolayer cells. This study reveals that FGFR signaling in the prostate CSCs promote their stemness characteristics and these CSCs may possess increased metastatic potential shown by changes in their gene expression. This study provides a novel *in vitro* model to study FGFR signaling in prostate cancer cell lines and utilizes a novel induced pluripotent stem cell-derived cell line to improve our understanding of prostate CSCs at a cellular and molecular level. The findings from this research may assist in screening for patient subgroups who would benefit from the TKI treatment targeting FGFR as an alternative treatment option.

Chapter 1

The importance of regulatory ubiquitination in cancer and metastasis

CELL CYCLE
2017, VOL. 16, NO. 7, 634–648
http://dx.doi.org/10.1080/15384101.2017.1288326

Taylor & Francis
Taylor & Francis Group

REVIEW

OPEN ACCESS

The importance of regulatory ubiquitination in cancer and metastasis

L. H. Gallo[a], J. Ko[a], and D. J. Donoghue[a,b]

[a]Department of Chemistry and Biochemistry, University of California San Diego, La Jolla, CA, USA; [b]Moores UCSD Cancer Center, University of California San Diego, La Jolla, CA, USA

ABSTRACT
Ubiquitination serves as a degradation mechanism of proteins, but is involved in additional cellular processes such as activation of NFkB inflammatory response and DNA damage repair. We highlight the E2 ubiquitin conjugating enzymes, E3 ubiquitin ligases and Deubiquitinases that support the metastasis of a plethora of cancers. E3 ubiquitin ligases also modulate pluripotent cancer stem cells attributed to chemotherapy resistance. We further describe mutations in E3 ubiquitin ligases that support tumor proliferation and adaptation to hypoxia. Thus, this review describes how tumors exploit members of the vast ubiquitin signaling pathways to support aberrant oncogenic signaling for survival and metastasis.

ARTICLE HISTORY
Received 9 December 2016
Revised 20 January 2017
Accepted 24 January 2017

KEYWORDS
deubiquitinase; ligase; metastasis; ubiquitination

Ubiquitination signaling overview

Ubiquitin (Ub), a highly conserved 76-amino acid protein expressed in all cell types, has 7 lysine residues (K6, K11, K27, K29, K33, K48, K63) that can be polymerized into var-ious linkages. The resulting linkage of Ub chains creates a certain topology that can be sampled by interacting proteins and dictates the fate of the substrate. For instance, K48-and K11-linked Ub chains adopt a "closed" or compact conformation and lead to 26S-mediated proteasomal degra-dation of substrates. In contrast, unanchored K63- or a mix of K63/M1-linked ubiquitination chains adopt an "open" conformation, and are involved in non-proteasomal func-
tions such as TAK1 and IKK complex activation culminat-ing in NFkB inflammatory signaling,[1,2] activation of DNA damage repair signaling[3] and B cell activation via MAPK by TAB2/TAB3.[4]

Ubiquitination is a conserved multistep process that begins with the activation of ubiquitin with ATP by the E1 ubiquitin activating enzyme, followed by the formation of a thioester linkage between the ubiquitin transferred from the E1 to the cysteine in the active site of an E2 ubiquitin con-jugating enzyme. The E3 ubiquitin ligase participates in the ubiquitination of a target substrate through the formation of an isopeptide bond between the carboxyl group of Gly76 of ubiquitin and the e-amine of Lys in the substrate. Deubi-quitinating enzymes (DUBs) remove the ubiquitin from the target substrates and recycle ubiquitin into the cytosolic pool.

Ubiquitination regulates the function and signaling of a pro-fusion of proteins in various cellular pathways. This review describes how various cancers take advantage of the misregu-lated expression of the members of the ubiquitination cascade for proliferation, survival and metastasis (Fig. 1).

The challenging route to metastasis

Cancer progression eventually may lead to metastasis, which is the final stage responsible for more than 90% of all terminal cancer deaths. Various genomic abnormalities must be present to allow cells of a primary tumor to ignore apoptotic signals, proliferate and survive. Before metastasis occurs, tumor cells undergo phenotypic changes through epithelial-mesenchymal transition (EMT) similar to signaling events during embryonic development. EMT is marked by a loss of cell-cell adhesion through decreased expression of E-cadherin, increased motility by actin reorganization and upregulated expression of N-cad-herin, Vimentin, Snail and Twist.[5] Cells are then able to move through the stroma, resist the episode of immune cells, survive and travel through the bloodstream. Finally, metastasized cells arrive at the secondary site, resisting rejection and apoptosis to form malignant microtumors. Eventually, these progress to clinically observable macro metastasized tumors. Only a small percentage of metastasized cells survive this migratory journey and successfully colonize the secondary tissue, classifying metastasis as a rare event.

Since most proteins undergo ubiquitination as a post-trans-lational modification in most cell types, it is not surprising that cancer cells exploit the members of the ubiquitination pathway to stabilize aberrant oncogenic signaling. This review describes that the misregulated expression of E2s, E3 ligases and DUBs contributes to the signaling of various oncogenes, leading to cancer progression and metastasis.

The overexpression of E2s supports aberrant oncogenic signaling in tumor metastasis

E2s play an active role in the regulation of cell cycle progres-sion, inflammation and the mechanisms by which they

CONTACT D. J. Donoghue ddonoghue@ucsd.edu Department of Chemistry and Biochemistry, University of California San Diego, La Jolla 92093-0367, CA, USA.

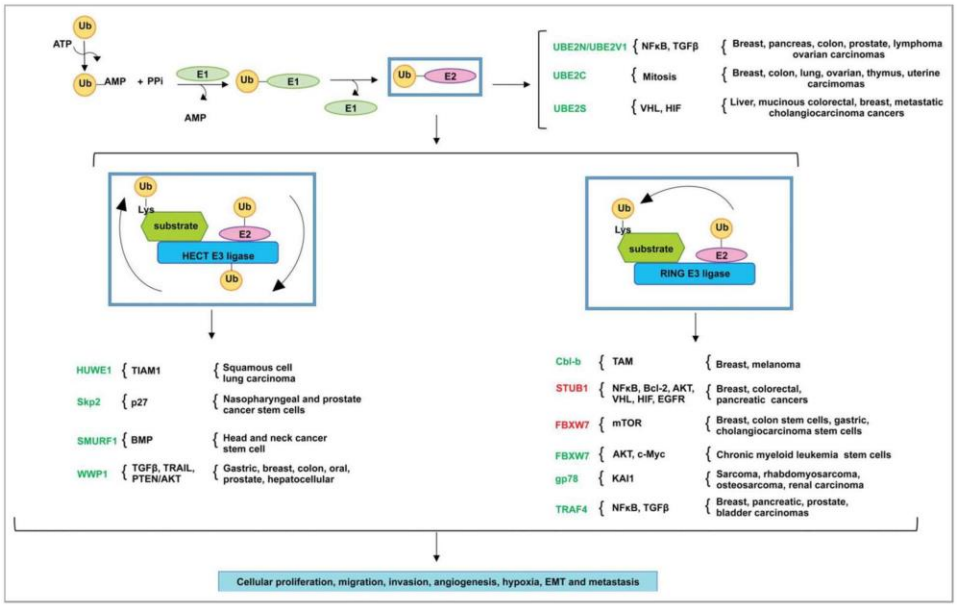

Figure 1.1. The misregulated expression of E2 ubiquitin conjugating enzymes and E3 ubiquitin ligases in various human cancers. The ubiquitination reaction ini-tiates with the activation of ubiquitin by ATP, in which ubiquitin is then transferred to the active site of E1 ubiquitin conjugating enzyme. The E1 transfers the ubiquitin to a Cys in the catalytic active site of the E2 ubiquitin conjugating enzyme. The HECT domain E3 ligases ubiquitinate the target substrates by 2 mecha-nisms: first, the ubiquitin is transferred from the active site of the E2 to the Cys in the active site of the E3, which then ubiquitinates the Lys residue in the tar-get substrate. RING- and RING-related domain E3 ligases, in contrast, serve as scaffolds to ubiquitinate target substrates in one step: the E2 transfers the ubiquitin directly to the Lys residue in the target substrate. Various tumors take advantage of the misregulated expression of E2s and E3s for the aberrant activa-tion of oncogenic pathways. E2s and E3s colored in green indicate the importance of their expression or overexpression in cancer, while those in red indicate their downregulated expression in cancer. These genomic events result in cancer cell proliferation, migration, invasion, angiogenesis, hypoxia, EMT and metastasis.

modulate cancer metastasis. There are approximately 40 E2 family members encoded by the human genome.[6] E2s share a highly conserved 150-amino acid catalytic core, the ubiquitin conjugating (UBC) domain, responsible for ubiquitination.

UBE2N/UBE2V1 modulates breast cancer metastasis

Ubiquitin-Conjugating Enzyme E2N (UBE2N, also known as UBC13), together with its co-factor UBE2V1 (also known as UEV1A), specifically builds Lys63-linked ubiquitin chains that are indispensable for NFkB inflammatory activation.[2] UBE2N is overexpressed in myriad tumors such as breast, pancreas, colon, prostate, lymphoma and ovarian carcinomas. UBE2N is required for breast cancer metastasis to the lung in vivo through TGFb-mediated activation of TAK1 and p38, culmi-nating in the expression of metastasis-associated genes CNN2, PLTP, IGFBP3, IL13RA2, CD44, VCAM-1 and ICAM-1 (Fig. 2). This requirement for UBE2N for metastatic spread is notable, given that UBE2N is not required for primary tumor forma-tion.[7] ShRNA-mediated inhibition of UBE2N or treatment of breast cancer cells with SB203580, small molecule inhibitor of p38 MAPK, interestingly result in the suppression of breast cancer metastasis to the lung.[7]

In addition, the cofactor for UBE2N, Ubiquitin-Conju-gating Enzyme E2 Variant 1 (UBE2V1) is upregulated in breast cancer and increases the invasiveness and migration of breast cancer cells, including tumor growth and upregu-lated metastasis to lymph nodes and lung, an effect that is dependent upon functional UBE2N. These tumors exhibit increased expression of Matrix Metalloproteinase-1 (MMP1) through activation of NFkB signaling[8] (Fig. 2), in which MMPs are involved in extracellular matrix degradation for tumor cell migration and invasion.[9] ShRNA-mediated inhi-bition of UBE2V1 ablates breast tumor growth and metasta-sis in vivo. UBE2V1, in marked contrast to UBE2N, lacks the catalytic Cys and therefore catalytically inactive to per-form the polyubiquitination of substrates.

It is not clear, however, whether these tumors exhibit the upregulated expression of both UBE2N and UBE2V1, or whether the upregulated expression of one member only is suf-ficient to aberrantly induce NFkB and TGFb signaling to drive metastasis. The UBE2N/UBE2V1 complex, critical for NFkB signaling, is overexpressed in some breast cancer samples; this may contribute to the hyperactivation of an inflammatory response in the tumor microenvironment. Collectively, these studies suggest that UBE2N/UBE2V1, responsible for the for-mation of Lys63-linked ubiquitin chains which are important to activate signaling pathways as opposed to triggering protein degradation, represent potentially important targets for thera-peutic intervention.[7-9]

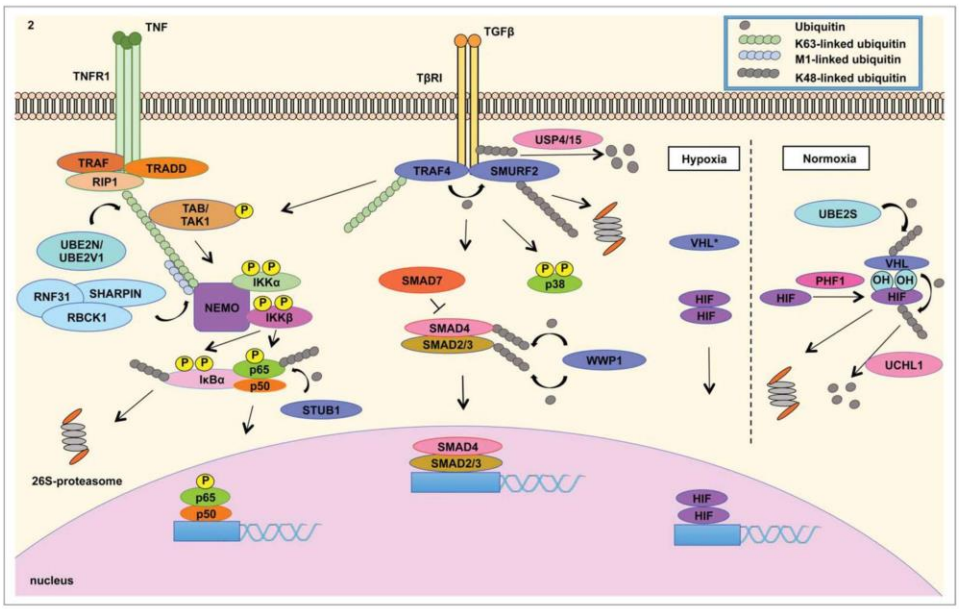

Figure 1.2. Misregulated expression of members of the ubiquitin cascade contributes to the aberrant signaling of various pathways in cancer. (LEFT) The UBE2N/UBE2V1 E2 ubiquitin conjugating enzyme complex catalyzes the Lys63-linked ubiquitination of NEMO that recruits the TAK1/TAB1/2 complex to activate the IKK complex, which is composed of IKKb, IKKa and NEMO. IKKb phosphorylates IkBa, which is Lys48-linked ubiquitinated and subsequently degraded by the 26S-proteasome.[2] This event releases NFkB to translocate into the nucleus to mediate the transcription of a signature of genes involved in inflammatory response. STUB1 E3 ligase negatively regulates NFkB signaling by catalyzing the degradation-inducing Lys48-linked ubiquitination of p65 subunit of NFkB.[23] (CENTER) In addition, cancer cells take advantage of overex-pressed TRAF4 to modulate TGFb signaling. TGFb activation culminates in the nuclear translocation of SMAD2/3/4 complex to modulate gene transcription. SMAD7 is a negative regulator of TGFb signaling by recruiting SMURF2 E3 ubiquitin ligase to ubiquitinate TbRI, leading to the proteasomal degradation of the receptor and mitiga-tion of signaling[79] TGFb signaling is regulated by TRAF4 E3 ligase mediated Lys48-linked ubiquitination of SMURF2 E3 ligase. The latter E3 ligase catalyzes the degrada-tion signal of TGFb receptor I (TbRI), in which these events mitigate the activation of the signaling pathway. TRAF4, on the other hand, is conjugated to Lys63-linked ubiquitin polymers to activate TAK1/TAB1/2 complex that induces the signaling of p38 MAPK and NFkB. TRAF4 further interacts with deubiquitinating enzyme USP15 and USP4, which remove the degradation signal from TGFb receptor I. These events contribute to the stabilization of TGFb signaling.[34] (RIGHT) Tumor adaptation to hyp-oxia is highly attributed to HIF signaling. Under normal oxygen level condition (normoxia), VHL E3 ligase binds to hydroxylated Proline residue in HIF catalyzed by PHD proteins. VHL then catalyzes the Lys48-linked ubiquitination of HIF, leading to proteasome degradation. UBE2S enzyme controls VHL protein stability. Under low oxygen conditions (hypoxia), inactivating of VHL (either by mutations or decreased expression) contributes to HIF isoform stabilization, which mediates the transcription of genes involved in tumor adaptation to hypoxia, including angiogenesis.[15,45] These signaling events governed by members of the ubiquitin cascade all contribute to EMT, cellular proliferation, migration, invasion, chemotherapy resistance and metastasis.

UBE2C regulates chromosomal alignment in mitosis

Overexpression of UBE2C (Ubiquitin-Conjugating Enzyme E2C, termed UBE2C or UBCH10) is detected in many cancers, including breast, colon, prostate, ovary, thymus, uterine and lung.[10-14] UBE2C functions with the Anaphase-promoting complex/cyclosome (APC/C) to ensure proper chromosome alignment and segregation in mitosis. UBE2C expression fluctuates during the cell cycle, peaking at prometaphase to regulate chromosomal segregation and decreasing in anaphase. Overexpression of UBE2C causes the missegregation of chromosomes (aneuploidy), chromosome misalignment and lagging, mitotic slippage and increased number of centrioles, in addition to a decrease in cyclin B1 levels. Mice engineered to overexpress UBE2C exhibit elevated lung tumor burden, including the emergence of lymphomas, lipomas, liver and skin tumors[11] (Fig. 1).

As misregulated expression of UBE2C contributes to the emergence of tumors in tissues and cells from various lineages, it is possible that this E2 modulates chromosomal segregation during mitosis of different cancers, representing a target to treat a broad range of tumors.

UBE2S regulates E3 ligase VHL in hypoxia

UBE2S, or Ubiquitin-Conjugating Enzyme E2S (also known as E2-EPF ubiquitin carrier protein (UCP)), catalyzes the ubiquitination of von Hippel-Lindau (VHL) protein, targeting it for proteasomal degradation.[15] VHL mediates the stability of HIF transcription factors that induce expression of protumorigenic and mitogenic growth factor genes such as VEGF, MMPs, SNAIL, TWIST and PDGF involved in hypoxia, EMT, angio-genesis, migration, proliferation and metastasis (Fig. 2).[16]

The overexpression of UBE2S and HIF1a, with low VHL expression, is detected in various tumors such as primary liver, mucinous colorectal and breast cancer, and in metastatic cholangiocarcinoma in soft tissue and metastatic colorectal cancer in lymph VHL controls the stability of hypoxia-inducible factors HIF-1 and HIF-2 that mediate the adaptation of cells to varying levels of oxygen. Overexpression of UBE2S in CAKI

cells (clear cell carcinoma derived from metastatic skin site) and C8161 (highly invasive and metastatic human melanoma cells) contributes to increased degradation of VHL, while it increases HIF1a expression and VEGF transcription, contributing to the increased proliferation and metastasis to the lung.[15] UBE2S is also amplified in pancreatic and neuroendocrine prostate cancer.[17,18]

In summary, this section illustrates that overexpression of E2 ubiquitin conjugating enzymes supports aberrant oncogenic signaling of inflammatory NFkB and TGFb, receptor tyrosine kinases, mitogenic growth factors and HIF transcription factors. These E2s drive aneuploidy, proliferation, migration and metastasis of a variety of tumors.

The misregulated expression of E3 ubiquitin ligases in cancer

There are approximately 600 E3 ubiquitin ligases encoded by the human genome and the mechanism of ubiquitination of target substrates depends upon the conserved catalytic domains: RING (Really Interesting New Gene), HECT (Homology to E6AP C Terminus) and RING-related (PHD, LIM, F-box, B-box and U-box). RING and RING-related E3 ligases catalyze a one-step reaction of ubiquitin transfer from the E2 to the lysine residue in the substrate. In contrast, HECT E3 ligases catalyze a 2-step reaction: first the ubiquitin is trans-ferred from the E2 to the cysteine in the active site of the E3
ligase, which then ubiquitinates the lysine residue in the target substrate.[19,20] (Fig. 1).

As with the E2 ubiquitin conjugating enzymes, misregulated expression of E3 ubiquitin ligases contributes to aberrant oncogenic signaling, metastasis and resistance to chemotherapy, including the modulation of pluripotency of cancer stem cells in tumor niches.

The downregulated expression of E3s in cancer STUB1 – more than just an E3 ligase

Cancer cells take advantage of downregulated expression of STIP1 Homology And U-Box Containing Protein 1 (STUB1), also known as CHIP, a U-box ligase that functions as a chaper-one for protein quality control and promotes the ubiquitination of various cell cycle regulators, such as c-Myc and SRC-3. STUB1 transcription is lower in malignant stage II and node-positive breast cancer than in stage I and node-negative patients. The downregulated expression of STUB1 upregulates NFkB signaling and anti-apoptotic proteins Bcl[i]2 and AKT, supporting inflammation, survival, invasiveness and metastatic potential of breast cancer cells[21,22] In colorectal cancer, STUB1 is the E3 ubiquitin ligase that regulates the stability of p65 sub-unit of NFkB (Fig. 2). Downregulated STUB1 in colorectal can-cer decreases the degradation of p65 subunit and increases the expression of NFkB-controlled VEGF, Cyclin D1, c-Myc, IL-8 and MMP-2 genes involved in angiogenesis and metastasis.[23]

In pancreatic cancer, STUB1 is a tumor suppressor and it modulates the stability of EGFR via proteasomal-mediated degradation of this receptor tyrosine kinase (RTK). STUB1 regu-lates the phosphorylation of Tyr845 and Tyr1068 of EGFR, activating downstream PI3K/AKT and Src/FAK/paxillin signaling pathways. Downregulated STUB1 expression increases oncogenic EGFR signaling and sensitizes pancreatic cancer cells to RTK inhibitor, erlotinib, which leads to apoptosis and decreased tumor volume in vivo.[24]

STUB1 modulates the proteasomal-mediated degradation of NFkB and EGFR oncogenes in various tumors (Fig. 1). Tumors harboring downregulated STUB1 expression exhibit aberrant NFkB signaling and some tumors may rely on RTK's for proliferative advantages. The role of STUB1 may extend beyond these pathways to include additional oncogenes in other tumors.

Despite its tumor suppressor function, enhanced STUB1 expression is observed in pancreatic, prostate breast and other cancers.[17,18,25] This suggests that further research will be required to unravel the tumor and context specific functions of this E3 ubiquitin-protein ligase.

FBXW7 – a key component of the SCF complex

F-Box And WD Repeat Domain Containing 7 (FBXW7) E3 ligase is a component of the SCF (SKP1, CUL-1, F-box protein) E3 ubiquitin ligase complex that regulates the stability of cell-cycle regulators such as c-Myc, cyclin E and Notch.[26]

FBXW7 is downregulated in breast, colorectal, gastric and cholangiocarcinoma (CCA) tumors correlated with poor prognosis and survival, elevated tumor invasion and occurrence of metastasis[27-29] (Fig. 1). FBXW7 regulates the stability and turnover of mTOR. Downregulated FBXW7 expression increases mTOR levels that support the metastastic potential of CCA tumors to the liver and lung. These tumors are sensitive to mTOR inhibitor rapamycin, which impairs tumor growth.[29]

In summary, this section illustrates that the downregulated expression of the E3 ubiquitin ligases stabilizes aberrant oncogenic signaling. Some of these reports, additionally, show that a rescue in the expression of these E3 ligases leads to increased degradation of key oncogenic signaling proteins, potentially resulting in the inhibition of tumor proliferation and metastasis.

The importance of the expression, or overexpression, of E3s in tumors

The contribution of Cbl-b to melanoma and breast cancer metastasis

The recruitment of immune system cells to the tumor microenvironment has been suggested to play an important role in tumor metastasis.[30] The E3 ligase activity of Casitas B-lineage lymphoma-b, Cbl-b or RNF56, is a negative regulator of anti-tumor function of natural killer (NK) cells. Genetic deletion of Cbl-b, or targeted inhibition of its E3 ubiquitin ligase activity, awakens the antitumor response of NK cells and educates these lymphoid cells to recognize and kill melanoma tumors, inhibiting lung metastasis. The TAM family of receptor tyrosine kinases, Tyro3, Axl and Mer, has been identified as substrates of Cbl-b for ubiquitination. Treatment of NK cells with selective TAM inhibitor, LDC1267, ablates melanoma and breast cancer metastasis.[31] This indicates that some E3 ligases, exemplified by Cbl-b, can modulate the immune system's ability to recognize and kill tumor cells.

HUWE1 controls cell-to-cell adhesion

In order for cancer cells to leave the primary tissue and metastasize to secondary sites, cell-to-cell adhesion must be disrupted for their movement through the stroma. The HECT, UBA, and WWE domain-containing protein 1 (HUWE1) E3 ubiquitin ligase has been implicated in the modulation of cell-to-cell adhesion. The expression of TIAM1, a guanine nucleotide exchange factor, at cell-to-cell junctions is critical to maintain cells in contact with one another. HUWE1-mediated degrada-tion of TIAM1 leads to scattering, dissemination and invasion of epithelial cells, including the dissemination and local inva-sion of metastatic lung cells. Knockdown of HUWE1 decreases the dissemination of cells, leading to the stabilization of TIAM1 at cell-to-cell junctions. Stage I and stage II squamous cell lung carcinoma tissue samples show an inverse correlation between HUWE1 and TIAM1 expression[32] (Fig. 1), suggesting that metastasis of lung cells may be modulated by the misregulated expression of HUWE1.

GP78 in sarcoma metastasis

The metastasis of sarcoma tumors is dependent upon the E3 ligase activity of GP78, also known as autocrine motility factor receptor (AMFR). GP78 is a RING-finger E3 ubiquitin ligase that localizes to the endoplasmic reticulum (ER) and it partici-pates in ER-associated degradation (ERAD), a pathway that leads to the degradation of misfolded or denatured proteins. Inhibition of GP78 expression in highly metastatic human sar-coma cells inhibits lung metastasis, but it does not affect pri-mary tumor growth. Stable gp78 knockdown decreases the survival of metastasized HT1080 sarcoma, RH30 rhabdomyo-sarcoma, HOS-MNNG osteosarcoma, including 786-O renal carcinoma (Fig. 1). The metastasis-suppressor KAI1 has been identified as a substrate of gp78-mediated degradation, in which an inverse correlation of KAI1 and GP78 expression is found in sarcoma samples. Downregulated gp78 leads to the accumulation of KAI1 that results in apoptosis and reduces the metastatic potential of sarcoma cells.[33] This event illustrates the importance of gp78 expression in sarcomas.

TRAF4 modulates inflammatory signaling of multiple tumors

Tumor necrosis factor receptor-associated factor 4 is a RING domain E3 ligase with well-documented signaling functions associated with the activation of TNFRs and IL-1R/TLRs, play-ing critical roles in immune system responses.[34]

TRAF4 has been implicated in the regulation of both SMAD-dependent and SMAD-independent TGFb receptor (TbRI)-induced signaling. TRAF4 ubiquitinates SMURF2 lead-ing to the degradation of the latter E3 ligase and enhancement of TGFb signaling. On the other hand, SMURF2 can ubiquiti-nate both TbRI and TRAF4 to terminate TGFb signaling. TRAF4 also interacts with deubiquitinating enzyme USP15, which deubiquitinates TbRI upon SMURF2-mediated ubiquiti-nation of TbRI, stabilizing this signaling pathway. In addition, TGFb induces the Lys63-linked ubiquitination of TRAF4 to promote TAK1 activation, leading to p38 and NFkB signaling[34] (Fig. 2).

TRAF4 is amplified in invasive breast carcinoma, pancreatic adenocarcinoma, prostate cancer and bladder carcinoma.[18,25,35] (Fig. 1). TRAF4 overexpression contributes to poor overall survival in ovarian cancer and, in breast cancer, it is correlated with ERBB2 amplification and bone metastasis. TRAF4 further supports the expression of EMT makers such as N-cadherin, Vimentin, Fibronectin and TGFb-associated expression of IL-11, PTHrP, CXCR4 and SNAIL. Knockdown of TRAF4 results in ablation of TGFb-induced phosphorylation of SMAD2 and p38 MAPK, showing the importance of TRAF4 in the regula-tion of SMAD-dependent and -independent signaling[34]

WWP1 – a phosphotyrosine binding E3

WW Domain Containing E3 Ubiquitin Protein Ligase 1 (WWP1) is a HECT domain E3 ubiquitin ligase that binds to phosphotyrosine (PPXY) domains in substrates.

WWP1 overexpression supports the proliferation and sur-vival of oral, and hepatocellular carcinoma (HCC).[36,37] (Fig. 1). Additionally, WWP1 positively regulates PTEN/AKT signaling to support the proliferation and cell cycle progression of gastric tumors, contributing to poor survival and lymph node metasta-sis[38] In breast cancer, WWP1 is overexpressed in 51% of trans-formed cell lines and supports the expression of estrogen receptor and Insulin-like growth factor receptor-1, resulting in aberrant proliferation. Inhibition of WWP1 expression sensi-tizes TRAIL-resistant breast cancer cells to TRAIL-induced activation of the extrinsic apoptotic pathway. In addition, effi-cient inhibition of breast cancer proliferation has been achieved by combining knockdown of WWP1 with anti-estrogen tamox-ifen drug therapy.[39-41] Lastly, WWP1 is frequently amplified and overexpressed in human prostate cancer, and is suggested to play a role in the inactivation of the TGFb tumor suppressor pathway by inactivation of Smad2, Smad4 and TbR1 in human cancer.[42]

Overall, this section illustrates that the overexpression of E3 ubiquitin ligases supports aberrant oncogenic signaling in various types of cancers. These reports show that inhibition of expression of each of these E3 ubiquitin ligase is sufficient to ablate tumor progression and metastasis.

Mutated E3 ligases proliferate different tumors

A list of mutations in E3 ubiquitin ligases, and their potential biologic effects in various tumors, is described in Table 1. We herein bring attention to the fact that mutated E3 ligases contribute to tumor hypoxia and vascularization, and upregulated inflammatory NFkB and growth factor mitogenic signaling pathways.

VHL adapts renal cell carcinoma to hypoxia

VHL is part of the VCB E3 ubiquitin ligase complex further composed of elongin B, elongin C and cullin-2. Under nor-moxia, VHL induces the ubiquitination of HIF1a for degrada-tion. On the other hand, inactivation of VHL results in the stabilization of HIF isoforms that support vascularization and adaptation of tumors to hypoxia[16] (Fig. 2).

Germ line mutations in tumor suppressor VHL cause von Hippel-Lindau syndrome characterized by the emergence of highly vascularized tumors, such as clear cell renal cell carci-noma (ccRCC), central nervous system hemagioblastoma, pheochromocytoma and pancreatic cysts.[16,43] Inactivated VHL

Table 1.1. Mutations in E3 ligases identified in cancers (partial list).

E3 Ligase	Mutation	Tumor	Biological Effect	Therapy	Reference
c-Cbl	Y371C/D/H	aCML, JMML			47-49
	S376F	aCML	transformation of 32D cells; decreased FLT3 ubiquitination		48
	L380P	aCML, MF, JMML			48,49
	C381R/Y	CMML, JMML			48,49
	C384R/Y	CMML, JMML, MDS-MPDu			48,49
	C396G/R	CMML, JMML			48,49
	H398Y	CMML	transformation of 32D cells; decreased FLT3 ubiquitination		48
	C401S	JMML			47
	C404R	JMML			49
	W408C/R	aCML, JMML			48,49
	G415V	JMML			49
	P417A	aCML	transformation of 32D cells; decreased FLT3 ubiquitination		48
	P417L	CMML			48
	F418L	aCML			48
	R420Q (proliferation of 32Dcells)	AML, aCML, MF, sAML	32D transformation; reduced FLT3 ubiquitination; inhibition of PDGFR and EGFR internalization		46,48,50
	R420L	aCML			48
	N454D	CMML			48
	R462X	aCML			48
	1106 del (66 bp)	JMML			47
	1228–2 A>G splice site	JMML			47
	c.1227–1227 C 4 del ggtac	CMML			48
	1190 del 99bp	JMML			49
	1227 C 4C>T splice site	JMML			49
	1228 - 2A>G splice site	JMML			49
	int C 5 G>A	aCML			48
	int C 4 C>T	CMML			48
	int - 1 G>C	CMML			48
Fbxw7	E113D	Colorectal, pancreatic			62,92
	E192A	Breast, liver		Sirolimus, Vorinostat: stable disease	62
	R222	colorectal		Temsirolimus, Bevacizumab, Cetuximab: stable disease	62
	W244	bladder, cervix		Sirolimus, Hydroxichloroquine: stable disease (bladder)	62
	R278	Colorectal, stomach			62,93
	S282	head and neck		Temsirolimus, Bevacizumab, Valproic acid: stable disease	62
	K299fs	melanoma			58
	W406	melanoma			58
	G423R/V	Melanoma, uterine	lower tumor volume in vivo compared with FBXW7 WT		58,94
	G437	T-ALL			53
	R441G/L/Q/W	Breast, NSCLC, T-ALL, uterine			53,56,95,96
	R465C/H	T-ALL, colorectal, endometrial, ovarian, extrahepatic, metastatic lung adenocarcinoma	R465H: metastatic lung adenocarcinoma	Temsirolimus: stable disease (R465H in metastatic lung adenocarcinoma); Everolimus, Anastrozole: progressive disease (R465H in ovarian cancer)	53,62,63
	R479G/P/Q	colorectal, head and neck, T-ALL			53,62
	W486	melanoma	increased melanoma tumor volume in vivo compared with FBXW7 WT		58
	G499Vfs 25	colorectal		Sirolimus, Hydroxichloroquine: stable disease	62
	R505C/G	colorectal, melanoma, intrahepatic, T-ALL	R505C: increased melanoma tumor volume in vivo compared with FBXW7 WT	Everolimus, Pazopanib: stable disease (R505C in colorectal cancer); Everolimus, Anakinra: progressive disease (R505C in colorectal cancer)	53,58,62
	S562L	melanoma	similar tumor volume in vivo compared with FBXW7 WT		58
	R658	melanoma, pleura		Sirolimus, Lapatinib: progressive disease (pleura)	58,62
	R689W	T-ALL			53
	726C1 G>A splice	teratoma		Temsirolimus, Bevacizumab, Carboplatin: stable disease	62
RNF31	Q584H	ABC DLBCL	upregulation of LUBAC linear polyubiquitination of NEMO; increased NFkB signaling		52

(Continued on next page)

Table 1.1. (Continued)

E3 Ligase	Mutation	Tumor	Biological Effect	Therapy	Reference
	Q622L	ABC DLBCL	upregulation of LUBAC linear polyubiquitination of NEMO; increased NFkB signaling		52
VHL	S72P	ccRCC	stabilization of HIF1		45
	N78K/S/Y	ccRCC	stabilization of HIF1		45
	V84E	ccRCC	stabilization of HIF1		45
	P86H	ccRCC	stabilization of HIF1		45
	W88C	ccRCC	stabilization of HIF1		45
	G93E	ccRCC	stabilization of HIF1		45
	Y98H/N	ccRCC	stabilization of HIF1		45
	L101P	ccRCC	stabilization of HIF1		45
	Y112D/H/N	ccRCC	stabilization of HIF1		45
	G114R	ccRCC	stabilization of HIF1		45
	W117L/R	ccRCC	stabilization of HIF1		45
	P119L	ccRCC	stabilization of HIF1		45
	D121G/Y	ccRCC	stabilization of HIF1		45
	V130D/P	ccRCC	stabilization of HIF1		45
	L153P	ccRCC	stabilization of HIF1		45
	K159N	ccRCC	stabilization of HIF1		45
	R161P/Q	ccRCC	stabilization of HIF1		45
	L169P	ccRCC	stabilization of HIF1		45
	V170E	ccRCC	stabilization of HIF1		45
	I180V	ccRCC	stabilization of HIF1		45
	L63fsX67	ccRCC	stabilization of HIF1		45
	H115SfsX17	ccRCC	stabilization of HIF1		45
	L153TfsX21	ccRCC	stabilization of HIF1		45
	R117fsX25	ccRCC	stabilization of HIF1		45

is observed in approximately 80–90% of ccRCC, which includes >90% of allelic deletion or loss of heterozygosity, >50% muta-tions and approximately 10% of promoter hypermethylation.[44] Over 800 distinct mutations in VHL have been detected in spo-radic and hereditary ccRCC, of which the majority results in loss of VHL function.[45]

Mutated VHL causes tumors to become sensitive to PI3K p110b inhibitor, TGX221, which decreases the proliferation, migration and invasion of cells.[44] In silico analysis revealed that the majority of missense mutations affecting the surface of VHL impact the interaction of VHL with HIF isoforms, elongin B, elongin C and other binding partners such as p53 and PKC. For instance, the L101P mutation, and other VHL disease-caus-ing mutations such as N78S, S80N and Y98H/N cause a dra-matic loss-of-function in VHL and stabilize HIF1 isoforms. In addition, frameshift mutations in exons 1, 2 and 3, with the exception of Glu204fsX44 at the very end of exon 3, inactivate VHL and lead to increased stability of HIF isoforms (Table 1). Such alterations in VHL possibly affect the hydroxylation of HIF isoforms by prolyl 4-hydroxylases (Fig. 2).[45] Hence, the stabilization of HIF isoforms by inactivation of the E3 ligase activity of VHL possibly contributes to hypoxia and the highly vascularized characteristics observed in these cancers.

c-Cbl drives myeloproliferative neoplasms

Casitas B-Lineage Lymphoma, c-Cbl or RNF55, is member of the Cbl family of E3 ubiquitin ligases previously mentioned. Muta-tions in c-Cbl in myeloproliferative neoplasms usually occur due to acquired 11q uniparental disomy, an event similar to loss of heterozygosity in which a part of the DNA is lost from one chro-mosome but the remaining homolog is duplicated resulting in 2 copies at the locus per cell. Myeloproliferative neoplasms include chronic myelomonocytic leukemia (CMML), atypical chronic myeloid leukemia (aCML; BCR-ABL negative), myelofribrosis (MF), secondary acute myelogenous leukemia (sAML), acute myeloid leukemia and juvenile myelomonocytic leukemia (JMML).[46-49] Homozygous mutations in c-Cbl in myeloprolifera-tive neoplasms contribute to poor survival rates of patients. Mutations in c-Cbl contribute to earlier presentation of JMML disease (age of 12 months at diagnosis) compared with patients without these alterations (29 months).[47,49]

c-Cbl mutations themselves are able to lead to neoplasms, as they have been identified in JMML tumors that do not harbor any other mutated RAS, PTN11 or NF1 genes known to be involved in JMML.[47] The mutations S376F (aCML), H398Y (CMML), P417A (aCML) and R420Q (AML, aCML, MF, sAML) in c-Cbl when co-transfected with FLT3 confer IL3-independence in 32D cells reflecting their oncogenic transforming activities (Table 1). These mutations also impair c-Cbl-mediated ubiquiti-nation of FLT3 and internalization of EGFR and PDGFR,[46,48,50] while they induce activated phospho-STAT5 signaling.[50] Muta-tion at the "hot spot" Y371 site of c-Cbl is rarely found in other myeloid neoplasms. The Y371C/D/H mutations located in the linker domain adjacent to the RING domain have been identified in JMML patients (Table 1). A similar phosphomimic mutation to Asp, Y371E, constitutively activates the autoubiquitination E3 ligase activity of c-Cbl and it interacts with EGFR,[51] showing that c-Cbl modulates RTK signaling.

Activating mutations in c-Cbl lead to constitutive RTK sig-naling by impairing receptor internalization and degradation, driving myeloproliferative disorders.

Mutations in RNF31 in ABC DLBCL

The Linear Polyubiquitin Chain Assembly Complex (LUBAC) is composed of RNF31 (or HOIP), RBCK1 (or HOIL-1) and SHARPIN. LUBAC catalyzes the linear ubiquitination of

NEMO, a scaffold member of the IKK complex that activates the canonical NFkB signaling pathway (Fig. 2).

Activated B cell-like (ABC) subtype of diffuse large B-cell lymphoma (DLBCL) malignant progression is dependent upon constitutive B-cell receptor (BCR) activation that upregulates NFkB signaling. Inhibition of RNF31 or SHARPIN decreases LUBAC-mediated linear polyubiquitination of NEMO and impaires IKK and NFkB activation, leading to a decrease in viability of ABC DLBCL.[52] In addition, inhibition of RNF31 sensitizes ABC DLBCL tumors to Bruton agammaglobulinemia tyrosine kinase (BTK) inhibitor, Ibrutinib, and IRF4 transcrip-tion factor inhibitor, Lenalidomine, leading to decreased viabil-ity of this subclass of B-cell lymphoma.

Two rare germline SNP polymorphisms in RNF31 are enriched 8-fold in ABC DLBCL biopsies (Table 1). These muta-tions, Q584H and Q622L, are found in the ubiquitin-associated domain of RNF31 known to interact with the ubiquitin-like domain of RBCK1, leading to upregulation of LUBAC-mediated linear polyubiquitination of NEMO, increased IKK and NFkB activation in ABC DLBCL tumors.[52]

Inactivating driver mutations in FBXW7

Mutations in FBXW7 have been identified in various tumors (Table 1). The F-box domain of FBXW7 is important for the interaction with the SCF complex, while the WD40 domain recognizes phosphorylation sites in a conserved Cdc4 phospho-degron motif in the target substrate.[26] Inactivating mutations in the WD40 domain of FBXW7 often impair substrate binding and subsequently diminish protein turnover, contributing to aberrant oncogenic signaling of targets mentioned below.

T cell acute lymphoblastic leukemia (T-ALL) is a malignant neoplasm characterized by mutations mostly in NOTCH1 and FBXW7.[53] Mutations in FBXW7, studied in a population of pediatric Chinese T-ALL patients, contribute to poor overall survival and higher incidence of tumor relapse. These FBXW7 mutations affect codons R465, R479, R505 and R689 in the WD40 domain, critical for the interaction with the PEST domain of NOTCH1. These mutations may further impact signaling pathways beyond NOTCH1, since FBXW7 mediates the stability of oncogenic proteins such as mTOR, Cyclin E and MYC.

In addition, mutations in FBXW7 are frequently found in various cancers, but particularly uterine, colorectal, bladder and cervical carcinoma.[54-57] In melanoma, some FBXW7 mutations have been reported in the absence of the classic BRAF V600E and NRAS G12D, G13R and Q61K/L/S mutations. This may indicate that mutations in FBXW7 are drivers of cancer progres-sion.[58] As a proof-of-concept for the inactivating mutations in FBXW7, knockdown of FBXW7 in melanoma cell lines leads to the accumulation of NOTCH1, HEY1 and downstream effectors Cyclin E, Aurora A and MYC, resulting in increased tumorigenesis.[59-61] In addition, this event leads to the upregulation of angiogenesis-promoting genes such as IL-6, CXCL2, SERPINE1 and PGF1, and increased phosphorylation of STAT3. Mice grafted with melanoma cells with knockdown FBXW7, treated with NOTCH1 inhibitors dibenzazepine (DBZ) and compound E, showed substantial melanoma tumor shrinkage.[58]

Other inactivating mutations in FBXW7 were identified in various advanced cancers such as colorectal, squamous head and neck, bladder, cervix, endometrial, liver, ovarian, mesothelioma, pancreatic and teratoma. In these tumors, most of these mutations concomitantly occur with mutations in TP53, fol-lowed by KRAS, PI3KCA and APC.[62] As mTOR is a down-stream target of FBXW7, tumors harboring inactivating mutations in FBXW7 are sensitive to mTOR inhibitors. For instance, treatment of patients, whose tumors exhibit mutated FBXW7, with mTOR inhibitors (Sirolimus, Everolimus, and Temsirolimus) resulted in tumor shrinkage.[62] In addition, Temsirolimus showed promising results in a patient with meta-static lung adenocarcinoma with mutated FBXW7 R465H,
leading to shrinkage of mediastinal lymphadenopathy (Table 1).[63]

E3 ubiquitin ligases in pluripotent cancer stem cells

Conventional chemotherapies often fail to target metastasized tumors, which may be due to the emergence of a subpopulation of cells, the cancer initiating cells or cancer stem cells (CSCs). CSCs are not only capable of self-renewal and differentiation like normal stem cells, but they are also capable of tumor initia-tion, relapse, chemotherapeutic resistance and metastasis.

CSCs are characterized by upregulated expression of embryonic stem cells markers, SOX2 (SRY-Box 2), OCT4 (Octamer-Binding Protein 4) and NANOG (Nanog Homeobox). These transcription factors are the key regulators of pluripotency, activating self-renewal-associated genes and inhibiting differentiation by suppressing lineage-specific transcription factors. Expression of these regulators confers stem cell-like characteristics, and silencing them results in decreased tumorigenicity. CSC's express surface markers CD133 and CD44, including increased expression of aldehyde dehydrogenase (ALDH) and increased ATP binding cassette (ABC) transporter drug efflux, which all contribute to chemotherapy resistance[64] (Fig. 3A).

E3 ligases are strongly associated with either promoting or suppressing the CSC population in various cancers (Fig. 3B). Investigating the mechanisms by which E3 ligases confer stem-cell like characteristics to a subpopulation of tumorigenic cells is of great interest to develop novel compounds to selectively target CSC's, possibly overcoming metastasis.

SMURF1 in head and neck cancer stem cells

SMURF1 (SMAD specific E3 ubiquitin protein ligase 1) suppresses bone marrow morphogenic (BMP) signaling contributing to the maintenance of the CSC subpopulation ($ALDH^{high}$/$CD44^{high}$) in head and neck squamous cell carcinoma (HNSCC). BMP proteins are growth factor members of the TGFb superfamily that restrict haematopoietic stem cell prolif-eration and induce cellular differentiation. The overexpression of SMURF1 in CSCs derived from HNSCC leads to decreased levels of SMADs 1/5/8 and attenuates BMP signaling, keeping cells in an undifferentiated stem-cell like phenotype.[65]

Skp2 in nasopharyngeal and prostate cancer stem cells

Skp2 (S-phase kinase-associated protein 2 also known as FBXL1) is an F-box protein; one of its main targets for degradation is the G1/S cyclin-dependent kinase inhibitor p27, a tumor suppressor.

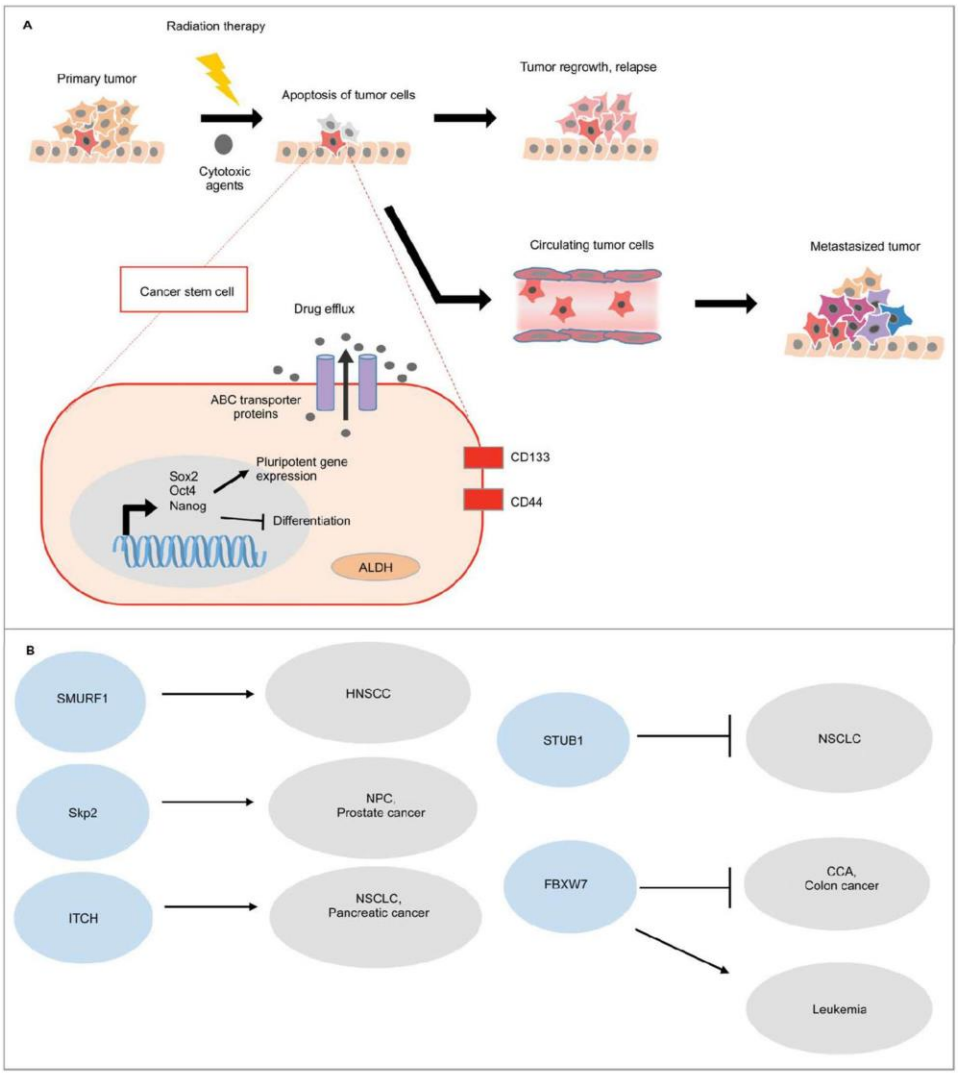

Figure 1.3. E3 ubiquitin ligases in pluripotent stem cells. (A) Cancer stem cells are characterized by the upregulation of Sox2, Oct4, and Nanog, which activates self-renewal associated genes and inhibits cellular differentiation. Cell surface markers, CD133 and CD44 are associated with CSC properties. Conventional chemotherapeutic agents target differentiated cells, thus quiescent CSCs are innately chemo-resistant. Moreover, CSCs show increased ABC multi-drug transporters, which pump the cytotoxic drugs out of the cells. CSCs also show high aldehyde dehydrogenase activity (ALDH), which detoxifies the aldehydes generated by the chemotherapeutic agents. As a result, the surviving CSCs can re-populate or metastasize, and these cancer cells that possess self-renewal advantages are very challenging to eradicate by using conventional che-motherapeutic agents.[64] (B) E3 ligases can either promote or suppress CSCs in different cancers.

Overexpression of Skp2 correlates with poor prognosis of nasopharyngeal carcinoma (NPC), one of the most common head and neck carcinomas,[66] and of prostate cancer[67] (Fig. 1). NPC patients with high expression of Skp2 have a correlation with tumor recurrence and metastasis. Knockdown of Skp2 decreases sphere colony formation of NPC cell lines, and impairs the proliferation of the ALDH1^{C} subpopulation of cells, indicating reduced CSC phenotypes.[66] In prostate cancer, a small molecule inhibitor of Skp2 reduces prostate CSC population through p53-independent cellular senescence and inhibition of aerobic glycolysis. Moreover, the Skp2 inhibitor sensitizes prostate CSC's to doxorubicin and cyclophosphamide drug treatments.[67]

Taken together, Skp2 promotes CSC properties and decreases drug treatment efficacy, showing the importance of targeting Skp2 to ablate CSC in tumor niches.

ITCH in lung cancer stem cells

ITCH is a HECT E3 ligase that performs essential regulatory functions in immune cells such as ubiquitination of Bcl10, PKC and PLC-γ, leading to nuclear translocation of NFκB and NFAT (nuclear factor of activated T-cells) during T-cell signaling activation. ITCH further regulates the stability of p63 and Notch.[68]

Desmethylclomipramine (DCMI), identified via high-throughput screening as a specific inhibitor of E3 ligase activity of ITCH,[69] has shown promising chemotherapeutic action against non-small cell lung CSCs in patient samples whom acquired resistance to chemotherapeutic drugs Cisplatin, Gemcitabine and Paclitaxel. DCMI leads to reduced sphere forming ability and inhibition of proliferation of this subpopulation of lung cancer stem cells. In addition, shRNA-mediated silencing of *ITCH* decreases ALDH-positive lung CSCs and sensitizes cells to Gemcitabine-induced apoptosis.[70]

FBXW7 in colonic and leukemia cancer stem cell maintenance

FBXW7 is known to target oncoproteins such as mTOR, cyclin-E, Jun, Myc and Notch1 for degradation, which are usually involved in the signaling of various cancers. The role of FBXW7 in the maintenance of normal stem cells has been previously shown.[71] However, the role of FBXW7 in the maintenance of CSCs can vary, depending on the type of tumor (Fig. 3.B).

In colon cancer, downregulated FBXW7 expression promotes EMT as shown by the increased epxression of mesenchymal stem cell markers, SOX2, OCT4 and NANOG, leading to invasive phenotype, greater tumor initiating potential and non-adherent growth ability. As previously mentioned, mTOR is a downstream target of FBXW7. Treatment of colon cancer cells with the mTOR inhibitor rapamycin suppresses their migration and tumor-sphere formation.[72] Loss of *FBXW7* is also associated with stem-like competence in cholangiocarcinoma (CCA), and rapamycin treatment of CCA cells suppresses invasion, metastatic potential and tumor sphere formation.[29]

In contrast, expression of FBXW7 is critical in the maintenance of leukemia-initiating cells (LICs) in chronic myeloid leukemia (CML), a disease associated with the BCR-ABL fusion protein. FBXW7 supports stem cell properties in LICs and maintains these cells in a quiescent state. Inhibition of *FBXW7* expression decreases colony formation potential, eliminates leukemic cell infiltration in peripheral blood, spleen, liver and lungs, and leads to induction of apoptosis in a p53-dependent manner. In addition, knockdown of *FBXW7* causes LIC's to differentiate and enter the cell cycle becoming sensitized to imatinib and cytosine arabinoside drug treatments.[73]

In summary, the levels in the expression of E3 ubiquitin ligases maintain a subpopulation of cancer stem cells in an undifferentiated state (Fig. 3.A and 3.B). Most of these reports show that inhibition of E3 ligase expression, with the exception of FBXW7 in LIC's, sensitizes CSC's to chemotherapeutic agents suggesting a clinical approach to eradicate this subpopulation of cells attributed to chemotherapy resistance and metastasis.

The misregulated expression of DUBs in metastatic cancers

Deubiquitinating enzymes (DUBs) play the reverse role of E3 ligases by cleaving the isopeptide bond between the ubiquitin and the substrate. DUBs have been described to play important roles in cellular processes, such as gene transcription, DNA repair and cell cycle progression. There are about 80 functional DUBs and they can be divided into 6 classes: ubiquitin-specific proteases (USPs), ubiquitin C-terminal hydrolases (UCHs), ovarian-tumor proteases (OTUs), Machado-Joseph disease protein domain proteases (MJD), JAMM/MPN domain-associated metallopeptidases (JAMMs) and monocyte chemotactic protein-induced protein (MCPIP).[74]

In cancer, DUBs can stabilize proteins by removing the degradation-inducing ubiquitin signal, contributing to aberrant signaling (Fig. 4). Many studies have shown that deregulation of DUBs is involved in cancer progression, recurrence and metastasis (Table 2).

USP7 promotes APL, aggressive prostate cancer, and NSCLC metastasis

USP7 (also known as HAUSP, Herpesvirus-associated ubiquitin protease) plays a crucial role in regulating tumor suppressors p53 and PTEN. A small molecule inhibitor of USP7 (HBX 41,108) inhibits USP7-mediated deubiquitination of p53 and induces apoptosis in colon carcinoma, suggesting the therapeutic potential in targeting USP7.[75] USP7 is frequently overexpressed in non-small cell lung carcinoma (NSCLC) and also correlates with lymph node metastasis. Inhibition of *USP7* upregulates E-cadherin and downregulates Vimentin and N-cadherin, indicating USP7 promotes EMT in NSCLC.[76]

Moreover, USP7 may contribute to cancer by modulating the nuclear localization of PTEN. Acute promyelocytic leukemia (APL) harboring the t(15;17) chromosomal translocation, which encodes the PML–RARα fusion protein that inhibits differentiation, exhibits aberrant nuclear exclusion of PTEN. As USP7 co-localizes to nuclear bodies, studies using prostate and colon tumor models have shown USP7 to interact with and deubiquitinate PTEN, leading to the nuclear exclusion and impairment of tumor suppressor function of PTEN. In addition, USP7 is overexpressed in prostate cancer tissue, in which the USP7/PTEN signaling axis is misregulated.[77]

Interestingly, murine ES cells expressing mutant p53 can retain pluripotency and normal karyotype through a mechanism in which USP7, Nedd4, Aurora kinase, Trim24 and the chaperonin containing TCP1 complex (CCT) participate in binding mutant p53, thus inducing a conformational shift toward a WT conformation. Exploiting this gain-of-function mechanism has been proposed as a possible path toward future p53-targeted cancer therapy.[78]

USP4 and USP9X support oncogenic signaling in various tumors

Ubiquitin-specific peptidase 4 (USP4) is overexpressed in multiple cancers, such as breast and lung cancers (Table 2). Some cancers rely on aberrant TGFβ signaling for the purposes of

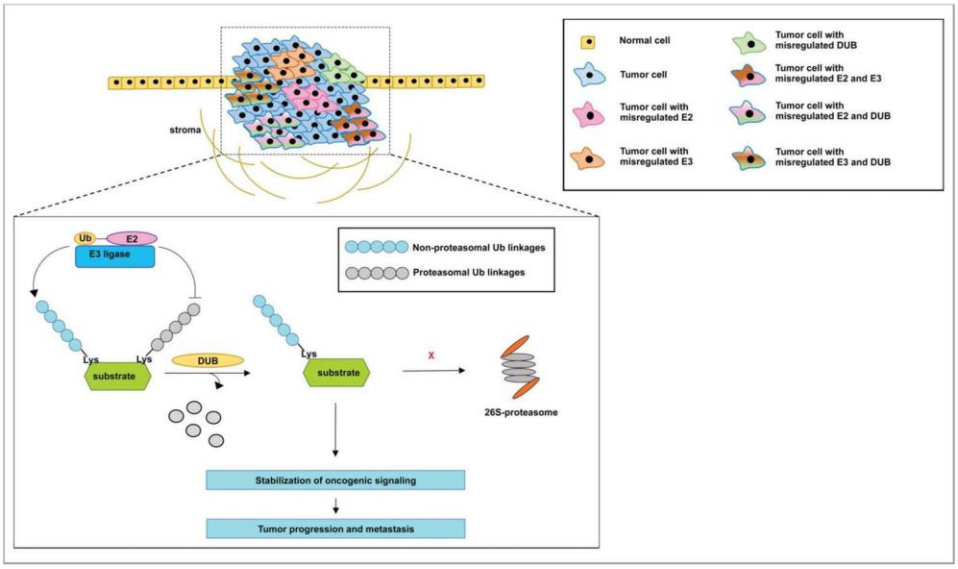

Figure 1.4. Proposed model of the mechanism by which the misregulated expression of E2s, E3s and DUB's may contribute to tumorigenesis and metastasis. The informa-tion from the reports described in this review reveals that inhibition of E2s, E3s and DUB's with either small interfering RNA or small molecule inhibitors is sufficient to inhibit the progression and metastasis of tumors. However, some of these reports show that the misregulated expression of the members of the ubiquitination pathway occurs in multiple tumors. It is not clear whether a subpopulation of cells within a tumor, for instance, may rely on the misregulated expression of one member only or on a combination of the misregulated expression of these proteins to support aberrant oncogenic signaling. In addition, it is not clearly demonstrated whether the misre-gulated expression of E2s and E3s stabilizes oncogenic signaling via the catalysis of non-proteasomal ubiquitin linkages, while DUB's remove ubiquitin linkages that would otherwise lead to proteasomal degradation. Nevertheless, we describe a common conclusion from multiple reports that members of the ubiquitination pathway drive tumor aggressiveness and culminate in metastasis.

EMT, proliferation, invasion and metastasis. As previously mentioned, TGFb-induced activation of TbRI eventually results in the ubiquitination of TbRI and subsequent mem-brane internalization and degradation of the receptor, termi-nating downstream signaling. USP4 overexpression is detected in invasive breast carcinoma and it enhances aberrant TGFb signaling. A mechanism by which this oncogenic signaling occurs has been proposed. AKT-mediated phosphorylation of USP4 at a consensus motif stabilizes this DUB, which in turn deubiquitinates the TGFb-induced activated TbRI and leads to the stabilization of downstream activation of phosphorylated SMAD2 and SMAD2/SMAD4 complex formation (Fig. 2). USP4-mediated stabilization of TGFb signaling leads to the expression of metastasis-inducing genes such as IL-11, CXCR4 and MMPs in breast cancer cells.[79]

In addition, the overexpression of another DUB - USP9X - has been detected in follicular lymphoma, breast and colon adenocarcinomas, and small cell lung carcinoma[80] (Table 2). Various lymphomas, such as B- and mantle-cell lymphomas and multiple myeloma usually rely on the overexpressed MCL1, a member of the pro-survival BCL family of proteins. In multiple myeloma, overexpression of USP9X is correlated with poor survival. A mechanism by which MCL1 is stabilized has been proposed. The overexpression of USP9X results in the deubiquitination of MCL1 by this DUB, stabilizing pro-survival oncogenic signaling in cancers. Although knocking down USP9X does not affect cell proliferation in vitro, it does sensitize tumors to ABT-737 small molecule antagonist of BCL proteins resulting in apoptosis.[80] More recently, in non-small cell lung carcinoma, inhibition of USP9X by either siRNA knockdown or via a small molecule inhibitor WP1130 decreased MCL1 expression and sensitized cells to radiation therapy.[81]

UCH-L1 plays a contradicting role in different tumors

Overexpression of UCH-L1 (Ubiquitin C-terminal hydrolase L1) in gastric cancer promotes colony formation, migration

Table 1.2. Aberrant expression of DUBs associated with cancers.

DUB	Upregulated in Tumor	EMT and/or Metastasis	Signaling Effect	Reference
USP9X (stabilization)	Follicular lymphoma, Diffuse Large B-cell Lymphoma, breast adenocarcinoma, colon adenocarcinoma, small cell lung carcinoma	Lymph node	Mcl1	80, 82-84,86
UCHL1	Gastric (in liver metastasis), NSCLC, breast (can also be downregulated), prostate (downregulated)	Liver, lung	Akt, Erk1/2, p38 MAPK, JNK	87-89
OTUB1	Colorectal, breast, prostate	Liver, pelvic, ovary, lymph node	TGFb, MAPK, FOXM1	

and liver metastasis of gastric cancer cells *in vitro* due to significant upregulation of AKT and Erk1/2 signaling.[82] Moreover, UCH-L1 is overexpressed in highly invasive NSCLC and melanoma. In lung cells, UCH-L1 supports the EGF-induced activation of Akt, JNK, and p38 MAPK signaling.[83]

In addition, high expression of UCH-L1 positively correlates with that of HIF1α and hence activation of hypoxia conditions in some breast and lung cancer, and it contributes to poor overall survival and distant metastasis-free survival in breast, lung and melanoma cancer. UCH-L1 is shown to deubiquitinate and stabilize HIF1α, inducing hypoxia (Fig. 2). UCHL1 expression supports breast and melanoma metastasis to lungs; inhibition of metastasis is achieved by a UCH-L1 inhibitor, LDN57444.[84]

However, the role of UCH-L1 is not as straightforward as suggested by these studies. Another study reported that *UCHL1* can be downregulated in other breast cancer tissue samples and cell lines due to frequent gene methylation. Overexpression of UCHL1 in MB231 breast cells significantly decreases proliferation due to G0/G1 cell cycle arrest and apoptosis.[85] Similarly, this DUB is downregulated in some prostate cancer samples and in LNCaP cell line, and overexpression of UCHL1 suppresses the proliferation and anchorage-independent growth of LNCaP cells.[86] Further research will be required to unravel the contradicting role of UCH-L1 in different cancers.

OTUB1 contributes to drug resistance and promotes metastasis

OTU domain-containing ubiquitin aldehyde-binding protein 1 (OTUB1) plays diverse roles such as stabilizing p53, inhibiting K63-linked polyubiquitination for DNA double strand break repair by targeting UBE2N for degradation, the E2 enzyme that catalyzes this ubiquitin linkage in proteins members of the NFκB pathway. High expression of OTUB1 is detected in approximately 50% of colorectal cancer and correlates with lymph node status, liver, pelvic and ovary distant metastasis, in addition to low overall and progression-free survival rates. OTUB1 is also found to be important in prostate cancer by regulating androgen signaling.[87,88] In breast cancer, OTUB1 decreases the Lys48-linked ubiquitination of FOXM1 stabilizing the expression of the protein. FOXM1 is a transcription factor that is important for DNA damage responses and its overexpression is associated with genotoxic drug resistance in tumors. Hence, the overexpression of OTUB1 contributes to the aberrant proliferation and epirubicin resistance of MCF7 cells and correlates with poor survival and chemotherapy resistance of breast cancer cohort.[89] In summary, it is evident that some DUBS are either upregulated or downregulated in some tumors, promoting oncogenic signaling.

Concluding remarks

The information presented herein reveals a common pattern: the misregulated expression of various E2 ubiquitin conjugating enzymes, E3 ubiquitin ligases and DUBs supports aberrant oncogenic signaling in a plethora of tumors. Since the misregulated expression of these proteins overlaps among many different types of cancers, there may exist subpopulations of cells within tumors exhibiting the misregulated expression of a specific member of the ubiquitination pathway. Alternatively, cells may take advantage of a combinatorial misregulated expression of these proteins to support oncogenic signaling. Lastly, it is not clear whether E2s and E3s catalyze non-proteasomal ubiquitin linkages that stabilize the function of oncogenes, and/or DUB's remove the ubiquitin linkages that would otherwise result in the degradation of oncogenes. Several models are presented by which members of the ubiquitination pathway support oncogenic signaling in cancers (Fig. 4). Nevertheless, it is clear that the inhibition of a specific E2, E3 or DUB seems to halt tumor progression and metastasis.

The development of chemotherapeutic agents against E2s, E3s and DUBs, is an attractive strategy that may lead to the inhibition of multiple oncogenic pathways in tumors. So far, the FDA has approved very few drugs targeting members of the ubiquitination cascade. Proteasome inhibitors, Bortezomib and Carfilzomib, are limited to multiple myeloma and mantle cell lymphoma treatments. Various strategies to develop inhibitors to target E1s, E2s, E3s have been recently described.[90] For instance, targeting the MDM2 E3 ligase - a p53 negative regulator - with RG7112 (cis-imidazoline analogs) has been tested in clinical trials for the treatment of advanced solid and hematological malignancies, including liposarcoma.[91]

An interesting concept to enhance the ubiquitination and degradation of "undruggable" oncogenic proteins is the development of protein-targeting chimeric molecules (PROTACs). These molecules are bifunctional in which they include an E3 ligase-recruiting moiety linked by a short linker to a ligand that targets the substrate of interest, placing them in proximity for ubiquitination leading to subsequent degradation.[90] Therefore, targeting the E3 ligases and their co-expressed substrates with PROTAC may be a promising therapeutic intervention in various tumors herein described.

Major advances have been made to target oncogenic protein kinases in clinical settings through the development of TKIs. Here, we present evidence from multiple papers demonstrating that mechanistic studies of the ubiquitination pathway will open new therapeutic approaches, potentially allowing the development of novel inhibitors to suppress cancer progression and metastasis.

Disclosure of potential conflicts of interest

No potential conflicts of interest were disclosed.

Acknowledgements

We thank all laboratory members for advice and encouragement, particularly April N. Meyer.

Funding

We also acknowledge generous support from the UC 820 San Diego Foundation.

References

[1] Emmerich CH, Ordureau A, Strickson S, Arthur JS, Pedrioli PG, Komander D, Cohen P. Activation of the canonical IKK complex by K63/M1-linked hybrid ubiquitin chains. Proc Natl Acad Sci U S A 2013; 110:15247-52; PMID:23986494; http://dx.doi.org/10.1073/pnas.1314715110

[2] Chen J, Chen ZJ. Regulation of NF-kappaB by ubiquitination. Curr Opin Immunol 2013; 25:4-12; PMID:23312890; http://dx.doi.org/10.1016/j.coi.2012.12.005

[3] Messick TE, Greenberg RA. The ubiquitin landscape at DNA double-strand breaks. J Cell Biol 2009; 187:319-26; PMID:19948475; http://dx.doi.org/10.1083/jcb.200908074

[4] Ori D, Kato H, Sanjo H, Tartey S, Mino T, Akira S, Takeuchi O. Essential roles of K63-linked polyubiquitin-binding proteins TAB2 and TAB3 in B cell activation via MAPKs. J Immunol 2013; 190:4037-45; PMID:23509369; http://dx.doi.org/10.4049/jimmunol.1300173

[5] Cheung KJ, Ewald AJ. A collective route to metastasis: Seeding by tumor cell clusters. Science 2016; 352:167-9; PMID:27124449; http://dx.doi.org/10.1126/science.aaf6546

[6] Clague MJ, Heride C, Urbe S. The demographics of the ubiquitin system. Trends Cell Biol 2015; 25:417-26; PMID:25906909; http://dx.doi.org/10.1016/j.tcb.2015.03.002

[7] Wu X, Zhang W, Font-Burgada J, Palmer T, Hamil AS, Biswas SK, Poidinger M, Borcherding N, Xie Q, Ellies LG, et al. Ubiquitin-conjugating enzyme Ubc13 controls breast cancer metastasis through a TAK1-p38 MAP kinase cascade. Proc Natl Acad Sci U S A 2014; 111:13870-5; PMID:25189770; http://dx.doi.org/10.1073/pnas.1414358111

[8] Wu Z, Shen S, Zhang Z, Zhang W, Xiao W. Ubiquitin-conjugating enzyme complex Uev1A-Ubc13 promotes breast cancer metastasis through nuclear factor-small ka, CyrillicB mediated matrix metalloproteinase-1 gene regulation. Breast Cancer Res 2014; 16:R75; PMID:25022892; http://dx.doi.org/10.1186/bcr3692

[9] Deryugina EI, Quigley JP. Matrix metalloproteinases and tumor metastasis. Cancer Metastasis Rev 2006; 25:9-34; PMID:16680569; http://dx.doi.org/10.1007/s10555-006-7886-9

[10] Fujita T, Ikeda H, Kawasaki K, Taira N, Ogasawara Y, Nakagawara A, Doihara H. Clinicopathological relevance of UbcH10 in breast cancer. Cancer Sci 2009; 100:238-48; PMID:19038004; http://dx.doi.org/10.1111/j.1349-7006.2008.01026.x

[11] van Ree JH, Jeganathan KB, Malureanu L, van Deursen JM. Overexpression of the E2 ubiquitin-conjugating enzyme UbcH10 causes chromosome missegregation and tumor formation. J Cell Biol 2010; 188:83-100; PMID:20065091; http://dx.doi.org/10.1083/jcb.200906147

[12] Narayan G, Bourdon V, Chaganti S, Arias-Pulido H, Nandula SV, Rao PH, Gissmann L, Durst M, Schneider A, Pothuri B, et al. Gene dosage alterations revealed by cDNA microarray analysis in cervical cancer: identification of candidate amplified and overexpressed genes. Genes Chromosomes Cancer 2007; 46:373-84; PMID:17243165; http://dx.doi.org/10.1002/gcc.20418

[13] Tzelepi V, Zhang J, Lu JF, Kleb B, Wu G, Wan X, Hoang A, Efstathiou E, Sircar K, Navone NM, et al. Modeling a lethal prostate cancer variant with small-cell carcinoma features. Clin Cancer Res 2012; 18:666-77; PMID:22156612; http://dx.doi.org/10.1158/1078-0432.CCR-11-1867

[14] Takahashi Y, Ishii Y, Nishida Y, Ikarashi M, Nagata T, Nakamura T, Yamamori S, Asai S. Detection of aberrations of ubiquitin-conjugating enzyme E2C gene (UBE2C) in advanced colon cancer with liver metastases by DNA microarray and two-color FISH. Cancer Genet Cytogenet 2006; 168:30-5; PMID:16772118; http://dx.doi.org/10.1016/j.cancergencyto.2005.12.011

[15] Jung CR, Hwang KS, Yoo J, Cho WK, Kim JM, Kim WH, Im DS. E2-EPF UCP targets pVHL for degradation and associates with tumor growth and metastasis. Nat Med 2006; 12:809-16; PMID:16819549; http://dx.doi.org/10.1038/nm1440

[16] Rankin EB, Giaccia AJ. Hypoxic control of metastasis. Science 2016; 352:175-80; PMID:27124451; http://dx.doi.org/10.1126/science.aaf4405

[17] Witkiewicz AK, McMillan EA, Balaji U, Baek G, Lin WC, Mansour J, Mollaee M, Wagner KU, Koduru P, Yopp A, et al. Whole-exome sequencing of pancreatic cancer defines genetic diversity and therapeutic targets. Nat Commun 2015; 6:6744; PMID:25855536; http://dx.doi.org/10.1038/ncomms7744

[18] Beltran H, Prandi D, Mosquera JM, Benelli M, Puca L, Cyrta J, Marotz C, Giannopoulou E, Chakravarthi BV, Varambally S, et al. Divergent clonal evolution of castration-resistant neuroendocrine prostate cancer. Nat Med 2016; 22:298-305; PMID:26855148; http://dx.doi.org/10.1038/nm.4045

[19] Berndsen CE, Wolberger C. New insights into ubiquitin E3 ligase mechanism. Nat Struct Mol Biol 2014; 21:301-7; PMID:24699078; http://dx.doi.org/10.1038/nsmb.2780

[20] Deshaies RJ, Joazeiro CA. RING domain E3 ubiquitin ligases. Annu Rev Biochem 2009; 78:399-434; PMID:19489725; http://dx.doi.org/10.1146/annurev.biochem.78.101807.093809

[21] Jang KW, Lee KH, Kim SH, Jin T, Choi EY, Jeon HJ, Kim E, Han YS, Chung JH. Ubiquitin ligase CHIP induces TRAF2 proteasomal degradation and NF-kappaB inactivation to regulate breast cancer cell invasion. J Cell Biochem 2011; 112:3612-20; PMID:21793045; http://dx.doi.org/10.1002/jcb.23292

[22] Kajiro M, Hirota R, Nakajima Y, Kawanowa K, So-ma K, Ito I, Yamaguchi Y, Ohie SH, Kobayashi Y, Seino Y, et al. The ubiquitin ligase CHIP acts as an upstream regulator of oncogenic pathways. Nat Cell Biol 2009; 11:312-9; PMID:19198599; http://dx.doi.org/10.1038/ncb1839

[23] Wang Y, Ren F, Wang Y, Feng Y, Wang D, Jia B, Qiu Y, Wang S, Yu J, Sung JJ, et al. CHIP/Stub1 functions as a tumor suppressor and represses NF-kappaB-mediated signaling in colorectal cancer. Carcinogenesis 2014; 35:983-91; PMID:24302614; http://dx.doi.org/10.1093/carcin/bgt393

[24] Wang T, Yang J, Xu J, Li J, Cao Z, Zhou L, You L, Shu H, Lu Z, Li H, et al. CHIP is a novel tumor suppressor in pancreatic cancer through targeting EGFR. Oncotarget 2014; 5:1969-86; PMID:24722501; http://dx.doi.org/10.18632/oncotarget.1890

[25] Eirew P, Steif A, Khattra J, Ha G, Yap D, Farahani H, Gelmon K, Chia S, Mar C, Wan A, et al. Dynamics of genomic clones in breast cancer patient xenografts at single-cell resolution. Nature 2015; 518:422-6; PMID:25470049; http://dx.doi.org/10.1038/nature13952

[26] Welcker M, Clurman BE. FBW7 ubiquitin ligase: a tumour suppressor at the crossroads of cell division, growth and differentiation. Nat Rev Cancer 2008; 8:83-93; PMID:18094723; http://dx.doi.org/10.1038/nrc2290

[27] Ibusuki M, Yamamoto Y, Shinriki S, Ando Y, Iwase H. Reduced expression of ubiquitin ligase FBXW7 mRNA is associated with poor prognosis in breast cancer patients. Cancer Sci 2011; 102:439-45; PMID:21134077; http://dx.doi.org/10.1111/j.1349-7006.2010.01801.x

[28] Iwatsuki M, Mimori K, Ishii H, Yokobori T, Takatsuno Y, Sato T, Toh H, Onoyama I, Nakayama KI, Baba H, et al. Loss of FBXW7, a cell cycle regulating gene, in colorectal cancer: clinical significance. Int J Cancer 2010; 126:1828-37; PMID:19739118

[29] Yang H, Lu X, Liu Z, Chen L, Xu Y, Wang Y, Wei G, Chen Y. FBXW7 suppresses epithelial-mesenchymal transition, stemness and metastatic potential of cholangiocarcinoma cells. Oncotarget 2015; 6:6310-25; PMID:25749036; http://dx.doi.org/10.18632/oncotarget.3355

[30] Quail DF, Joyce JA. Microenvironmental regulation of tumor progression and metastasis. Nat Med 2013; 19:1423-37; PMID:24202395; http://dx.doi.org/10.1038/nm.3394

[31] Paolino M, Choidas A, Wallner S, Pranjic B, Uribesalgo I, Loeser S, Jamieson AM, Langdon WY, Ikeda F, Fededa JP, et al. The E3 ligase Cbl-b and TAM receptors regulate cancer metastasis via natural killer cells. Nature 2014; 507:508-12; PMID:24553136; http://dx.doi.org/10.1038/nature12998

[32] Vaughan L, Tan CT, Chapman A, Nonaka D, Mack NA, Smith D, Booton R, Hurlstone AF, Malliri A. HUWE1 ubiquitylates and degrades the RAC activator TIAM1 promoting cell-cell adhesion disassembly, migration, and invasion. Cell reports 2015; 10:88-102; PMID:25543140; http://dx.doi.org/10.1016/j.celrep.2014.12.012

[33] Tsai YC, Mendoza A, Mariano JM, Zhou M, Kostova Z, Chen B, Veenstra T, Hewitt SM, Helman LJ, Khanna C, et al. The ubiquitin ligase gp78 promotes sarcoma metastasis by targeting KAI1 for degradation. Nat Med 2007; 13:1504-9; PMID:18037895; http://dx.doi.org/10.1038/nm1686

[34] Zhang L, Zhou F, Garcia de Vinuesa A, de Kruijf EM, Mesker WE, Hui L, Drabsch Y, Li Y, Bauer A, Rousseau A, et al. TRAF4 promotes TGF-beta receptor signaling and drives breast cancer metastasis. Mol

Cell 2013; 51:559-72; PMID:23973329; http://dx.doi.org/10.1016/j.molcel.2013.07.014

[35] Martelotto LG, De Filippo MR, Ng CK, Natrajan R, Fuhrmann L, Cyrta J, Piscuoglio S, Wen HC, Lim RS, Shen R, et al. Genomic landscape of adenoid cystic carcinoma of the breast. J Pathol 2015; 237:179-89; PMID:26095796; http://dx.doi.org/10.1002/path.4573

[36] Lin JH, Hsieh SC, Chen JN, Tsai MH, Chang CC. WWP1 gene is a potential molecular target of human oral cancer. Oral Surg Oral Med Oral Pathol Oral Radiol 2013; 116:221-31; PMID:23849376; http://dx.doi.org/10.1016/j.oooo.2013.05.006

[37] Cheng Q, Cao X, Yuan F, Li G, Tong T. Knockdown of WWP1 inhibits growth and induces apoptosis in hepatoma carcinoma cells through the activation of caspase3 and p53. Biochem Biophys Res Commun 2014; 448:248-54; PMID:24792179; http://dx.doi.org/10.1016/j.bbrc.2014.04.117

[38] Zhang L, Wu Z, Ma Z, Liu H, Wu Y, Zhang Q. WWP1 as a potential tumor oncogene regulates PTEN-Akt signaling pathway in human gastric carcinoma. Tumour Biol 2015; 36:787-98; PMID:25293520; http://dx.doi.org/10.1007/s13277-014-2696-0

[39] Chen C, Zhou Z, Ross JS, Zhou W, Dong JT. The amplified WWP1 gene is a potential molecular target in breast cancer. Int J Cancer 2007; 121:80-7; PMID:17330240; http://dx.doi.org/10.1002/ijc.22653

[40] Chen C, Zhou Z, Sheehan CE, Slodkowska E, Sheehan CB, Boguniewicz A, Ross JS. Overexpression of WWP1 is associated with the estrogen receptor and insulin-like growth factor receptor 1 in breast carcinoma. Int J Cancer 2009; 124:2829-36; PMID:19267401; http://dx.doi.org/10.1002/ijc.24266

[41] Zhou Z, Liu R, Chen C. The WWP1 ubiquitin E3 ligase increases TRAIL resistance in breast cancer. Int J Cancer 2012; 130:1504-10; PMID:21480222; http://dx.doi.org/10.1002/ijc.26122

[42] Chen C, Sun X, Guo P, Dong XY, Sethi P, Zhou W, Zhou Z, Petros J, Frierson HF, Jr., Vessella RL, et al. Ubiquitin E3 ligase WWP1 as an oncogenic factor in human prostate cancer. Oncogene 2007; 26:2386-94; PMID:17016436; http://dx.doi.org/10.1038/sj.onc.1210021

[43] Maher ER, Neumann HP, Richard S. von Hippel-Lindau disease: a clinical and scientific review. Eur J Hum Genet 2011; 19:617-23; PMID:21386872; http://dx.doi.org/10.1038/ejhg.2010.175

[44] Feng C, Sun Y, Ding G, Wu Z, Jiang H, Wang L, Ding Q, Wen H. PI3Kbeta inhibitor TGX221 selectively inhibits renal cell carcinoma cells with both VHL and SETD2 mutations and links multiple pathways. Scientific reports 2015; 5:9465; PMID:25853938; http://dx.doi.org/10.1038/srep09465

[45] Rechsteiner MP, von Teichman A, Nowicka A, Sulser T, Schraml P, Moch H. VHL gene mutations and their effects on hypoxia inducible factor HIFalpha: identification of potential driver and passenger mutations. Cancer Res 2011; 71:5500-11; PMID:21715564; http://dx.doi.org/10.1158/0008-5472.CAN-11-0757

[46] Makishima H, Cazzolli H, Szpurka H, Dunbar A, Tiu R, Huh J, Muramatsu H, O'Keefe C, Hsi E, Paquette RL, et al. Mutations of e3 ubiquitin ligase cbl family members constitute a novel common pathogenic lesion in myeloid malignancies. J Clin Oncol 2009; 27:6109-16; PMID:19901108; http://dx.doi.org/10.1200/JCO.2009.23.7503

[47] Muramatsu H, Makishima H, Jankowska AM, Cazzolli H, O'Keefe C, Yoshida N, Xu Y, Nishio N, Hama A, Yagasaki H, et al. Mutations of an E3 ubiquitin ligase c-Cbl but not TET2 mutations are pathogenic in juvenile myelomonocytic leukemia. Blood 2010; 115:1969-75; PMID:20008299; http://dx.doi.org/10.1182/blood-2009-06-226340

[48] Grand FH, Hidalgo-Curtis CE, Ernst T, Zoi K, Zoi C, McGuire C, Kreil S, Jones A, Score J, Metzgeroth G, et al. Frequent CBL mutations associated with 11q acquired uniparental disomy in myeloproliferative neoplasms. Blood 2009; 113:6182-92; PMID:19387008; http://dx.doi.org/10.1182/blood-2008-12-194548

[49] Loh ML, Sakai DS, Flotho C, Kang M, Fliegauf M, Archambeault S, Mullighan CG, Chen L, Bergstraesser E, Bueso-Ramos CE, et al. Mutations in CBL occur frequently in juvenile myelomonocytic leukemia. Blood 2009; 114:1859-63; PMID:19571318; http://dx.doi.org/10.1182/blood-2009-01-198416

[50] Sargin B, Choudhary C, Crosetto N, Schmidt MH, Grundler R, Rensinghoff M, Thiessen C, Tickenbrock L, Schwable J, Brandts C, et al. Flt3-dependent transformation by inactivating c-Cbl mutations in AML. Blood 2007; 110:1004-12; PMID:17446348; http://dx.doi.org/10.1182/blood-2007-01-066076

[51] Kassenbrock CK, Anderson SM. Regulation of ubiquitin protein ligase activity in c-Cbl by phosphorylation-induced conformational change and constitutive activation by tyrosine to glutamate point mutations. J Biol Chem 2004; 279:28017-27; PMID:15117950; http://dx.doi.org/10.1074/jbc.M404114200

[52] Yang Y, Schmitz R, Mitala J, Whiting A, Xiao W, Ceribelli M, Wright GW, Zhao H, Yang Y, Xu W, et al. Essential role of the linear ubiquitin chain assembly complex in lymphoma revealed by rare germline polymorphisms. Cancer Dis 2014; 4:480-93; PMID:24491438; http://dx.doi.org/10.1158/2159-8290.CD-13-0915

[53] Yuan L, Lu L, Yang Y, Sun H, Chen X, Huang Y, Wang X, Zou L, Bao L. Genetic mutational profiling analysis of T cell acute lymphoblastic leukemia reveal mutant FBXW7 as a prognostic indicator for inferior survival. Ann Hematol 2015; 94:1817-28; PMID:26341754; http://dx.doi.org/10.1007/s00277-015-2474-0

[54] Cancer Genome Atlas Research N. Comprehensive molecular characterization of urothelial bladder carcinoma. Nature 2014; 507:315-22; PMID:24476821; http://dx.doi.org/10.1038/nature12965

[55] Seshagiri S, Stawiski EW, Durinck S, Modrusan Z, Storm EE, Conboy CB, Chaudhuri S, Guan Y, Janakiraman V, Jaiswal BS, et al. Recurrent R-spondin fusions in colon cancer. Nature 2012; 488:660-4; PMID:22895193; http://dx.doi.org/10.1038/nature11282

[56] Jones S, Stransky N, McCord CL, Cerami E, Lagowski J, Kelly D, Angiuoli SV, Sausen M, Kann L, Shukla M, et al. Genomic analyses of gynaecologic carcinosarcomas reveal frequent mutations in chromatin remodelling genes. Nat Commun 2014; 5:5006; PMID:25233892; http://dx.doi.org/10.1038/ncomms6006

[57] Muller E, Brault B, Holmes A, Legros A, Jeannot E, Campitelli M, Rousselin A, Goardon N, Frebourg T, Krieger S, et al. Genetic profiles of cervical tumors by high-throughput sequencing for personalized medical care. Cancer Med 2015; 4:1484-93; PMID:26155992; http://dx.doi.org/10.1002/cam4.492

[58] Aydin IT, Melamed RD, Adams SJ, Castillo-Martin M, Demir A, Bryk D, Brunner G, Cordon-Cardo C, Osman I, Rabadan R, et al. FBXW7 mutations in melanoma and a new therapeutic paradigm. J Natl Cancer Inst 2014; 106:dju107; PMID:24838835; http://dx.doi.org/10.1093/jnci/dju107

[59] Sato M, Rodriguez-Barrueco R, Yu J, Do C, Silva JM, Gautier J. MYC is a critical target of FBXW7. Oncotarget 2015; 6:3292-305; PMID:25669969; http://dx.doi.org/10.18632/oncotarget.3203

[60] Fujii Y, Yada M, Nishiyama M, Kamura T, Takahashi H, Tsunematsu R, Susaki E, Nakagawa T, Matsumoto A, Nakayama KI. Fbxw7 contributes to tumor suppression by targeting multiple proteins for ubiquitin-dependent degradation. Cancer Sci 2006; 97:729-36; PMID:16863506; http://dx.doi.org/10.1111/j.1349-7006.2006.00239.x

[61] Richards MW, Burgess SG, Poon E, Carstensen A, Eilers M, Chesler L, Bayliss R. Structural basis of N-Myc binding by Aurora-A and its destabilization by kinase inhibitors. Proc Natl Acad Sci U S A 2016; 113:13726-31; PMID:27837025; http://dx.doi.org/10.1073/pnas.1610626113

[62] Jardim DL, Wheler JJ, Hess K, Tsimberidou AM, Zinner R, Janku F, Subbiah V, Naing A, Piha-Paul SA, Westin SN, et al. FBXW7 mutations in patients with advanced cancers: clinical and molecular characteristics and outcomes with mTOR inhibitors. PLoS One 2014; 9:e89388; PMID:24586741; http://dx.doi.org/10.1371/journal.pone.0089388

[63] Villaruz LC, Socinski MA. Temsirolimus therapy in a patient with lung adenocarcinoma harboring an FBXW7 mutation. Lung cancer (Amsterdam, Netherlands) 2014; 83:300-1; PMID:24360397; http://dx.doi.org/10.1016/j.lungcan.2013.11.018

[64] Morrison BJ, Morris JC, Steel JC. Lung cancer-initiating cells: a novel target for cancer therapy. Target Oncol 2013; 8:159-72; PMID:23314952; http://dx.doi.org/10.1007/s11523-012-0247-4

[65] Khammanivong A, Gopalakrishnan R, Dickerson EB. SMURF1 silencing diminishes a CD44-high cancer stem cell-like population in head and neck squamous cell carcinoma. Mol Cancer 2014; 13:260; PMID:25471937; http://dx.doi.org/10.1186/1476-4598-13-260

[66] Wang J, Huang Y, Guan Z, Zhang JL, Su HK, Zhang W, Yue CF, Yan M, Guan S, Liu QQ. E3-ligase Skp2 predicts poor prognosis and maintains cancer stem cell pool in nasopharyngeal carcinoma. Oncotarget 2014; 5:5591-601; PMID:25015320; http://dx.doi.org/10.18632/oncotarget.2149

[67] Chan CH, Morrow JK, Li CF, Gao Y, Jin G, Moten A, Stagg LJ, Ladbury JE, Cai Z, Xu D, et al. Pharmacological inactivation of Skp2 SCF ubiquitin ligase restricts cancer stem cell traits and cancer progression. Cell 2013; 154:556-68; PMID:23911321; http://dx.doi.org/10.1016/j.cell.2013.06.048

[68] Aki D, Zhang W, Liu YC. The E3 ligase Itch in immune regulation and beyond. Immunol Rev 2015; 266:6-26; PMID:26085204; http://dx.doi.org/10.1111/imr.12301

[69] Rossi M, Rotblat B, Ansell K, Amelio I, Caraglia M, Misso G, Bernassola F, Cavasotto CN, Knight RA, Ciechanover A, et al. High throughput screening for inhibitors of the HECT ubiquitin E3 ligase ITCH identifies antidepressant drugs as regulators of autophagy. Cell Death Dis 2014; 5:e1203; http://dx.doi.org/10.1038/cddis.2014.113

[70] Bongiorno-Borbone L, Giacobbe A, Compagnone M, Eramo A, De Maria R, Peschiaroli A, Melino G. Anti-tumoral effect of desmethylclomipramine in lung cancer stem cells. Oncotarget 2015; 6:16926-38; PMID:26219257; http://dx.doi.org/10.18632/oncotarget.4700

[71] Takeishi S, Nakayama KI. Role of Fbxw7 in the maintenance of normal stem cells and cancer-initiating cells. Br J Cancer 2014; 111:1054-9; PMID:24853181; http://dx.doi.org/10.1038/bjc.2014.259

[72] Wang Y, Liu Y, Lu J, Zhang P, Wang Y, Xu Y, Wang Z, Mao JH, Wei G. Rapamycin inhibits FBXW7 loss-induced epithelial-mesenchymal transition and cancer stem cell-like characteristics in colorectal cancer cells. Biochem Biophys Res Commun 2013; 434:352-6; PMID:23558291; http://dx.doi.org/10.1016/j.bbrc.2013.03.077

[73] Takeishi S, Matsumoto A, Onoyama I, Naka K, Hirao A, Nakayama KI. Ablation of Fbxw7 eliminates leukemia-initiating cells by preventing quiescence. Cancer Cell 2013; 23:347-61; PMID:23518349; http://dx.doi.org/10.1016/j.ccr.2013.01.026

[74] D'Arcy P, Wang X, Linder S. Deubiquitinase inhibition as a cancer therapeutic strategy. Pharmacol Ther 2015; 147:32-54; PMID:25444757; http://dx.doi.org/10.1016/j.pharmthera.2014.11.002

[75] Colland F, Formstecher E, Jacq X, Reverdy C, Planquette C, Conrath S, Trouplin V, Bianchi J, Aushev VN, Camonis J, et al. Small-molecule inhibitor of USP7/HAUSP ubiquitin protease stabilizes and activates p53 in cells. Mol Cancer Ther 2009; 8:2286-95; PMID:19671755; http://dx.doi.org/10.1158/1535-7163.MCT-09-0097

[76] Zhao GY, Lin ZW, Lu CL, Gu J, Yuan YF, Xu FK, Liu RH, Ge D, Ding JY. USP7 overexpression predicts a poor prognosis in lung squamous cell carcinoma and large cell carcinoma. Tumour Biol 2015; 36:1721-9; PMID:25519684; http://dx.doi.org/10.1007/s13277-014-2773-4

[77] Song MS, Salmena L, Carracedo A, Egia A, Lo-Coco F, Teruya-Feldstein J, Pandolfi PP. The deubiquitinylation and localization of PTEN are regulated by a HAUSP-PML network. Nature 2008; 455:813-7; PMID:18716620; http://dx.doi.org/10.1038/nature07290

[78] Rivlin N, Katz S, Doody M, Sheffer M, Horesh S, Molchadsky A, Koifman G, Shetzer Y, Goldfinger N, Rotter V, et al. Rescue of embryonic stem cells from cellular transformation by proteomic stabilization of mutant p53 and conversion into WT conformation. Proc Natl Acad Sci U S A 2014; 111:7006-11; PMID:24778235; http://dx.doi.org/10.1073/pnas.1320428111

[79] Zhang L, Zhou F, Drabsch Y, Gao R, Snaar-Jagalska BE, Mickanin C, Huang H, Sheppard KA, Porter JA, Lu CX, et al. USP4 is regulated by AKT phosphorylation and directly deubiquitylates TGF-beta type I receptor. Nat Cell Biol 2012; 14:717-26; PMID:22706160; http://dx.doi.org/10.1038/ncb2522

[80] Schwickart M, Huang X, Lill JR, Liu J, Ferrando R, French DM, Maecker H, O'Rourke K, Bazan F, Eastham-Anderson J, et al. Deubiquitinase USP9X stabilizes MCL1 and promotes tumour cell survival. Nature 2010; 463:103-7; PMID:20023629; http://dx.doi.org/10.1038/nature08646

[81] Kushwaha D, O'Leary C, Cron KR, Deraska P, Zhu K, D'Andrea AD, Kozono D. USP9X inhibition promotes radiation-induced apoptosis in non-small cell lung cancer cells expressing mid-to-high MCL1. Cancer Biol Ther 2015; 16:392-401; PMID:25692226; http://dx.doi.org/10.1080/15384047.2014.1002358

[82] Gu YY, Yang M, Zhao M, Luo Q, Yang L, Peng H, Wang J, Huang SK, Zheng ZX, Yuan XH, et al. The de-ubiquitinase UCHL1 promotes gastric cancer metastasis via the Akt and Erk1/2 pathways. Tumour Biol 2015; 36:8379-87; PMID:26018507; http://dx.doi.org/10.1007/s13277-015-3566-0

[83] Kim HJ, Kim YM, Lim S, Nam YK, Jeong J, Kim HJ, Lee KJ. Ubiquitin C-terminal hydrolase-L1 is a key regulator of tumor cell invasion and metastasis. Oncogene 2009; 28:117-27; PMID:18820707; http://dx.doi.org/10.1038/onc.2008.364

[84] Goto Y, Zeng L, Yeom CJ, Zhu Y, Morinibu A, Shinomiya K, Kobayashi M, Hirota K, Itasaka S, Yoshimura M, et al. UCHL1 provides diagnostic and antimetastatic strategies due to its deubiquitinating effect on HIF-1alpha. Nat Commun 2015; 6:6153; PMID:25615526; http://dx.doi.org/10.1038/ncomms7153

[85] Xiang T, Li L, Yin X, Yuan C, Tan C, Su X, Xiong L, Putti TC, Oberst M, Kelly K, et al. The ubiquitin peptidase UCHL1 induces G0/G1 cell cycle arrest and apoptosis through stabilizing p53 and is frequently silenced in breast cancer. PLoS One 2012; 7:e29783; PMID:22279545; http://dx.doi.org/10.1371/journal.pone.0029783

[86] Ummanni R, Jost E, Braig M, Lohmann F, Mundt F, Barett C, Schlomm T, Sauter G, Senff T, Bokemeyer C, et al. Ubiquitin carboxyl-terminal hydrolase 1 (UCHL1) is a potential tumour suppressor in prostate cancer and is frequently silenced by promoter methylation. Mol Cancer 2011; 10:129; PMID:21999842; http://dx.doi.org/10.1186/1476-4598-10-129

[87] Iglesias-Gato D, Chuan YC, Jiang N, Svensson C, Bao J, Paul I, Egevad L, Kessler BM, Wikstrom P, Niu Y, et al. OTUB1 de-ubiquitinating enzyme promotes prostate cancer cell invasion in vitro and tumorigenesis in vivo. Mol Cancer 2015; 14:8; PMID:25623341; http://dx.doi.org/10.1186/s12943-014-0280-2

[88] Zhou Y, Wu J, Fu X, Du W, Zhou L, Meng X, Yu H, Lin J, Ye W, Liu J, et al. OTUB1 promotes metastasis and serves as a marker of poor prognosis in colorectal cancer. Mol Cancer 2014; 13:258; PMID:25431208; http://dx.doi.org/10.1186/1476-4598-13-258

[89] Karunarathna U, Kongsema M, Zona S, Gong C, Cabrera E, Gomes AR, Man EP, Khongkow P, Tsang JW, Khoo US, et al. OTUB1 inhibits the ubiquitination and degradation of FOXM1 in breast cancer and epirubicin resistance. Oncogene 2016; 35:1433-44; PMID:26148240; http://dx.doi.org/10.1038/onc.2015.208

[90] Huang X, Dixit VM. Drugging the undruggables: exploring the ubiquitin system for drug development. Cell Res 2016; 26:484-98; PMID:27002218; http://dx.doi.org/10.1038/cr.2016.31

[91] Burgess A, Chia KM, Haupt S, Thomas D, Haupt Y, Lim E. Clinical Overview of MDM2/X-Targeted Therapies. Front Oncol 2016; 6:7; PMID:26858935; http://dx.doi.org/10.3389/fonc.2016.00007

[92] Cancer Genome Atlas N. Comprehensive molecular characterization of human colon and rectal cancer. Nature 2012; 487:330-7; PMID:22810696; http://dx.doi.org/10.1038/nature11252

[93] Cancer Genome Atlas Research N. Comprehensive molecular characterization of gastric adenocarcinoma. Nature 2014; 513:202-9; PMID:25079317; http://dx.doi.org/10.1038/nature13480

[94] Cancer Genome Atlas Research N, Kandoth C, Schultz N, Cherniack AD, Akbani R, Liu Y, Shen H, Robertson AG, Pashtan I, Shen R, et al. Integrated genomic characterization of endometrial carcinoma. Nature 2013; 497:67-73; PMID:23636398; http://dx.doi.org/10.1038/nature12113

[95] Campbell JD, Alexandrov A, Kim J, Wala J, Berger AH, Pedamallu CS, Shukla SA, Guo G, Brooks AN, Murray BA, et al. Distinct patterns of somatic genome alterations in lung adenocarcinomas and squamous cell carcinomas. Nat Genet 2016; 48:607-16; PMID:27158780; http://dx.doi.org/10.1038/ng.3564

[96] Stephens PJ, Tarpey PS, Davies H, Van Loo P, Greenman C, Wedge DC, Nik-Zainal S, Martin S, Varela I, Bignell GR, et al. The landscape of cancer genes and mutational processes in breast cancer. Nature 2012; 486:400-4; PMID:22722201

ACKNOWLEDGEMENTS

Chapter 1, in full, is a reprint of the review article as it appears in Cell Cycle. Gallo LH, Ko J, Donoghue DJ. The importance of regulatory ubiquitination in cancer and metastasis. Cell Cycle. 2017;16(7):634–648. doi:10.1080/15384101.2017.1288326. The dissertation author was a co-author of this review but did not perform the research described by the review. The dissertation author was responsible for the following specific subsections of this review in its entirety; E3 ubiquitin ligases in pluripotent cancer stem cells, SMURF1 in head and neck cancer stem cells, Skp2 in nasopharyngeal and prostate cancer stem cells, ITCH in lung cancer stem cells, FBXW7 in colonic and leukemia cancer stem cell maintenance, The misregulated expression of DUBs in metastatic cancers, USP7 promotes APL, aggressive prostate cancer, and NSCLC metastasis, USP4 and USP9X support oncogenic signaling in various tumors, UCH-L1 plays a contradicting role in different tumors, OTUB1 contributes to drug resistance and promotes metastasis. The dissertation author also assisted with other figures, tables, and other sections as well. Co-authors include Leandro H Gallo and Daniel J Donoghue.

Chapter 2

Characterization of FGFR Signaling in Prostate Cancer Stem Cells and Inhibition via TKI treatment

ABSTRACT

Metastatic castrate-resistant prostate cancer remains uncurable and novel therapies are needed to better treat patients. Aberrant fibroblast growth factor receptor (FGFR) signaling has been implicated in advanced prostate cancer, and FGFR1 is suggested to be a promising therapeutic target along with the current androgen deprivation therapy. Three-dimensional (3D) spheroids of frequently studied prostate cancer cell lines, PC3, DU145 and LNCaP were examined to select for prostate cancer stem cells (CSCs), establishing a novel *in vitro* model to study endogenous FGFR signaling. FGFR inhibition using three different TKIs, Dovitinib, BGJ398, and PD166866 in 3D spheroids of PC3, DU145 and LNCaP, and induced pluripotent stem (iPS) 87 cells resulted in the decrease of cell survival and proliferation of these spheroids. Especially, the prostate CSCs in PC3 cell line were shown to have increased metastatic potential as EMT markers were examined, and TKIs targeting FGFR1 was shown to decrease the mesenchymal markers. As prostate cancer is overwhelmingly heterogeneous, this study enhances our understanding of FGFR signaling and its inhibition in prostate cancer at a molecular level through the comparison of AR-positive and AR-negative cell lines, and of the bulk population and CSCs, and of common cell lines and a novel iPSC-derived cell line. Collectively, the findings provided here may assist in screening for suitable subgroups of prostate cancer patients and improving their treatment options.

INTRODUCTION

Prostate cancer statistics

Prostate cancer is the second most common cancer among men in the United States according to the American Cancer Society (1). Worldwide, it is the second most common, and the most frequently diagnosed cancer among men in 105 countries. In terms of mortality, prostate cancer is the second leading cause of cancer deaths among men in the Unites States and fifth leading cause worldwide, being the leading cause of cancer death among men in 46 countries (2). The 5-year survival rate for non-metastatic prostate cancer (stages I- III) patients is about 99%, however, for metastatic prostate cancer (stage IV) patients, the rate drops to about 30% (1).

The prostate is a part of the male reproductive system located under the bladder, producing prostate fluid that is added to semen. It is a walnut-sized gland surrounded by a capsule of connective tissue and is composed of epithelial acini arranged in a fibromuscular stromal network including smooth muscle cells, fibroblasts, and endothelial cells and neurons. The gland cells consist of luminal cells, basal cells, and neuroendocrine cells surrounded by the basement membrane (3). About 95% of all prostate cancers arise from these gland cells, which is called an adenocarcinoma. Depending on clinical and pathological characteristics, subtypes of the adenocarcinoma are further distinguished. Apart from the gland cells, smooth muscle cells surrounding the epithelial acini can give rise to prostate cancer, which is called a sarcoma, although it is very rare (4).

Luminal cells produce prostate-specific antigen called PSA, and small amounts of PSA ordinarily circulate in the blood. However, when serum PSA levels increase to over 4.0 ng/ml, it

can indicate abnormal activity of the luminal cells such as infection, inflammation, or prostate cancer. PSA tests and digital rectal exams are useful tools utilized by doctors to determine the further need of needle biopsy to diagnose prostate cancer (5).

In the progression of prostate cancer, normal cells start displaying abnormalities, and lead to prostatic intraepithelial neoplasia (PIN). PIN is a precursor of prostatic carcinoma and it features luminal cell over-growth and a reduction in the number of basal cells. PIN lesions progress to invasive adenocarcinoma displaying a more luminal phenotype with loss of the basal cell layer and basement membrane (6, 7). In the development of advanced prostate cancer with varying tumor grades, genetic changes such as phosphatase and tensin homolog (PTEN) loss or mutation take place in addition to androgen signaling dysregulation, which promotes progression of prostate cancer (8, 9, 10). In a molecular level, loss of PTEN leads to overactivation of Akt signaling which increases tumor cell survival and proliferation promotes chemotherapy and radiation resistance (11). Other tumor suppressor genes, TP53, and RB1 are also frequently altered in prostate cancer patients, and in fact, DNA and RNA sequencing of clinically obtained biopsies of mCRPC tumors revealed 53.3% of TP53, 40.7% of PTEN, and 9.3% of RB1 to show genetic alterations mostly copy losses (12). Unfortunately, the cooperative loss of PTEN, TP53, and RB1 is associated with increased risk of relapse and death in prostate cancer patients (13).

Androgen signaling and androgen deprivation therapy

Androgens are male sex hormones produced primarily by the testes, which are required for the development of the male reproductive system, and play a role in metabolic homeostasis (14). Testosterone is a type of androgen and upon entering prostate cells, is converted to dihydrotestosterone (DHT) mediated by 5α-reductase enzymes in an irreversible manner (15).

Both testosterone and DHT can bind to androgen receptor (AR), which consists of a poorly conserved N-terminal domain, a highly conserved deoxyribonucleic acid (DNA)-binding domain (DBD) and a moderately conserved ligand-binding domain (LBD) (10). Upon androgen ligands binding to AR, it dimerizes and becomes phosphorylated and is translocated to the nucleus. Modulated by cofactors, AR binds to chromosomal DNA and activates target gene expression (16).

AR is found to be highly expressed in the majority of cases of castration resistant prostate cancer (CRPC) patients which has made the AR pathway a main target in androgen deprivation therapy (ADT) for advanced prostate cancer patients. The understanding that androgen deprivation is an effective treatment for prostate cancer was first demonstrated in 1941 (17). In 2012, A second-generation AR inhibitor, Enzalutamide, was approved by the U.S. Food and Drug Administration (FDA), for improving the survival of CRPC patients by about 4.8 months compared to placebo group, which was considered a great advancement (18). Enzalutamide is a competitive binder of androgens, it prevents the translocation of the AR to the nucleus, and within the nucleus, it inhibits AR binding to DNA, which impedes further transcription of tumor genes (19).

Another potent AR inhibitor, Apalutamide, was approved by FDA in 2018. It showed significant clinical efficacy, increasing the metastasis-free survival by 24.3 months of CRPC patients (20). AR inhibitors can be combined with an inhibitor of cytochrome P450 17α−hydroxy/17,20-lyase (CYP17) enzymes, abiraterone acetate, that suppresses androgen biosynthesis for more effective treatment (21).

Although ADT is effective at initial stage for “hormone naïve” prostate cancer, androgen-independent tumor cells eventually emerge as they adapt to the limited availability of

androgen. To compensate, tumor cells up-regulate androgen synthesis, or overexpress ARs, or make AR mutants or splicing variants with increased functional activity such as AR-V7 that lacks the LBD and can be activated in a ligand-independent manner (22). Total androgen inhibition can give rise to more aggressive AR-negative prostate cancer and most of the patients relapse and develop mCRPC, which is "hormone refractory", emphasizing the importance of finding new therapeutic strategies (23, 24). Even in the castration-resistant state, current therapies rely on AR antagonists, but increasing efforts are being made to explore both AR pathway and non-AR pathways to intervene in the progression of CRPC (23, 24).

Growth factors and their receptors in prostate cancer

There have been numerous studies investigating the role of growth factors such as fibroblast growth factors (FGFs), vascular endothelial growth factors (VEGFs), and insulin-like growth factors (IGFs) and their receptors in promoting benign prostatic hyperplasia and prostate cancer. Results of these studies utilizing various prostate cancer cell lines and xenografts were extensively reviewed by Joy L. Ware in 1993 (25).

Recent studies have found the involvement of FGFR in promoting prostate cancer. Of note, Armstrong *et al.* (26) reported that FGFR1 is upregulated in CRPC patient samples and is associated with higher risk of relapse and poor patient survival. Sahadevan *et al.* (27) reported that FGFR1 and FGFR4 were overexpressed in prostate cancer patient samples and that inhibition of FGFR4 via siRNA knockdown decreased cell proliferation and invasion in DU145 cells which are one of the most frequently studied prostate cancer lines. Acevedo *et al*. (28) reported that it is the activation of FGFR1 that drives prostate cancer progression and epithelial-

to-mesenchymal transition (EMT) using a mouse model, emphasizing the role of FGFR1 in prostate cancer.

In addition, a study conducted by MD Anderson Cancer Center in 2014 (29) reported that FGFR1 was upregulated in clinical prostate tumor samples via RNA sequencing. They found that treatment with Dovitinib, an inhibitor targeting FGFR and other receptors, showed a promising antitumor effect depending on FGFR1 expression in their clinical study and mouse models. They concluded that Dovitinib showed its antitumor effect by targeting the tumor microenvironment, which is the interaction between the prostate cancer cells and the osteoblasts mediated by FGFR signaling. Dovitinib was also found to show its anti-tumor effect by reducing angiogenesis.

Activation of FGFR and its downstream signaling cascade

FGFRs are a part of the receptor tyrosine kinase (RTK) family that are essential in many biological responses. Humans have 58 RTKs, which are grouped into twenty subfamilies. All RTKs have similar overall structure with a ligand-binding extracellular domain, transmembrane helix, and a cytoplasmic region that contains the tyrosine kinase domain (30).

FGF/FGFR signaling pathways includes eighteen secreted FGFs that are categorized into six subfamilies and four FGF receptors (FGFR1-4). The secreted FGFs along with heparin sulfate proteoglycans bind to immunoglobulin-like domains II and III, and the linker region between these domains of FGFRs, displaying different ligand binding specificity. (31).

FGF ligand binding to the FGFRs triggers receptor dimerization and trans-autophosphorylation of tyrosine residues in the kinase domain. The kinase domain includes an activation loop, masked by tyrosine residues, and phosphorylation of specific tyrosine residues in multiple steps within the activation loop induces a conformation change, disrupting this

autoinhibitory state. The activation of receptors triggers the signaling outcome of four major downstream signaling pathways of JAK/STAT, Ras/MAPK, PI3K/AKT, and PLC-γ, (32).

The signal transducer and activator of transcription (STAT) proteins are components of signal-dependent transcription-factor pathways that are often activated by the JAK family and dimerize and translocate to the nucleus. Then the STATs bind to DNA, recruit coactivators, and induce target gene transcription. Among the STATs, STAT3 is the most over-activated in cancer cells, followed by STAT5. STAT3 regulates many biological functions such as cell survival, apoptosis, and wound healing, and STAT5 is involved in hematopoiesis and immune regulation (33).

The RAS-mitogen activated protein kinase (MAPK) pathway comprises several key signaling components of RAS-RAF-MEK-ERK-MAPK, and regulate cell growth, differentiation, proliferation, apoptosis and migration functions (34). In advanced prostate cancer, upregulation of MAPK expression was reported to correlate with poor survival and relapse (35).

Phosphatidylinositol-3 kinases (PI3Ks) constitute a lipid kinase family. Once growth factor receptors are activated, PI3K is recruited to the membrane or to adaptors, and phosphorylate phosphatidylinositol-4,5-bisphosphate (PIP2) to phosphatidylinositol-3,4,5-trisphosphate (PIP3). PIP3 leads to the activation of Akt, a serine/threonine kinase, which then mediates various cellular process including cellular survival, inhibition of apoptosis, growth and proliferation. PTEN is a phosphatase, negatively regulating Akt activation through PIP3 dephosphorylation (36). The PI3K/Akt pathway is frequently dysregulated in various cancers through deletion and mutation of *PTEN* gene or overexpression and overactivation of Akt, and it

is suggested to be responsible for chemotherapy and radiation resistance and tumor invasion and metastasis (36, 37).

Phospholipase Cγ (PLCγ) is an enzyme in phosphoinositide metabolism, hydrolyzing PIP2, which modulates functions such as cytoskeletal reorganization, cytokinesis, and membrane dynamics. PLCγ is associated with tumor cell invasion including in prostate cancer (38).

Aberrant FGFR signaling has been implicated in numerous developmental diseases and various solid cancers and hematological malignancies through receptor mutations and overexpression, chromosomal translocation, or FGF overexpression, impacting downstream signaling which regulates various biological functions. (31, 32). FGFR has emerged as a promising target in lung cancer, breast cancer and prostate cancer (40, 41, 42). As mentioned earlier, FGFR1 overexpression was reported in prostate cancer patient samples, and efforts have been made to target FGFR signaling, utilizing small molecule inhibitors (29).

Small molecule inhibitors of tyrosine kinases

Small-molecule tyrosine kinase inhibitors can be grouped into ATP-site inhibitors, as all kinases have a conserved activation loop or non-ATP competitive allosteric inhibitors with more selectivity. The ATP-site inhibitors can be further divided into type I and type II depending on the structure of the inhibitor-target complex. Type I inhibitors bind to the active conformation of the target, referred to as DFG-in conformation, the phenylalanine of the DFG motif creating a hydrophobic interaction. On the other hand, Type II inhibitors bind to the inactive conformation, referred to as DFG-out conformation with disrupted hydrophobic pocket, and hinder the conformation required for the transfer of ATP phosphate (43).

Dovitinib and BGJ398 are both Type I inhibitors, and their target include FGFRs with different selectivity and potency, and have been utilized in clinical trials and shown promising antitumor activity in cancer treatment. Dovitinib is a multi-kinase inhibitor of the benzimidalzole-quinolinone class found through chemical library screening and first designed and synthesized in 2005 **(Figure 2.1)**. The crystal structure of Dovitinib bound to FGFR1 is shown in **Figure 2.2** (44). Dovitinib shows an inhibitory effect on a variety of RTKs including FGFRs VEGFRs, and Platelet-derived Growth Factor Receptors (PDGFRs) (44, 45). These multi-TKIs such as Dovitinib can have beneficial effects through targeting multiple RTKs involved in tumorigenesis, however, they can also lead to high toxicity and various off-target effects. To reduce these adverse effects, efforts have been made to develop FGFR-selective inhibitors such as BGJ398, exhibiting high selectivity towards FGFR1-3 with nanomolar potency (45) **(Figure 2.3)**. The crystal structure of BGJ398 bound to FGFR1 is shown in **Figure 2.4** (45).

Another FGFR inhibitor, PD166866, was compared to Dovitinib and BGJ398 in this study to show improved potency and advancement of new generation TKI inhibitors. PD166866 was developed through screening a compound library in 1998, displaying nanomolar potency in cell free assays with significantly higher activity than other tyrosine kinase inhibitor molecules available at the time (46) **(Figure 2.5)**.

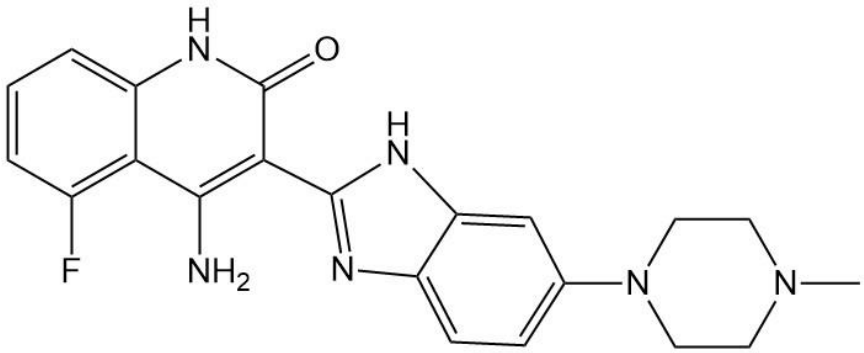

Figure 2.1. The structure of Dovitinib.
4-Amino-5-fluoro-3-[5-(4-methylpiperazin-1-yl)-1H-benzimidazol-2-yl]quinolin-2(1H)-one

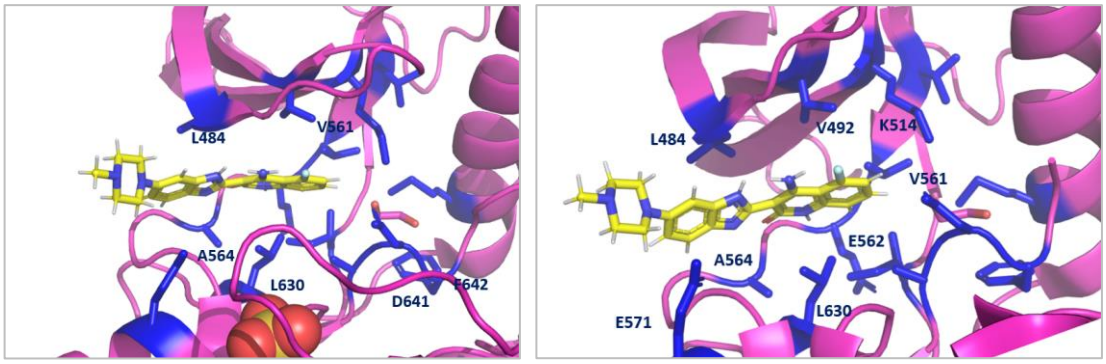

Figure 2.2. The crystal structure of the FGFR1 kinase domain in complex with Dovitinib (PDB code: 5A46).
(1H-benzimidazol-2-yl)quinolin-2(1H)-one moiety of Dovitinib is shown to occupy the ATP binding pocket of FGFR1 through hydrophobic contacts with L484, V492, I545 (residue not shown) A563, V561 and L630, in DFG- in conformation and hydrogen bonds (E562 and A564) with the hinge region between the two lobes of FGFR1.

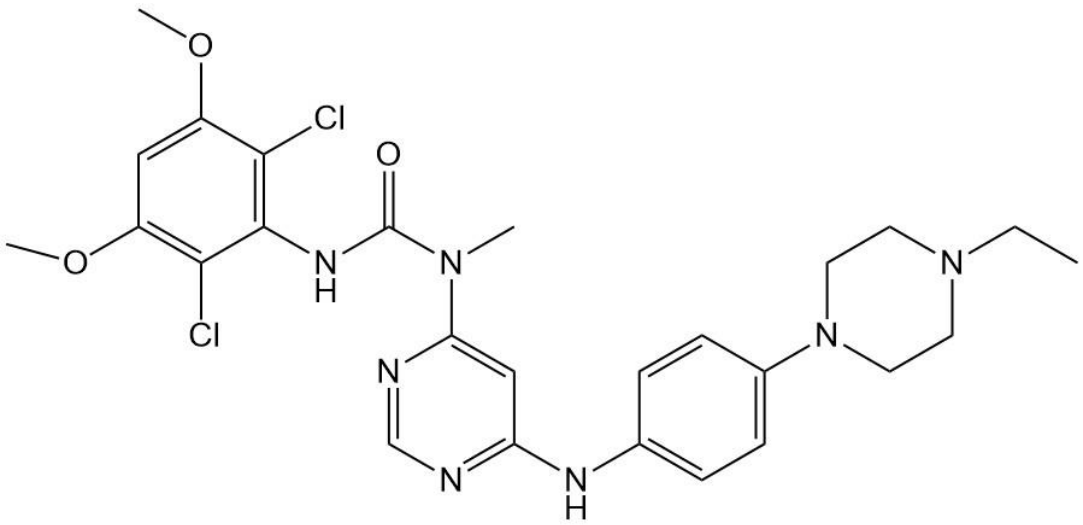

Figure 2.3. The structure of BGJ398.
3-(2,6-dichloro-3,5-dimethoxy-phenyl)-1-{6-[4-(4-ethyl-piperazin-1-yl)-phenylamino]-pyrimidin-4-yl}-1-methyl-urea.

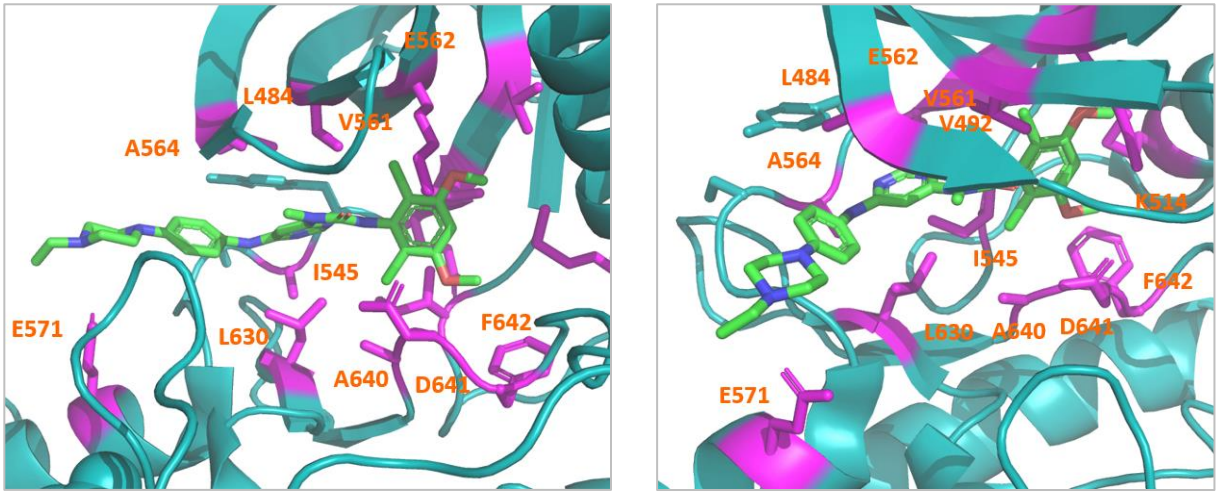

Figure 2.4. The crystal structure of the FGFR1 kinase domain in complex with BGJ398 (PDB code: 3TT0).

The dichloro-dimethoxy phenyl moiety of the BGJ398 compound (shown in green) fits the ATP binding site in a rigid manner in the perpendicular orientation, conferring specific interaction with FGFR1-3 over other kinases such as VEGFRs. The BGJ398 inhibitor makes hydrophobic contacts with L484, A512, I545, V561, Y563 and L630 of FGFR1 as shown.

Additionally, the pyrimidine nitrogen and the adjacent NH of the BGJ398 form multiple hydrogen bonds with A564 located in the hinge region of the ATP site and the urea carbonyl group forms a water-mediated hydrogen bond to K514 in the back pocket. Furthermore, the 4-(4-Ethylpiperazin-1-yl) aniline moiety of the compound forms hydrogen bonds with A564 and E571 in the hinge region as well as displays hydrophobic interactions with L478 and G561 (residues not shown).

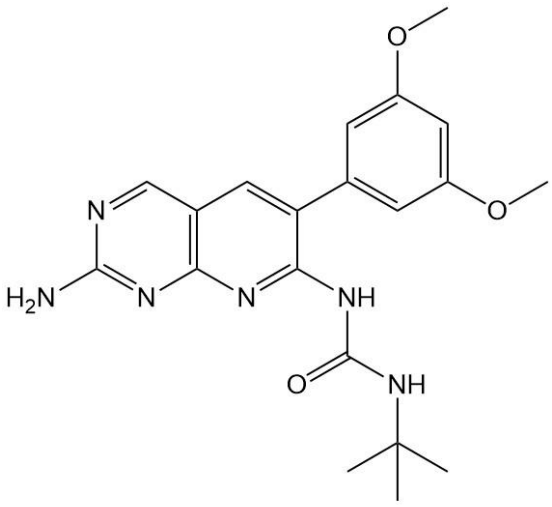

Figure 2.5. The structure of PD166866.

N-[2-amino-6-(3,5-dimethoxyphenyl)pyrido[2,3-d]pyrimidin-7-yl]-N'-(1,1-dimethylethyl)-urea.

Treatment effect of Dovitinib targeting bone microenvironment

Dovitinib primarily targets fms-like tyrosine kinase 3 (FLT3), Proto-Oncogene Receptor Tyrosine Kinase (c-KIT), FGFR1, FGFR3, vascular endothelial growth factor receptor (VEGFR)1, VEGFR2, VEGFR3, and PDGFRs (44). As mentioned earlier, a study conducted by MD Anderson Cancer Center in 2014 (29) utilized Dovitinib in their clinical study of prostate cancer, showing its promising antitumor effect by targeting the bone microenvironment.

Prostate cancer metastasis is commonly found in bone by metastasizing through lymph or blood vessels. Bone is a type of connective tissue, which constantly undergoes remodeling of bone deposition and resorption by osteoblasts and osteoclasts, respectively. During the remodeling process, various growth factors, cytokines and chemokines are released from the bone matrix that can be exploited by tumor cells. Interactions of normal cells of the bone and the prostate cancer cells establish a positive feedback loop to favor tumor growth in bone as well as to boost the activity of osteoblast cells, resulting in excess of bone deposition. The disrupted homeostasis by the metastases of prostate cancer causes severe bone pain and fractures to patients. Currently, the only treatment option is to slow down the formation of bone lesions (29, 47). Additionally, prostate tumor cells in bone promote angiogenesis, a formation of new blood vessels by vascular endothelial cells. Angiogenesis occurs during normal development process such as wound healing, however, tumor cells take advantage of the process to get access to nutrients and oxygen, an essential process for tumor cell growth. Angiogenic activators such as VEGF, FGF, and PDGF are secreted from the tumor cells to attract endothelial cells (48, 49).

Wan *et al.* (29) reported that Dovitinib treatment reduced tumor burden in bone both in mouse models and in patients and reduced angiogenesis. Interestingly, they have only observed these antitumor effects with FGFR1-overexpressing models, concluding that the interaction of

prostate tumor cells and the osteoblasts are mediated by FGFR signaling and in part reducing angiogenesis through the suppression of VEGFR signaling.

Cancer metastasis

Cancer-related deaths are mostly due to cancer metastasis. However, metastasis is a rare and challenging process for tumor cells (49). For tumor cells to migrate to a distant location, first they need to be detached from their environment, which means a decrease in cell to cell adhesion. This process is often explained through the epithelial-mesenchymal transition (EMT) model (50). EMT is a biological process that occurs both in normal cells for organ development and maturation of immune system and in tumor cells prior to cancer metastasis (50, 51). It is believed that cancer cells utilize EMT mechanism to migrate to secondary sites, which allows tumor cells to be detached from their primary tumor. The cells undergoing EMT display decreased epithelial marker of E-cadherin and increased mesenchymal markers such as N-cadherin, vimentin, fibronectin, β-catenin, and transcription factors of Snail, slug, zeb1, and twist (51).

Most tumor cells undergo detachment-induced cell death when they are detached from the primary tumor or the surrounding tissue. Only a small population of cells can survive the anchorage-independent condition. Anchorage-independence is considered a characteristic of more tumorigenic cells (52). These circulating tumor cells (CTCs) migrate through the endothelial barrier to enter the bloodstream either directly or via the lymphatic system. During tumor dissemination, only the CTCs that survive the immune surveillance can extravasate and repopulate, and findings on CTCs showing increased mesenchymal markers mediated by transforming growth factor (TGF)-β signaling (53).

Then the tumor cells undergo mesenchymal-epithelial transition (MET) to anchor themselves in the surrounding tissue to colonize at the new location (50, 53, 54). Tumor cells must promote angiogenesis for their proliferation and expansion to eventually form macrometastases which are clinically detectable (54). Additionally, signaling crosstalk between the tumor cells and the microenvironment is crucial. Accumulated findings show that different types of cancer develop metastasis in certain organs more frequently than others. For example, breast cancer and prostate cancer tend to metastasize to the bones, colorectal cancer to liver and lungs, and lung cancer to liver and adrenal glands (55, 56, 57, 58).

Cancer stem cells

Many studies suggest that cancer stem cells (CSCs) serve as the basis of metastases. CSCs are a small sub-population of cells in a bulk tumor. CSCs have self-renewal abilities, tumor-initiating capacity, abilities to survive the anchorage independent conditions, increased metastatic potential, exhibit chemoresistance, and contribute to tumor heterogenicity (59). CSCs are also called Tumor-Initiating Cells (TICs). In fact, the term TIC better depicts the nature of these cells as the cell of origin as well as the definition and identification of the CSCs are elusive and controversial (60, 61). In prostate cancer, many studies have reported the presence of prostate TICs or CSCs and their role in cancer progression and recurrence and therapeutic resistance (62).

Efforts have been made to identify and characterize CSCs although the CSC phenotype varies across types of tumor and even among cell lines from the same cancer type. For example, cells expressing cell surface markers of CD Molecules such as CD133, CD44, CD24, and CD166 can be isolated (63). Also, functionally, they have the ability to exclude Hoechst dye 33342 to be

identified as a side population in flow cytometry analysis (64). Similarly, they have increased levels of aldehyde dehydrogenase (ALDH) and among 19 isoforms of the ALDH family, ALDH1A1 is most frequently utilized, marking CSCs in lung, pancreatic and colon cancers and ALDH7A1 (65, 66) in prostate cancer.

Furthermore, CSCs can be characterized by their ability to generate spheroids (67, 68, 69). Studies have shown for solid cancers that colony-forming cells from solid tumors such as lung cancer, ovarian cancer or neuroblastoma are CSCs as they exhibit the anchorage independent growth, high clonogenicity and tumorigenicity (61).

Interestingly, FGFR expression has been associated with promoting stem cell-like properties in various cancer such as breast cancer (70), non-small cell lung cancer (71), and esophageal squamous cell carcinoma (72).

Relevance of 3D culture models in studies of cancer metastasis and cancer stem cells

Three-dimensional (3D) suspension culture systems are widely used to bridge the gap between traditional adherent 2D cultures and animal models by better recapitulating drug sensitivity and cell environment *in vivo* (73, 74, 75). Tumor spheroids growing to a diameter between 200 µm and 500 µm display a necrotic core as chemical gradients of oxygen and nutrients develop. The middle layer of the spheroid consists of quiescent cells, and the most outer layer of proliferating cells. Due to their 3D nature, spheroid cell clusters display preserved cell morphology, cell-to-cell interaction, and the cellular heterogenicity found in solid tumors. Drugs exerting their effect by generating reactive oxygen species cannot target the necrotic core effectively as little oxygen and nutrients can diffuse into the inner core. Additionally, chemotherapeutic agents designed to suppress proliferation do not have a great effect on the

slow-growing quiescent middle layer with an adapted metabolism. Moreover, 3D spheroids closely mimic the physical barriers found in real solid tumors, where chemotherapeutic agents cannot penetrate through the whole mass of cells. Thus, the spheroid cells mimic *in vivo* tumor physiology more effectively and are clinically more relevant in testing drug response and altered gene expression (73, 74, 75).

3D cultures do have limitations by lacking the dynamics of the surrounding extracellular matrix (ECM) and blood vessels that real tumors exploit for their expansion. So, patients-derived xenograft models are widely utilized in clinical studies, but the effect of treatments on animal models may not translate into successful outcomes for human patients. Growing efforts have been made to develop humanized microenvironments in xenograft models and to introduce vascularization by co-culturing cells and utilizing different scaffold and engineering tissues. For example, a group of investigators developed a protocol to engineer humanized bone in a murine host, which can shed light on the interactions between human cancer cells and human bone microenvironment *in vivo* (76).

Many researchers have utilized 3D culture methods such as hanging drop culture, microwells, Matrigel, poly 2-hydroxyethyl methacrylate (PolyHEMA)-coated dishes or special nonadherent conditions in serum-free medium to study various CSCs including prostate CSCs (77, 78). As mentioned earlier, CSCs are hypothesized to be associated with cancer metastasis, and possess the anchorage independent growth property to be studied in 3D cell culture models.

Studying prostate CSCs in 3D cell culture

In the study of prostate cancer, it is difficult to access to primary patient samples or metastases, thus, cell lines have been frequently utilized in pre-clinical settings. PC3, DU145 and

LNCaP are classic prostate cancer cell lines that have been the most commonly studied (79). The PC3 cell line was derived from a bone metastasis of prostatic adenocarcinoma origin and exhibits a poorly-differentiated adenocarcinoma (80), while the DU145 cell line was derived from a brain metastasis and possess less metastatic potential than the PC3 cell line (81). The LNCaP cell line was derived from a lymph node metastasis of prostatic adenocarcinoma and shows a response to androgens and low tumorigenicity unlike PC3 and DU145 cells. LNCaP cells have a mutated androgen receptor (T877A), which alters the binding specificity of its ligands (82).

The experimental models of prostate cancer are introduced in Table 2.1, and the advantages and disadvantages of each model is explained in Table 2.2.

Table 2.1. Experimental Models of Prostate Cancer.
The prostate cancer cell lines are shown with their first report year and their origin. The number of articles on Pubmed search engine is shown with the best estimate, and it is shown for the purpose of providing comparison of the most frequent usage of the three cells lines of DU145, PC3, and LNCaP. Their sublines were not included in the list.

Human PCa cell lines (2D culture)	Report Year	Origin	Number of articles on Pubmed	Reference
DU145	1975	Brain metastasis	5,378	(81)
PC3	1979	Bone metastasis	10,498	(80)
LNCaP	1980	Lymph node metastasis	8522	(79)
ARCaP	1996	Ascites fluid of a patient with advanced metastatic disease	56	(83)
MDA PCa 2a & MDA PCa 2b	1997	Bone metastasis	274	(84)
22Rv1	1999	CRPC derivative of CWR22 (primary tumor) xenograft	775	(85)

Table 3.1. Experimental Models of Prostate Cancer, continued.

VCaP (Vertebral-Cancer of the Prostate)	2001	Xenograft tumor from metastatic lesion to a lumbar vertebral body	330	(86)
KUCaP	2005	Xenograft tumor from liver metastasis	10	(87)
NCI-H660	2007	Metastatic site of an extrapulmonary small cell carcinoma arising from the prostate	21	(88)

3D culture (organoids)	Establishment	Characteristics	Reference
Patient tissue-derived organoids (PDOs)	▪ Generated from prostatectomy, metastasis and circulating tumor cells. ▪ First fully characterized organoid cell lines introduced in 2014.	▪ Reflect genetic mutations and diversity frequently observed in prostate cancer.	(89)
Stem cell (iPS)-derived organoids (iDOs)	▪ Co-culture of iPSCs with rodent urogenital sinus mesenchyme (an inductor of prostatic morphogenesis) in nude mice.	▪ First demonstration of iDOs to generate mature prostate structure.	(90)
Cell line spheroids	▪ Grown in non-adherent, serum-free conditions in suspension or in semisolid Matrigel.	▪ Different from organoids; free-floating instead of embedded in ECM, and lack the organization seen *in vivo*.	(91), (92), (77)

Table 4.1. Experimental Models of Prostate Cancer, continued.

Mouse models	Establishment	Characteristics	Reference
Xenograft models (immunodeficient)	▪ Generated by Cell line- or patient-derived engraftment. LNCaP, PC3, and DU145 are most commonly used. ▪ Subcutaneous, subrenal capsular, orthotopic transplantation.	▪ Human tumor surrounded by mice stroma.	(93)
Allograft models (immunocompetent)	▪ Derived from transgenic mouse models (i.e. 12T-10 transgenic prostate mouse model (2004, first reported prostate allograft model) , trp53-/-/Pten-/- transgenic mouse tumor)	▪ More accurate than xenografts; capable of modelling immune and micro-environmental changes.	(94), (95)
Genetically engineered mouse models (GEM)	▪ Generated by using viral oncogenes such as the SV 40 large T antigen Tag (i.e. TRAMP model, Lady model, p53 KO and mutations, pRB KO and mutations, PTEN KO, Nkx3.1 KO)	▪ Generated for studying gain- or loss-of-function of oncogenes, growth factor/receptors, and etc. ▪Better recapitulate genetic events occurring in human prostate cancer	(96), (97),

Table 2.2. Advantages and Disadvantages of Existing Prostate Cancer Models.
The comparison of advantages and disadvantages of 2D culture, 3D organoids, and mouse models are provided as below.

	2D culture (cell lines)	**3D culture (organoids)**	**Mouse models**	**References**
Advantages	▪ Capacity for unlimited growth ▪ Low cost ▪ Amenability to high throughput screening	▪ Harbor copy number signatures of primary prostate cancer (alterations commonly found in CRPC including *TP53*, *PIK3R1*, *FOXA1).* ▪ (iDOs) Unlimited source of iPSCs; Gene editing to introduce patient-specific mutations; Recapitulation of prostate tissue histology, including self-maintaining stromal compartment ▪ Retain features of the developmental stage ▪ Ex vivo testing of drug in a realistic time frame High throughput drug screening	▪ Able to maintain the histopathological characteristics and gene integrity of primary tumors from patients ▪ Human prostate tumors can be propagated *in vivo* for indefinite periods of time ▪ Intact endocrine system	(93), (98), (99), (100), (101)

Table 2.2. Advantages and Disadvantages of Existing Prostate Cancer Models, continued.

Disadvantages	▪ Lack cell-cell and cell-matrix interactions ▪ Genetic drift, lack of annotated clinical data ▪ Do not completely recapitulate the three-dimensional (3D) organization of cells and ECM within tissues and organs	▪ Low establishment rate, maintained for only 1–2 months with many cultures overtaken by normal epithelial cells present in the biopsy samples ▪ Lack of vascular system and immune influence	▪Discrepancy between the experimental and clinical outcomes due to differences in human and animal biology ▪ Engraftment and drug validation in mice usually requires >6 months ▪ Not amenable to high-throughput screening or genetic manipulation	(93), (98), (99), (100), (101)

Assay for cell survival and proliferation of prostate CSCs utilizing MTT

In analyzing the cell survival and proliferation, MTT (3-(4,5-dimethylthiazol-2-yl)-2,5-diphenyltetrazolium bromide) assay has been extensively adopted and utilized in cancer research since 1983 (103). This assay measures the solubilized purple colored formazan product with an absorbance maximum at 570 nm with a reference at 630nm using a spectrophotometer. Formazan is only produced by live cells with active mitochondrial activity involving NADH or similar reducing molecules that transfer electrons to MTT (**Figure 2.6**). The MTT assay provides a comparison of metabolically active cells to resting cells as the amount of formazan generated

from MTT is directly proportional to the number of cells in the range of 100 to 50,000 cells per well in a homogeneous cell population (104).

Furthermore, MTT assays are commonly utilized as cell viability assays. Assuming that cells have a similar level of mitochondrial activity within a homogeneous cell line or a primary cell type, the absorbance reading is proportional to the number of viable cells because only the live cells can reduce MTT to formazan. Different cell types possess varying metabolic activity, thus, for a comparison in a given cell line, the MTT assay allows researchers to compare the cell viability between samples. Linearity of viable cell number with absorbance readings extends the applications of the assay to be suitable for measuring cytotoxic effects of drugs that eventually lead to cell death (104, 105).

However, precautions need to be made when there are factors altering the metabolic ability in a given cell line. For example, it was reported that radiation exposed cells may have either hyperactive mitochondria or increased mitochondrial mass to show increased production of formazan so that the number of cells did not correspond to cell viability (106).

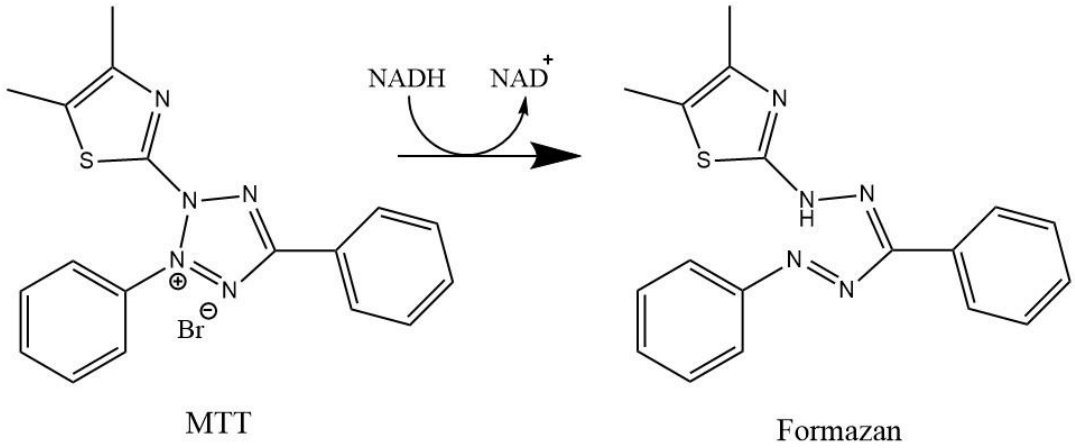

Figure 2.6. Reduction of MTT to Formazan.
The structure of MTT and Formazan is shown, and the best known reduction mechanism is indicated.

RESULTS

Expression of FGFRs and VEGFR2 in 2D monolayer cells of PC3, LNCaP and DU145

PC3, LNCaP and DU145 cells are the most commonly used cell lines in prostate cancer studies and they are derived from bone, lymph node, and brain metastases respectively. PC3 and DU145 are highly metastatic, and AR-negative, whereas LNCaP is less tumorigenic and AR-positive (107). Due to the heterogeneous nature of prostate cancer, we set out to investigate and characterize all three cells lines. Studies have indicated that fibroblast growth factor receptors (FGFRs) are associated with prostate cancer progression and metastasis and that targeting these receptors may serve as a potential therapeutic target alternative to androgen receptor (AR) signaling. In particular, Wan *et al.* (29) reported that FGFR1 was found highly expressed in primary tumors via RNA sequencing of patient samples and patient derived xenograft (PDX) models. Additionally, Sahadevan *et al.* (27) reported that significant overexpression of FGFR1 and FGFR4 was found in malignant prostate samples.

However, in our study only DU145 cells showed significant FGFR1 expression in 2D monolayer culture of the cell lines used (Figure 2.9. Lane 1 in first row panels). We also examined the presence of other FGFR isoforms and only detected expression of FGFR4 (Figure 2.9. Lane 1 in fourth row panels). It is believed that FGFR4 is predominantly expressed in PC3, DU145 and LNCaP cell lines, however, expression of FGFR1 is limited to the DU145 cell line. Additionally, we probed for the protein expression of FGFR2 and FGFR3, via western blot, yet we were unable to detect expression of either (Figure 2.9. Lane 1 in second row panels and third row panels). We then probed for the protein expression of VEGR2, a highly active kinase among the VEGFR family. VEGFR2 was of our interest because it is not only associated with increased

malignancy modulating angiogenesis, invasion, metastasis development, and bone destruction (109), but is also one of the main targets of Dovitinib, a TKI which was used in this study. None of the 2D monolayer culture of the cell lines showed positive expression of VEGFR2 (Figure 2.9. Lane 1 in fifth row panels). β-actin was used as a loading control (Figure 2.9. All lanes in sixth row panels).

Spheroid Formation Assays of PC3, LNCaP and DU145 Cells

We utilized sphere formation assays since cells grown as 3D spheroids display different gene expression patterns involved in cell proliferation, angiogenesis, cell interaction, and drug sensitivity compared to 2D monolayer cells. Increasing evidence has demonstrated that 3D cell culture systems are more clinically relevant since the results mimic human physiology and tumor biology better than traditional monolayer cell culture grown on tissue culture (110, 111). Moreover, anchorage-independent growth of 3D spheroids is a characteristic of stem cell-like properties and increased metastatic potential. (112, 113).

Using this 3D spheroid assay, we sought to examine if FGFRs are involved in the formation of 3D spheroids, and if these 3D spheroids possess stem cell-like characteristics. In culturing the 3D spheroids, there are various experimental protocols such as different medium composition, cell density, and culture substrates that can differ between research groups that give rise to different results. We set out our investigation to establish effective culture conditions. First, cell growth in basal media of DMEM/F12 versus RPMI 1640 was tested. The DMEM/F12 is routinely used for cancer stem cell (CSC) culture in various cancer cell types, and the RPMI 1640 is used for culturing prostate cancer cell lines. Growth PC3 spheroid cells were tested in basal media with different nutrient supplements, and these spheroids showed better growth in

RPMI 1640 basal medium (data not shown). We then compared different non-adherent plates of ultra low attachment plates and agarose gel-coated tissue culture dishes, in order to see differences in growth and protein expression patterns. However, we found no differences between these plate varieties, and utilized agarose gel-coated tissue culture dishes in this work (data not shown).

We compared growth and protein expression of PC3 spheroids using RPMI 1640 medium in the presence or absence of epidermal growth factor (EGF) in 40 ng/ml, and basic fibroblast growth factor (bFGF) in 50 ng/ml with knockout serum replacement (SR). SR is commonly used in culturing embryonic stem cells and induced pluripotent stem cells (114), however, to the best of our knowledge it hasn't been utilized for culturing prostate cancer cell lines and our study is the first to report this result. We found that PC3 spheroids were not able to proliferate efficiently with only one growth factor present without other supplements (data not shown), thus, 2% SR was added as a base condition. As seen by MTT assay, (Figure 2.7A) the numbers of spheroids were counted from six separate field views and analyzed using ImageJ software and graphed using GraphPad Prism (Figure 2.7B). The results show that 10% SR in RPMI 1640 medium supports the growth of PC3 spheroids more efficiently when compared to adding growth factors in our cell culture. This result is shown by the PC3 metabolic activity and cell count; thus, we utilized 10% SR as the sole supplement in the basal medium of RPMI 1640 for 3D spheroids culture throughout the study for all three prostate cancer cell lines.

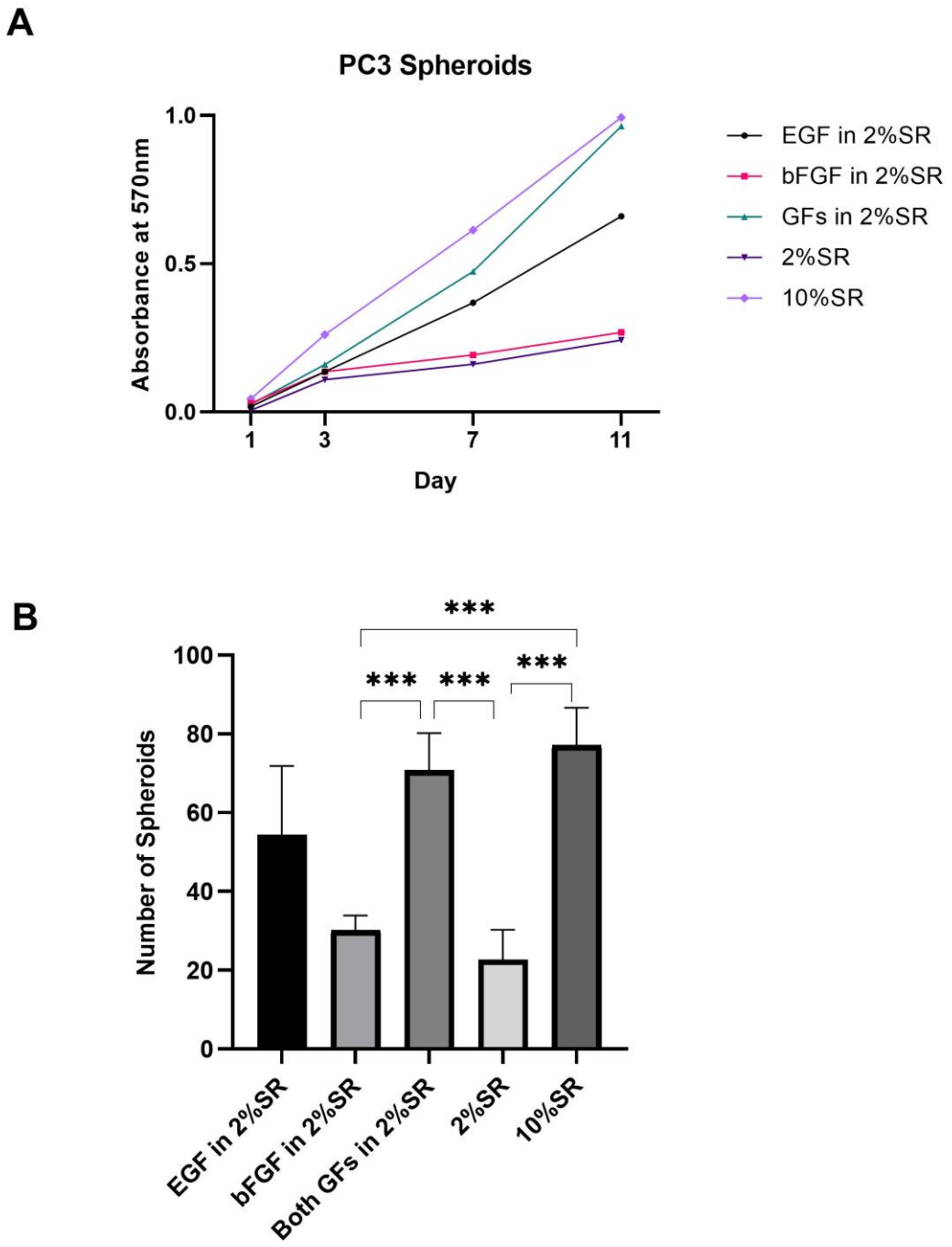

Figure 2.7. Proliferation of PC3 spheroids comparing culture conditions.
(A) MTT assay showing different metabolic activity of cells in different culture conditions. EGF and bFGF were used at 40 ng/ml and 50 ng/ml, respectively. (B) The number of spheroids from six random fields were counted using ImageJ. The error bars represent standard deviation. *P* values are from two-tailed paired *t* tests. *** $P<0.001$.

PC3, DU145, and LNCaP cells were cultured into spheroids, respectively, in the media conditions described above and they displayed different morphology and growth properties. Comparisons of 2D monolayer cells and 3D spheroids cells of each cell line are shown in images taken using a bright field microscope (Figure 2.8). PC3 spheroids appeared to have grape-like structures or loose clusters of cells indicating poor cell-cell contact. DU145 spheroids appeared to be tightly packed together indicating robust cell-to-cell adhesion and had irregular but rather round shape and overall smaller in size than LNCaP spheroids. LNCaP spheroids appeared larger but with robust cell-to-cell adhesion and formed somewhat round shape mass.

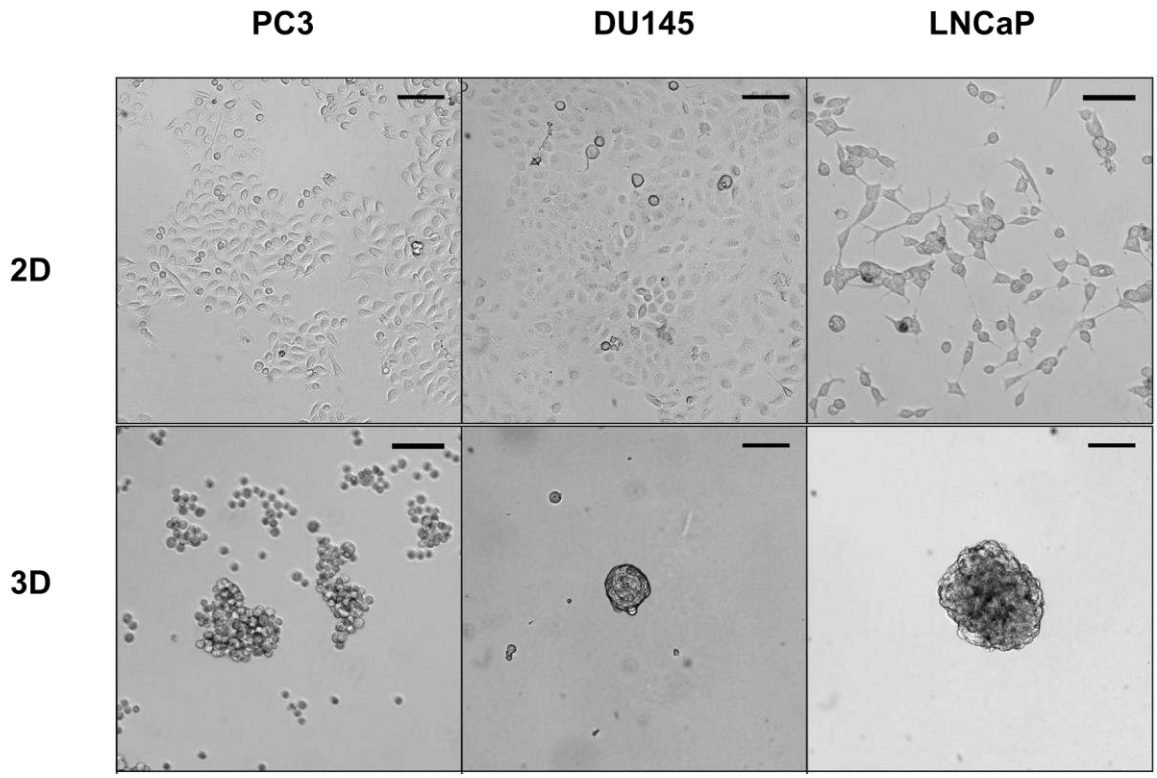

Figure 2.8. Brightfield microscope images of PC3, DU145, and LNCaP cells.
The top panels show cells cultured as 2D monolayer in the order of PC3, DU145 and LNCaP cells and the bottom panels show 3D spheroids of the cell lines at 14 days. The scale bars indicate 100 µm.

Expression of FGFRs, VEGFR2 and downstream cell signaling activation of 3D Spheroids of PC3, DU145 and LNCaP

In order to observe changes in protein expression, 3D spheroids of each cell line were collected on days 1, 4, 7, 11, and 14 and were subjected to westernblot analysis. Strikingly, we found that 3D spheroids of PC3 cells exhibited an increase in FGFR1 and VEGFR2 expression while the expression of FGFR4 decreased (Figure 2.9. Left panel, 1st row, lane 3-6; 5th row, lane 5, 6; 4th row, lane 1-6). DU145 spheroids maintained consistent expression of both FGFR1 and FGFR4, and showed an increase in VEGFR2 expression (Figure 2.9. Middle panel, 1st row, lane 1-6; 4th row, lane 1-6; 5th row, lane 4-6). LNCaP spheroids also showed an increase in FGFR1 expression, however expression of VEGFR2 was not detected (Figure 2.9. Right panel, 1st row; lane 2-6; 5th row, lane 1-6).

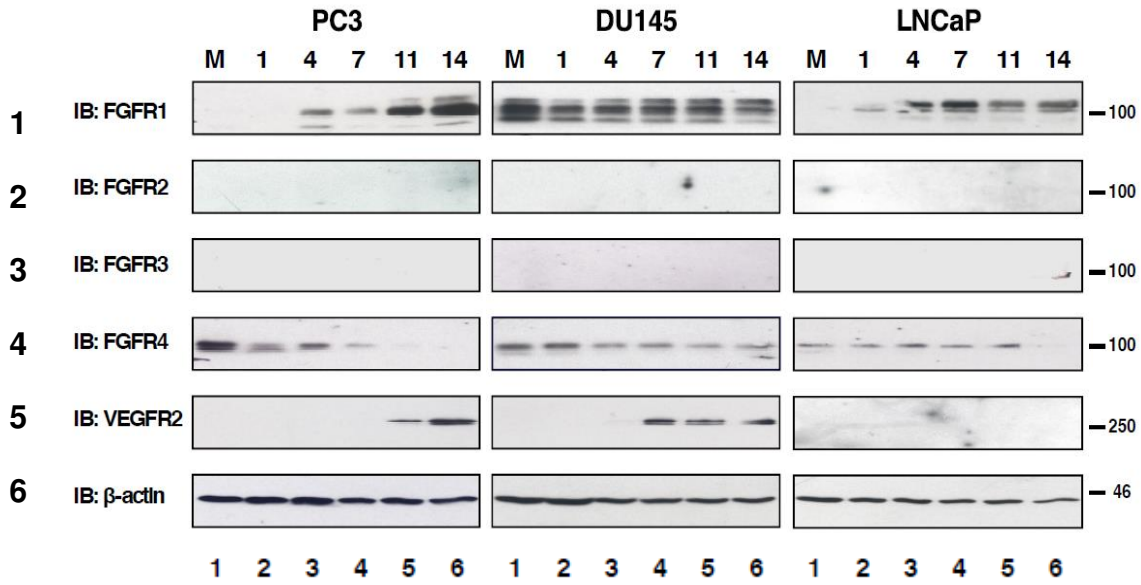

Figure 2.9. Expression of FGFRs and VEGFR2 in spheroids of PC3, DU145 and LNCaP. 2D monolayer cells and 3D spheroids of PC3, LNCaP and DU145 cells on days 1, 4, 7, 11, and 14 were subjected to Westernblot analysis for FGFR 1-4, and VEGFR2. Beta-actin was used as a loading control. M= 2D monolayer.

Of note, 3D spheroids of PC3 and DU145 increased or maintained FGFR1 expression, respectively, and both showed increased VEGFR2 expression. Despite an increase in VEGFR2 expression, this RTK was not activated, as seen though westernblot probed for phosphorylated VEGFR2 (data not shown). This data suggests that FGFR1 may be involved as an anchorage independent hallmark of prostate cancer cells, however, it is not clear whether this selection via 3D culture enriched for FGFR1-expressing cell population and/or the non-adherent culture condition promoted the survival of cells via overexpression of FGFR1. The positive expression of FGFR1 and FGFR4 in the spheroids of all three cell lines led us to examine the kinase activity of FGFR by immunoblotting with p-FGFR antisera and downstream signaling pathways using p-STAT5, p-MAPK, and p-AKT antisera.

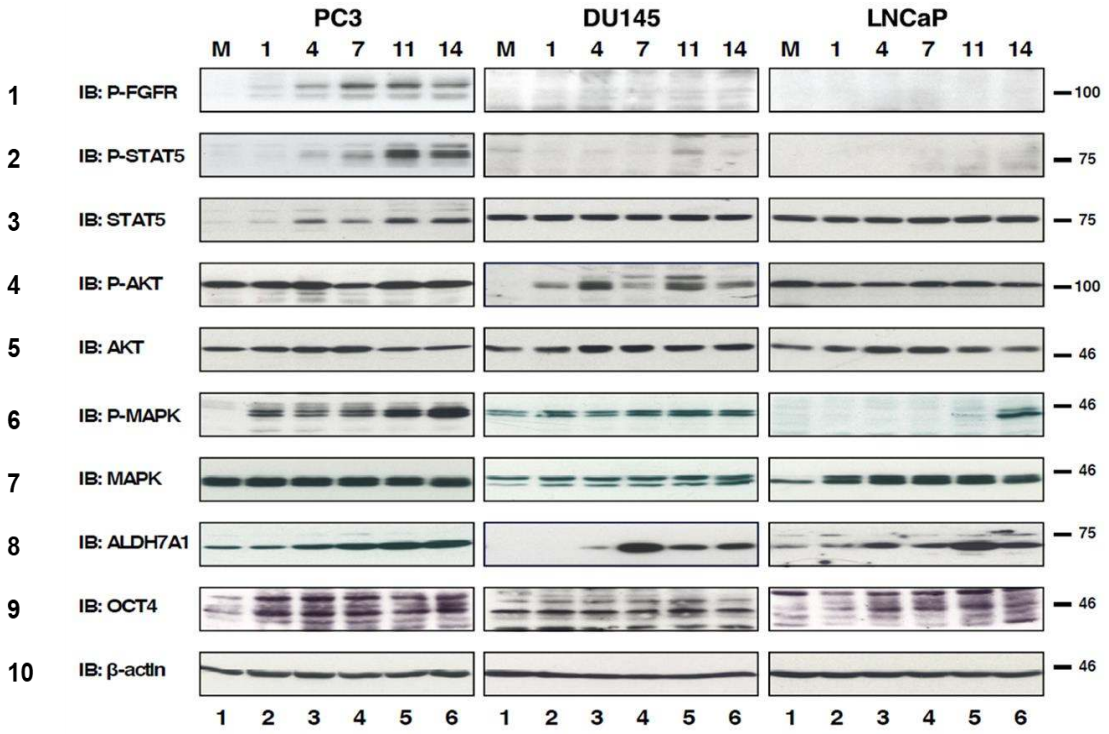

Figure 2.10. Expression and downstream cell signaling activation of FGFR of spheroids of PC3, DU145 and LNCaP.
(1st row) FGFR activation was shown by immunoblotting for phospho-Y653/654 FGFR antiserum and only PC3 spheroids showed positive signal. (2nd row) STAT5 activation was detected by immunoblotting for phospho-Y694-STAT5, and the same membrane was stripped and probed for total STAT5 expression shown immediately below. (4th row) AKT activation was detected by immunoblotting for phospho-S473-AKT, and the same membrane was stripped and probed for total AKT expression shown immediately below. (6th row) MAPK activation was shown by immunoblotting for phospho-T202/Y204-MAPK, and the same membrane was stripped and probed for total MAPK shown immediately below. (8th row) Total ALDH7A1 expression was shown significantly increasing. (9th row) OCT4 expression was shown slightly increasing for PC3 and LNCaP 3D spheroids and was shown maintaining for DU145 3D spheroids. (10th row) Beta-actin was used as a loading control. M= 2D monolayer.

We found FGFR kinase activity was most significant in PC3 spheroids via up-regulated p-FGFR, and p-STAT5, and p-MAPK while maintaining the constitutive p-AKT levels (Figure 2.10. Left panel, row 1,2,4, and 6). Expression of STAT5, AKT and MAPK was probed as a control (Figure 2.10. Left panel, row 3, 5 and 7). Compared to PC3 spheroids, DU145 spheroids showed modest activation of FGFR signaling pathway. Surprisingly, despite the most prominent

expression of FGFR1, we were not able to detect a phospho-FGFR signal from DU145 spheroids (Figure 2.10. Middle panel, row 1). Even with 3-fold increased amount of lysate and 2-fold increase in the antiserum usage, the phospho-FGFR signal was negative while non-specific background signal was enhanced (Data not shown). STAT5 was not found to be activated in DU145 spheroids (Figure 2.10. Middle panel, row 2). Although irregular, AKT was activated in the DU145 spheroids (Figure 2.10. Middle panel, row 3). This is surprising because AKT negatively regulates MAPK in prostate cancer (115), which is consistent with our findings in case of the monolayer cells (Figure 2.10. Middle panel, row 4 lane 1, compared to row 6 lane 1), suggesting that 3D spheroids may utilize FGFR signaling differently from 2D monolayer cells. MAPK activation was maintained throughout the 3D culture in DU145 cells (Figure 2.10. Middle panel, row 6). A phospho-FGFR signal was not detected in LNCaP spheroids, despite the increase in the protein expression of FGFR1 (Figure 2.10. Right panel, row 1). A Four-fold increase of lysate amount and 2-fold increase in the antiserum usage resulted in the negative p-FGFR signal similarly to DU145 spheroids (Data not shown). STAT5 was not found to be activated in LNCaP spheroids (Figure 2.10. Right panel, row 2). LNCaP cells harbor one deleted allele of *PTEN* and one mutated allele of *PTEN,* thus this cell line does not express the PTEN protein. Lacking this negative regulator, p-AKT was constitutively activated in both 2D and 3D LNCaP cells (Figure 2.10. Right panel, row 4). LNCaP monolayer cells did not activate MAPK as it may be negatively regulated by AKT (115), however, LNCaP spheroids showed activation of MAPK pathway while maintaining AKT activation (Figure 2.10. Right panel, row 6 lane 6).

To the best of our knowledge, this is the first report to demonstrate that 3D spheroids of prostate cancer cell lines predominantly express FGFR1 compared to other FGFRs in the culture conditions described.

Cancer stem cell Markers of 3D Spheroids of PC3, DU145 and LNCaP Cell Lines

We examined the hypothesis that anchorage independence is a characteristic of cancer stem cells by probing for cancer stem cell markers through westernblot. ALDH7A1 and OCT4 were chosen to show increased metastatic potential and stemness of the spheroids, respectively (66, 116, 117). ALDH7A1 detoxifies aldehyde compounds induced by chemotherapeutic agents to be associated with CSC markers in prostate cancer and is highly expressed in prostate primary tumors and matching bone metastases of those primary tumors (66). PC3, DU145 and LNCaP spheroid cells exhibited an increase in ALDH7A1 compared to their respective monolayer cells (Figure 2.10. All panels, 8th row). OCT4, an embryonic stem cell marker for self-renewal and maintenance of an undifferentiated state (117), was maintained throughout 3D culture with little increase (Figure 2.10. All panels, 9th row). The greatest increase observed was a 2-fold increase of the signal strength of PC3 spheroids at 14 day compared to the monolayer PC3 cells and the LNCaP spheroids at 14 day compared to the monolayer LNCaP cells analyzed in a semi-quantitative manner using ImageJ software (data not shown). Beta-actin was used as a loading control (Figure 2.10. All panels, 10th row).

Taken together, PC3, DU145, and PC3 spheroids may have increased metastatic potential *in vitro*, however, it is unclear if they have increased self-renewal abilities; however, there is a possibility that these spheroids are more progenitor-like cells. In fact, most stem cells undergo asymmetric cell divisions to generate one daughter stem cell and one differentiating daughter cell (93). To investigate the enrichment of more stem/progenitor cells more quantitative analysis would be required.

Although there are other CSC markers frequently used in studying prostate cancer stem cells. Collins *et al.* (118) and other studies (77, 7) have reported that $CD44^{+}/\alpha2\beta1$

integrin$^+$/CD133$^+$ cells mark a stem cell-like population in prostate cancer cells and these markers have been frequently used to isolate or identify this rare population (0.1–0.3%). However, the reliability of cell surface markers remains debatable especially depending on types of cell line. CD44$^+$/α2β1 integrin$^+$ population may possess higher tumorigenic properties compared to CD44$^-$/α2β1 integrin$^-$ population, however, nearly 100% of PC3 cells are CD44$^+$/α2β1 integrin$^+$ (119, 120). Indeed, we observed that approximately 100% of PC3 cells showed positive CD44$^+$ expression via immunofluorescence (data not shown).

On the other hand, the number of PC3 CD133$^+$ cells is extremely rare, thus, making the protein expression analysis inefficient. Although a few studies (77, 121) have reported that when prostate cancer cells were cultured into spheroids, CD133$^+$ cells showed enrichment in fluorescence activated cell sorting (FACS) analysis. However, Pfeiffer *et al.* (122) has reported that PC3 and LNCaP cell lines were not CD133 positive, as seen through FACS analysis, and only 0.01 ± 0.01% of DU145 cells showed expression for CD133. In fact, in our flow cytometry trials using PC3 cells, we obtained 0.4% of CD133$^+$ PC3 cells, however, depending on gating of the plot in analysis, the CD133$^+$ population may not be reliably estimated. (**Figure 2.11**) Moreover, our investigation of CD133$^+$ population in PC3 cells of monolayer and spheroids through immunofluorescence and westernblot resulted in negative findings consistently by several antisera from different manufacturers (data not shown).

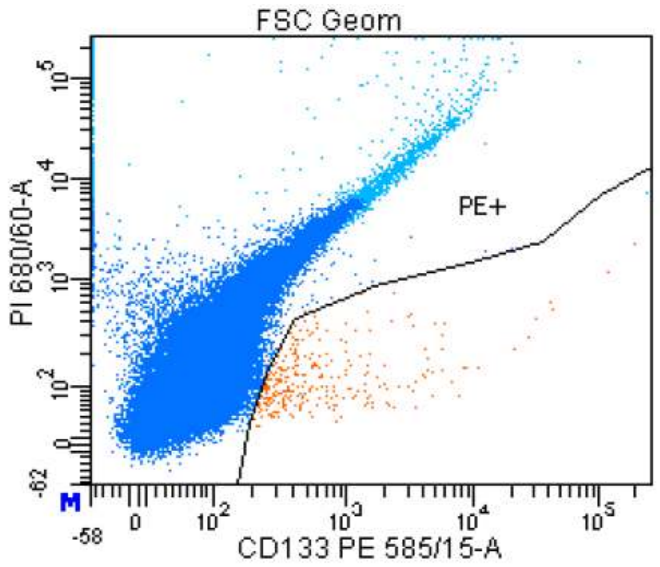

Figure 2.11. Flow cytometry analysis of PC3 cells.
Single PC3 cells were labeled with CD133 antibody conjugated with PE fluorophore. Dead cells were marked by high propidium iodide (PI) staining in the upper region shown in light blue. To the lower right, $CD133^+$ population was identified to be 0.4 % among live cells.

Quantification of the Anchorage-independent Cells in PC3, DU145 and LNCaP Spheroids using Soft Agar Colony Formation Assay

To quantify the proportion of the anchorage-independent spheroids in the total population, we utilized a soft agar colony formation assay. This method allows cells to grow in a non-adherent semi-solid agarose matrix from the initial seeding of single cells thus, the number of colonies represents the number of single cells that are capable of surviving and proliferating in an anchorage-independent condition in a semi-quantitative manner. The colony forming efficiency of cells is routinely used as a measure of tumorigenicity *in vitro* (122, 123).

Cells were dissociated into single cells and then plated with agarose with varying seeding densities as shown (Figure 2.12). Each cell line exhibited different colony forming efficiency that the seeding density range was not unified. Additionally, the average size of colonies at 4

weeks varied from one cell line to another, so the culture period and the minimum size of colonies counted was dependent on the cell line. Thus, a cell line to cell line comparison of the colony forming efficiency was not be made from the data presented in **Figure 2.12.**

The results show that there is a linear correlation between the number of cells seeded and the number of colonies generated from all three cell lines (Figure 2.12. A, B, C). However, the number of colonies at higher seeding densities showed a decreased percentage of colony-forming cells (Figure 2.12. D, E, F), probably due to the confined culture with limited nutrient and accumulated cellular waste. In conclusion, the results suggest that the anchorage independent population from all three cell lines are around 1%, which shows that anchorage independent growth, anoikis, is a rare property and these cells may be considered as a more stem cell-like population.

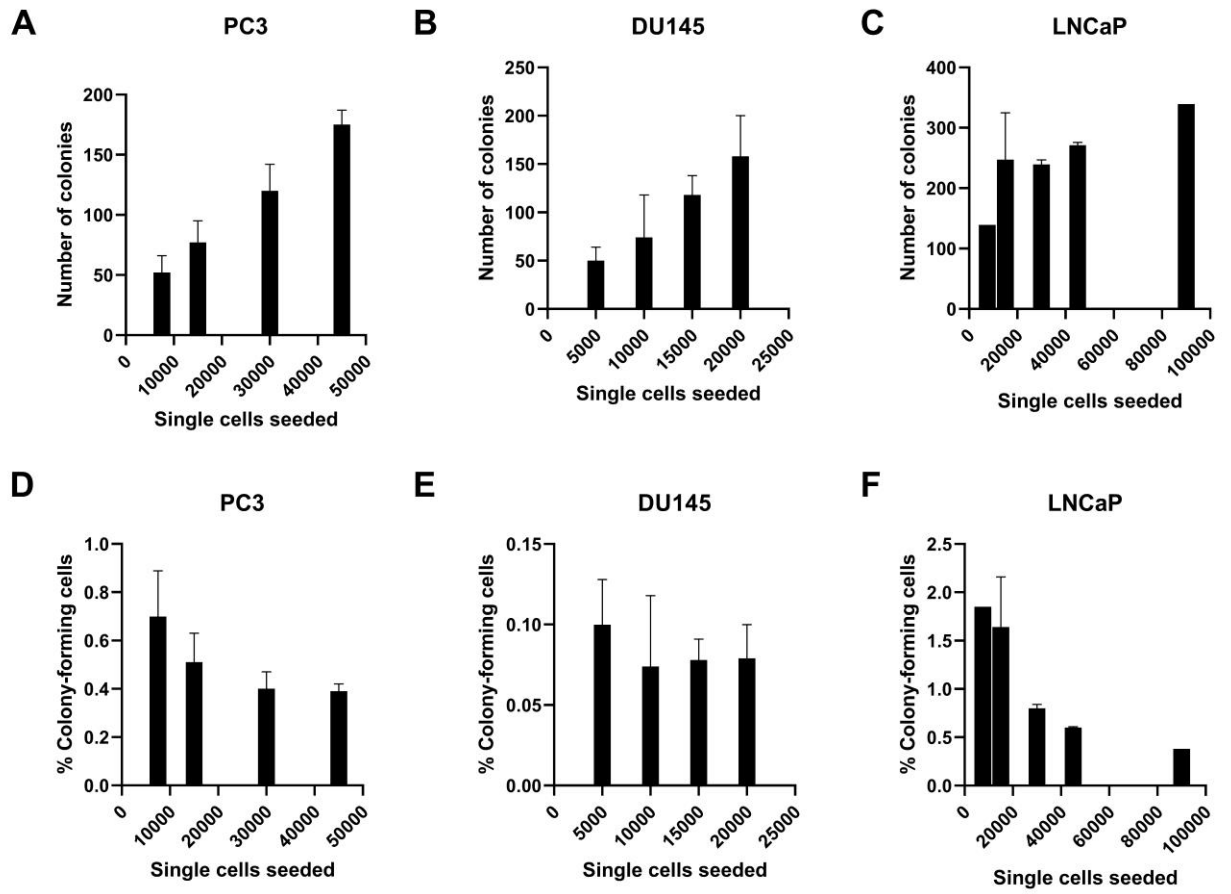

Figure 2.12. Anchorage independence of prostate cancer cell lines through soft agar colony formation assay.

Single cells of PC3, DU145 and LNCaP were seed into agarose mixture and the number of colonies and the percentage of colony forming cells were quantified using ImageJ software. The error bars represent standard deviation. (A) PC3 colonies that are larger than 10,000μm^2 in size are counted. (B) DU145 colonies that are larger than 10,000μm^2 in size are counted. (C) LNCaP colonies that are larger than 2,500μm^2 in size are counted. The first and the last data point do not have error bars. (D, E and F) The colony forming efficiency was calculated based on the number of colonies for total single cells seeded for PC3, DU145 and LNCaP. The error bars represent standard deviation.

Effect of FGFR Inhibition on Cell survival of 2D monolayer cells

Prior to our investigation of the importance of FGFR signaling in 3D spheroids of prostate cancer cell lines, we set out to compare the association of FGFR signaling in 2D monolayer cells for their survival. We blocked FGFR activity using the small molecule

inhibitors, Dovitinib and BGJ398, which have been examined in clinical trials for several cancers with defined FGFR genetic alterations. We included PD166866 in our comparison as it was reported to be a highly selective inhibitor towards FGFR1 in addition to other RTKs such as c-Src, PDGFR, EGFR (46). Dovitinib is a nanomolar multi-RTK inhibitor for receptors such as FLT3, VEGFR, and FGFR and has shown antitumor activity, reducing the bone metastasis and angiogenesis in PDX models and in a clinical trial for CRPC patients (29). BGJ398 is a nanomolar inhibitor for FGFR1-3 without significant biological effects towards other kinases. It has shown antitumor effects in clinical trials for patients with FGFR1-amplified squamous non-small-cell lung cancer and patients with FGFR3-mutant bladder and urothelial cancers (124).

We utilized an MTT assay to examine if PC3, DU145 and LNCaP cells depend on the FGFR signaling pathway for their survival and to determine if they were sensitive to inhibitor treatments. The cells were plated on to 24-well tissue culture plates in triplicate and each inhibitor at different concentrations was added for approximately 24 hours before the absorbance reading was measured. The viability of PC3 cells was reduced by all three inhibitors (Figure 2.13 A). The results show that BGJ398 and Dovitinib decreased the cell viability of PC3 cells at high concentrations, however, did not show meaningful IC50 (<100 μM). PD166866 exhibited a limited solubility issue at high concentrations so that the IC50 derived from the assay is not reliable. Interestingly, DU145 cells did not show clear dose-dependent response to any FGFR inhibitors as shown in the graph, which resulted in ambiguous IC50 determination (Figure 2.13B). LNCaP cells showed the best response to FGFR inhibitors among the three cell lines compared. The IC50 of PD166866 was not determined due to the limited solubility of the drug, while IC50 of BGJ398 was 5.77μM, and that of Dovitinib was 43.4μM (Figure 2.13C). Taken together, these data show that 2D monolayer cells of the prostate cancer cell lines do not respond

to FGFR inhibition in low micromolar range, suggesting that FGFR pathway is not critical regulating the survival of 2D cells.

It is expected that longer treatment of 48 hours or 72 hours would lower the cell viability more effectively, however, considering that the protein expression of FGFR in these 2D cells and the kinase activity are negative or below the detection threshold via westernblot analysis as shown in Figure 2.8, we concluded that FGFR signaling does not play a key role in cell survival of the 2D cells of PC3, DU145, and LNCaP cell lines.

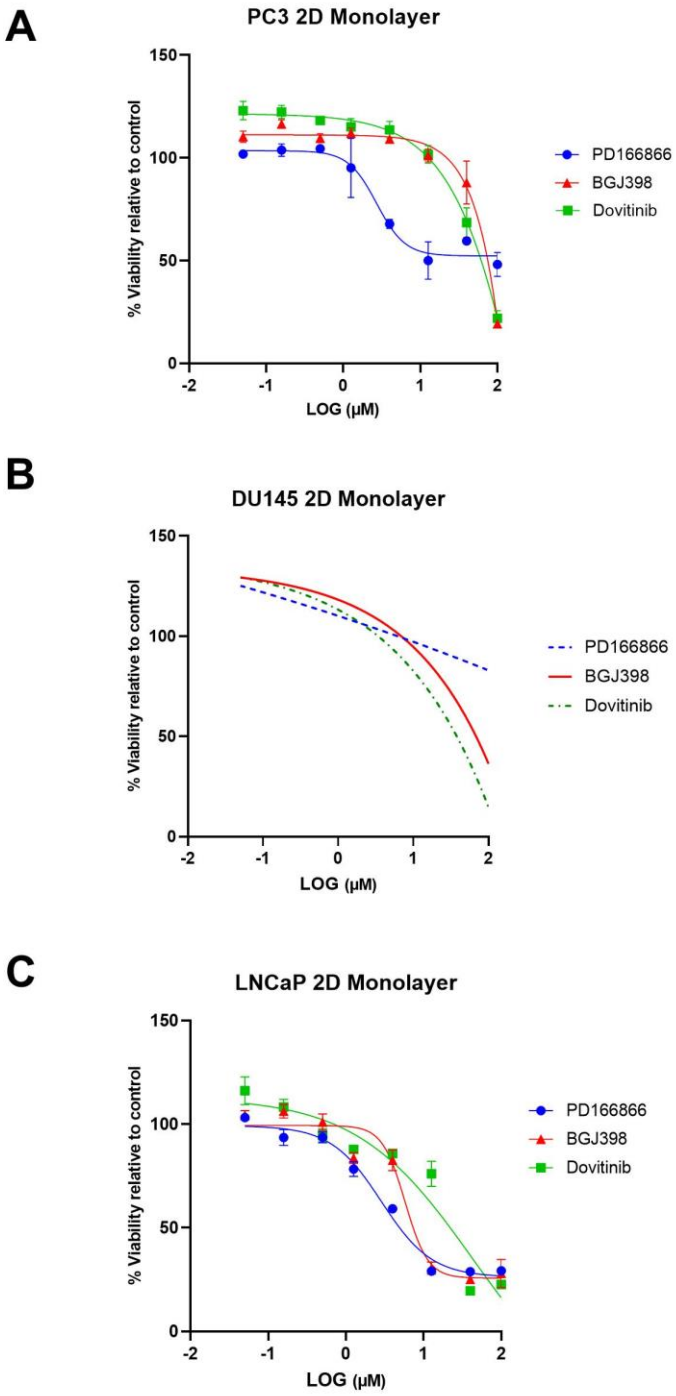

Figure 2.13. Effect of FGFR inhibitors on the cell viability of 2D monolayer cells of PC3, DU145 and LNCaP.

(A) PC3 cells were treated with 0.050, 0.15, 0.45, 1.35, 4.05, 12.15, 36.45 or 109.35 μM of PD166866, BGJ398, or Dovitinib for 24 hours. (B and C) DU145 and LNCaP cells were treated the same as described for PC3 cells.

Effect of FGFR Inhibition on Survival and Proliferation of 3D spheroids

Next, we examined our hypothesis that FGFR signaling is essential in the cell survival and proliferation of the spheroids of PC3, DU145 and LNCaP as the FGFR1 expression had increased as well as its downstream signaling was shown to be activated unlike in the monolayer cells. We utilized MTT assay accompanied by counting of the number of cells to examine if the cell viability and proliferation are affected by the inhibitor treatments more favorably than the 2D cells.

For this experiment, the experimental conditions for the cell lines were unified because the spheroids of PC3, DU145 and LNCaP exhibited different growth patterns.

First, the seeding density needed varying because DU145 and LNCaP spheroids showed very slow proliferation so that without the increase of the seeding density, the metabolic activity for showing the growth was not clearly discernable. Secondly, DU145 and LNCaP spheroids displayed tough physical barrier that acidified isopropanol was not able to completely lyse them for absorbance measurements. Thus, a measure was taken to concentrate the formazan product by removing supernatant by centrifuging before the lysis of the cells. These different protocols are described in the Figure 2.14 and Figure 2.15.

After modification of the protocol, growth pattern of all three types of spheroids are shown Figure 2.16. The spheroids of PC3 reached their maximum absorbance by MTT in 14 days from low seeding density. On the other hand, DU145 cells exhibited noticeably lower capacity for anchorage-independent growth than PC3 and LNCaP cells. DU145 cells needed high seeding density, the initial cell death was reflected during days 1-5 through MTT assay. However, the surviving DU145 cells give rise to spheroids that proliferate by 17 days to reach the maximum absorbance that can be measured by MTT assay. Lastly, spheroids of LNCaP

showed modest growth in the initial stage of sphere formation, however, their growth didn't show a noticeable increase after 5 days even by 17 days of prolonged culture and did not reach the maximum absorbance (approximately 1).

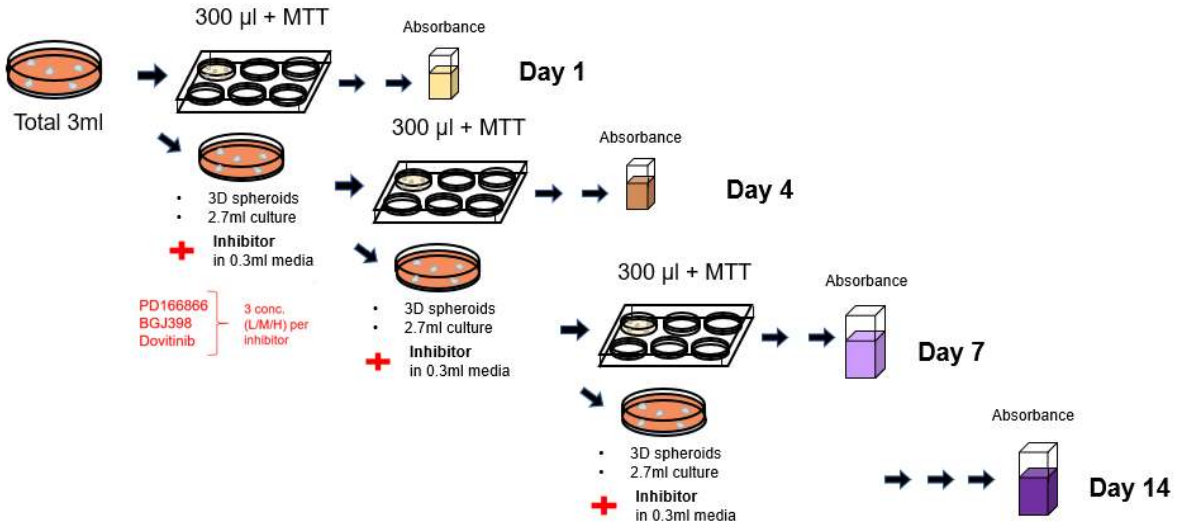

Figure 2.14. Schematic of MTT protocol for PC3 spheroids.
Single cells were seeded on agarose-coated 60mm TC plates with total volume of 3ml. Then 10% of the cell culture was taken out and moved to a plate where MTT reagent was added. This was incubated for 4 hours to allow the cells to metabolize the dye to formazan, and acidified isopropanol was added to lyse the cells. Then 1 hour later solution was transferred to a cuvette and the absorbance reading was taken at day 1. To the remaining culture, 300ul of media was added to make the total volume back to 3ml. For the treated groups, each inhibitor was added in DMSO vehicle with 300ul of media to make the total volume 3ml again. Samples from the same culture every 3-4 days for their growth and response to the inhibitor treatments at additional days indicated.

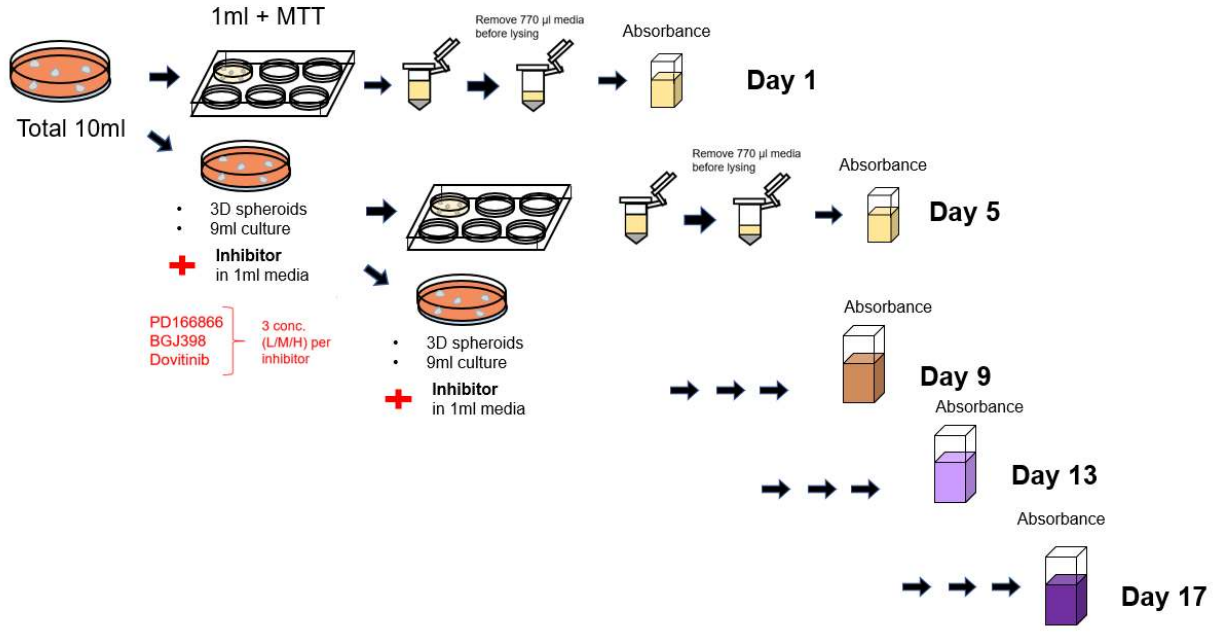

Figure 2.15. Schematic of the modified MTT protocol for DU145 and LNCaP spheroids. Single cells were seeded in the total volume of 10 mL culture on agarose-coated 10 mL tissue culture plates. 1 mL (10% of the total volume) of was taken out for MTT assay, and before the lysis, the cells were concentrated by removing extra media by centrifugation. With the lysing solvent added, it was vortexed and then incubated longer for further lysis. To the remaining culture, 1ml of media was added to make the total volume back to 10 mL. For the treated groups, each inhibitor was added in DMSO vehicle with 1mL of media to make the total volume 10 mL again. Samples from the same culture were examined every 4 days for their growth and response to the inhibitor treatments at additional days indicated.

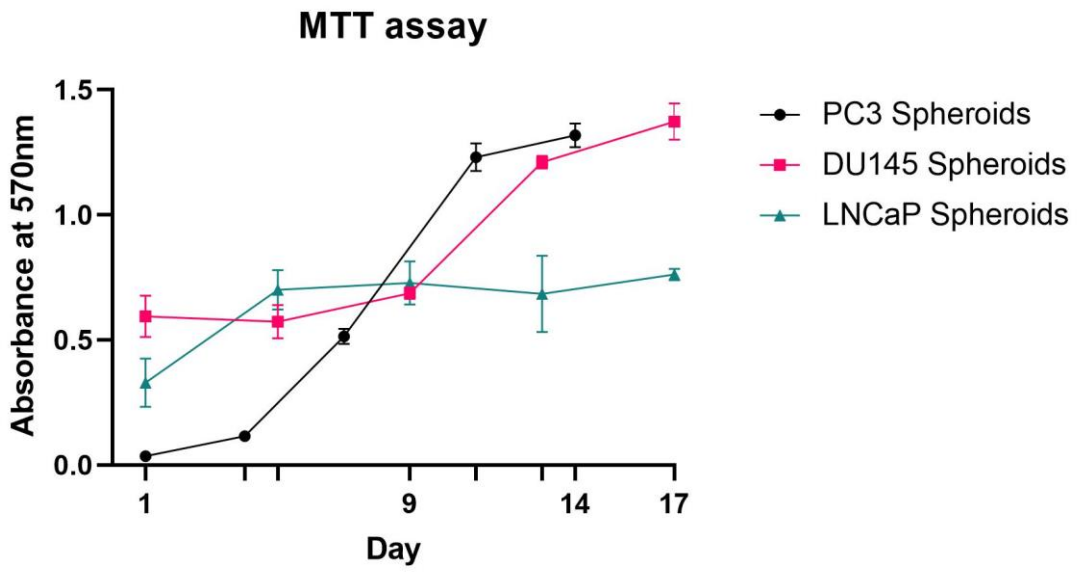

Figure 2.16. Metabolic activity of three prostate cancer cell lines.
Different growth patterns of spheroids were revealed by the MTT assay. PC3 spheroids showed relatively rapid increase and DU145 spheroids showed little changes in the absorbance value initially and showed similar increase to PC3 spheroids after 10 days. Lastly, LNCaP spheroids showed moderate increase in the absorbance initially and plateaued after 5 days.

Treatment with PD166866 (2–20 μM) was not as effective as other two inhibitors for PC3 spheroids, however, PD166866 successfully hindered cell proliferation at much higher concentrations (Figure 2.17A). BGJ398 (1–5 μM) showed its inhibitory effects and at high (5μM) dosage, and cells seemed to undergo apoptosis (Figure 2.17B). Dovitinib (0.5–2 μM) demonstrated potent anti-proliferative effects, and morphology of PC3 spheroids changed especially at high (2 μM) dosage (Figure 2.17C). Additionally, Dovitinib treated PC3 cells displayed granular nucleus and were larger in size (data not shown). It is believed that PC3 treated with Dovitinib for a prolonged period showed further differentiation into a neuroendocrine phenotype to show different morphology. This was not examined in our study to conclude if the PC3 spheroids did differentiated into a neuroendocrine phenotype.

The number of floating spheroids with the minimum size of 1,000 μm^2 was counted by

photographing 6 random field views under the microscope (Figure 2.18A). In addition, the number of single cells from the spheroids was counted by averaging the size of single cells and associating it with the area of spheroids measured (Figure 2.18B). It is noteworthy that although the number of single cells is an estimation, it shares the same trend as the number of spheroids by the inhibitor treatment. This data supports that FGFR inhibition results in the decrease of cell survival and proliferation as shown by MTT assay, the correlation of the metabolic activity has a linear association with the number of cells (Figure 2.19).

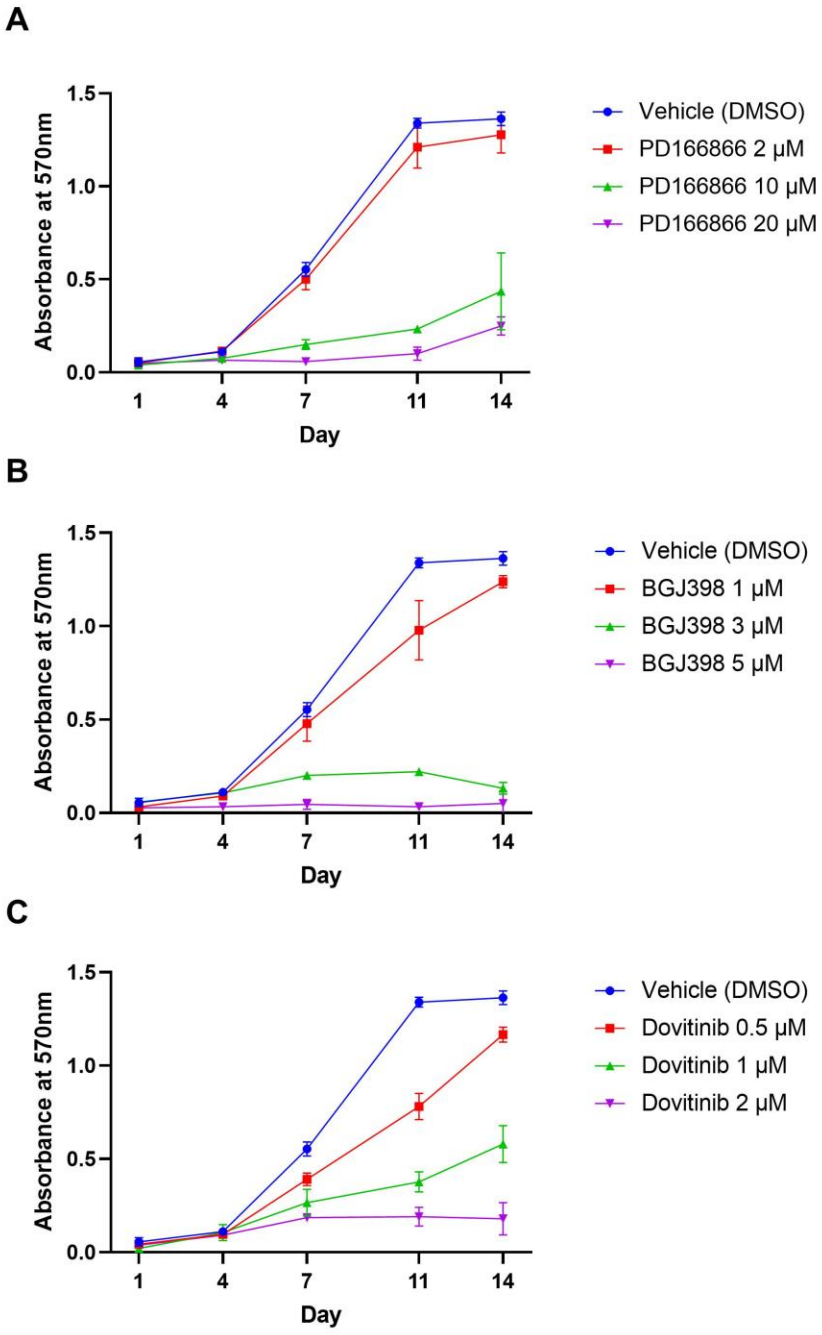

Figure 2.17. FGFR inhibitor treatment on PC3 spheroids.
Triplicate cultures of PC3 3D spheroids were grown in RPMI 1640 with 10% SR on agarose-coated dishes. Samples of cultures were taken and assayed by MTT metabolic assay indicating the number of viable cells on days 1, 4, 7, 11, and 14 to show the proliferation over time. (A) 2µM -20µM of PD166866 was treated. (B) 1µM -5µM of BGJ398 was treated. (C) 0.5µM -2µM of Dovitinib was treated. Triplicate experiment was performed, and error bars show the standard deviation.

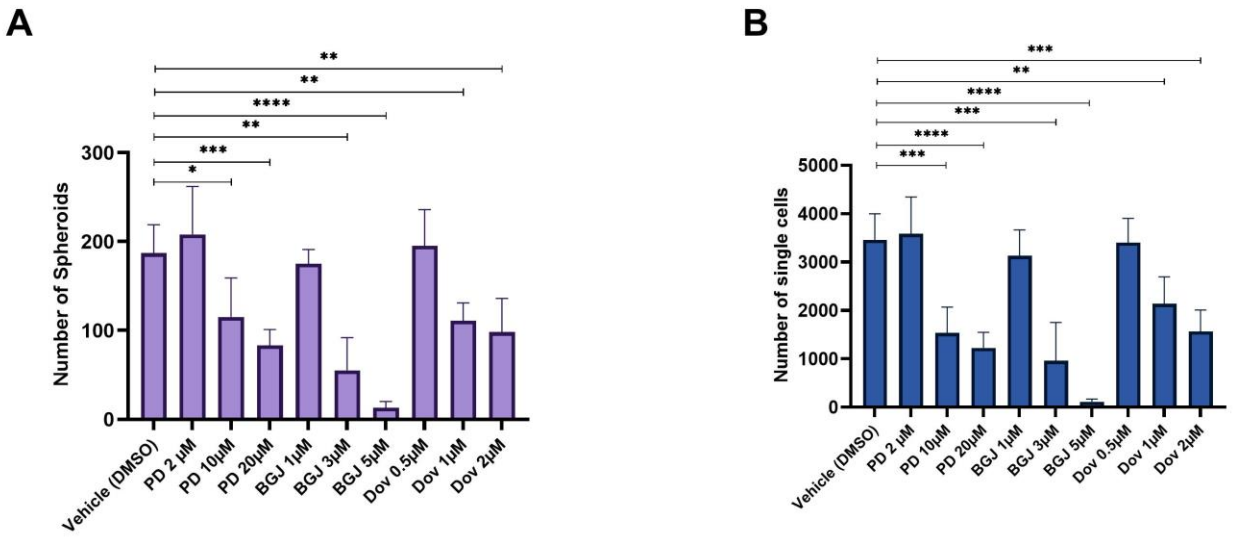

Figure 2.18. The effect of FGFR inhibitor treatment on the number of spheroids and the single cells of PC3.

(A) The number of spheroids (>1,000 μm^2) from total 6 random field views were counted using ImageJ software and the average number is shown. Error bars show the standard deviation. (B) The number of single cells were analyzed based on size of the spheroids measured and size of a single cell (approximately 210 μm^2) to estimate the number of single cells in the field view. Error bars show the standard deviation. *P* values are from two-tailed paired *t* tests. * = $P \leq 0.05$, ** = $P \leq 0.01$, *** = $P \leq 0.001$, **** = $P \leq 0.0001$. PD= PD166866, BGJ= BGJ398, Dov= Dovitinib.

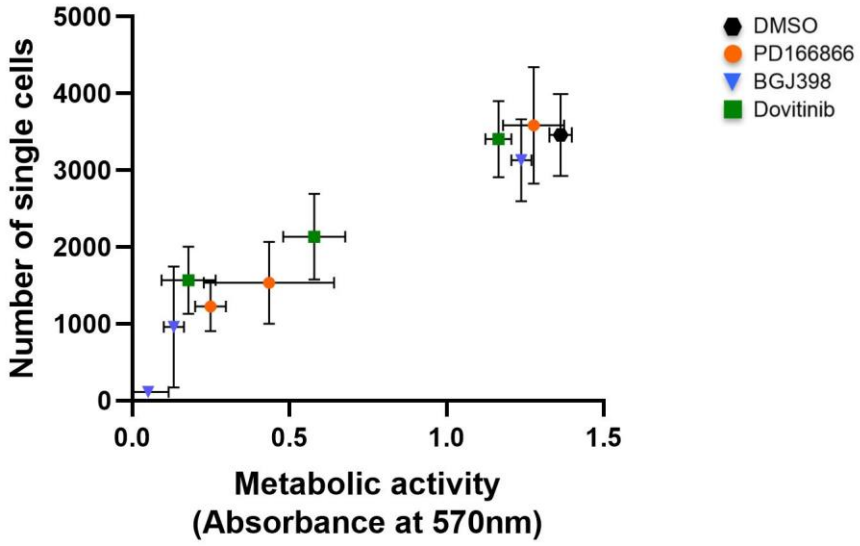

Figure 2.19. MTT assay as a tool for cell survival and proliferation.

The metabolic activity measured from the spheroids PC3 correlates to the number of cells by the linear association.

DU145 spheroids were sensitive to treatment with FGFR inhibitors PD166866, BGJ398, and Dovitinib, respectively, as shown in Figure 2.20 A, B, and C. These data suggest that although FGFR activation of DU145 spheroids was not observed via westernblot analysis, FGFRs may be weakly activated and the kinase activity may be critical in the cell survival and growth among an anchorage-independent subpopulation. Additionally, the number of floating spheroids with the minimum size of 500 μm^2 was counted by photographing 3 separate field views under the microscope (Figure 2.21A). An attempt was made to estimate the number of single cells from the spheroids was counted by averaging the size of single cells and associating it with the area of spheroids measured (Figure 2.21B). As seen from Figure 2.21C, DU145 spheroids build up a tough physical barrier that hinders the penetration of chemical reagents such as trypsin and other cell dissociation reagents. Furthermore, this barrier provides protection against mechanical impact such as vortexing, thus the estimation of single cells and single cell-like aggregates were best analyzed by association with the total area. The result shows that treatment with FGFR inhibitors showed a decrease in both the number of spheroids and the number of single cell-like aggregates. Taken together with the decreased metabolic activity shown via MTT assay, we can conclude that FGFR inhibition results in the decrease of cell survival and proliferation of DU145 spheroids.

LNCaP spheroids grew slowly compared to the other two cell lines, and the treatment with FGFR inhibitors further resulted in reduced growth (Figure 2.22 A, B, and C). The inhibitory effect of PD166866 (2–20 μM) was similar to that of PC3 spheroids. Notably, LNCaP spheroids were less responsive to treatment with BGJ398 treatment (2.5–10 μM). It is contrasting to the result shown with LNCaP monolayer, which was most sensitive to treatment with BGJ398 compared PC3 and DU145 monolayer cells. Dovitinib treatment (0.5–2 μM) resulted in anti-

proliferative effects, and there were no noticeable morphological changes of the spheroids after the inhibitor treatment. Additionally, the number of floating spheroids with the minimum size of 500 μm^2 was counted by photographing 3 separate field views under the microscope (Figure 2.23A). Similarly to DU145 spheroids, LNCaP spheroids have a physical barrier and tight contact between the cells that the counting of single cells was difficult. An attempt was made to estimate the number of single cells from the spheroids was counted by averaging the size of single cells and associating it with the area of spheroids measured (Figure 2.23B). The results show that FGFR inhibitor treatment did not effectively reduce the number of spheroids nor the number of single cell-like aggregates. A Student's *t*-test confirmed that this difference was insignificant. Taken together, it was found that LNCaP spheroids require higher concentration of FGFR inhibitor to decrease the cell survival and proliferation, especially for the anchorage independent LNCaP cells.

Collectively, FGFR signaling is involved in maintaining cell survival and promoting proliferation in different degrees among PC3, DU145 and LNCaP prostate cancer cell lines. Interestingly, DU145 spheroids responded more sensitively to the inhibitor treatments than their 2D cells, while LNCaP spheroids were less sensitive to inhibitor treatment compared to their 2D cells. This suggests that a rare subpopulation characterized as anchorage independent cells may not be the key factor in predicting the response to TKI treatment and the importance of FGFR signaling is different between cell lines. This led us to examine different aspects of FGFR activation and activation of downstream signaling from PC3, DU145 and LNCaP spheroids.

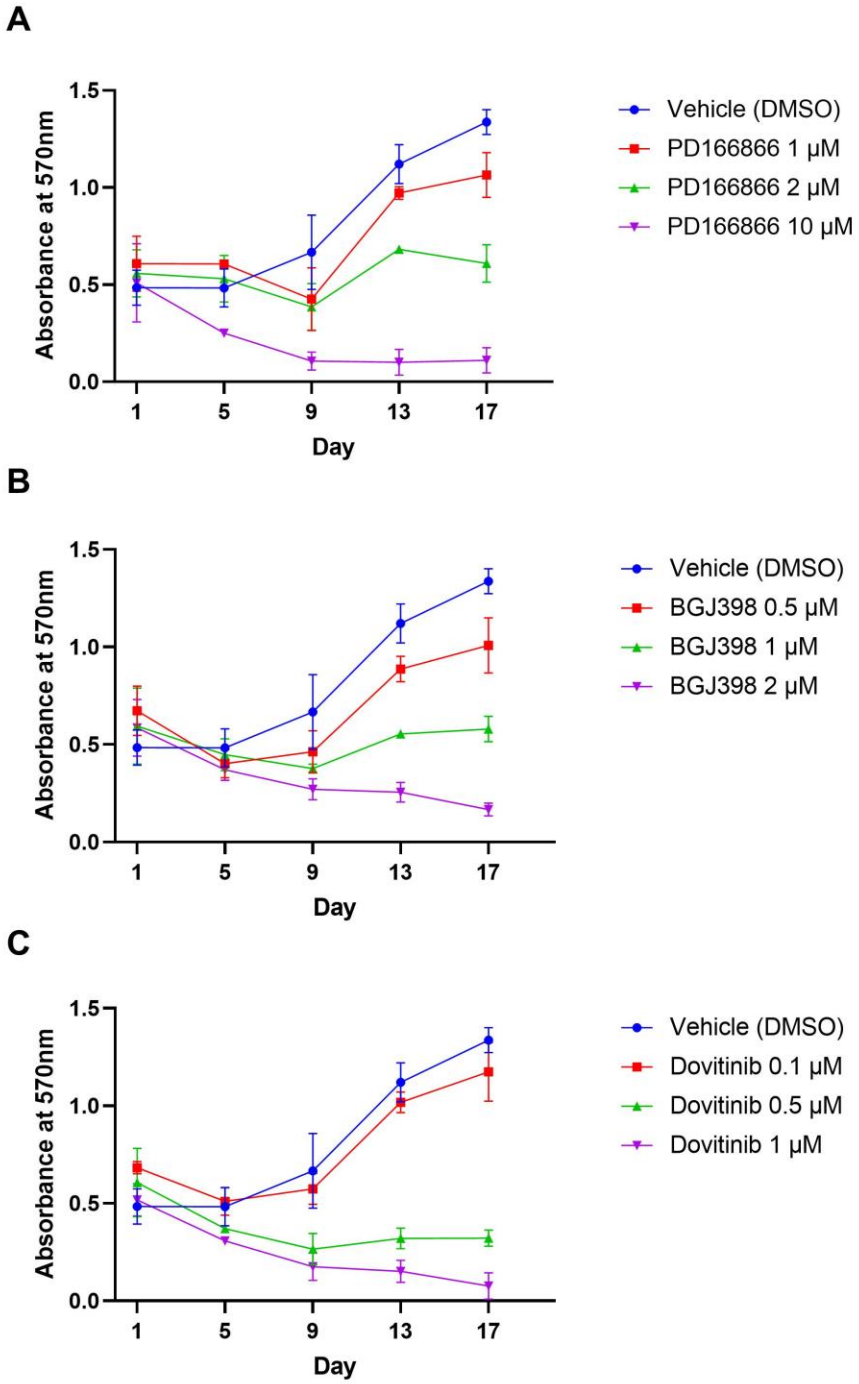

Figure 2.20. FGFR inhibition on DU145 spheroids.

Triplicate cultures of DU145 3D spheroids were grown in RPMI 1640 with 10% SR on agarose-coated dishes. As described in the material and method, samples of cultures were taken and assayed by MTT metabolic assay indicating the number of viable cells on days 1, 5, 9, 13, and 17 to show the proliferation over time. (A) 1μM -10μM of PD166866 was treated. (B) 0.5μM -2μM of BGJ398 was treated. (C) 0.5μM -2μM of Dovitinib was treated. Error bars show the standard deviation.

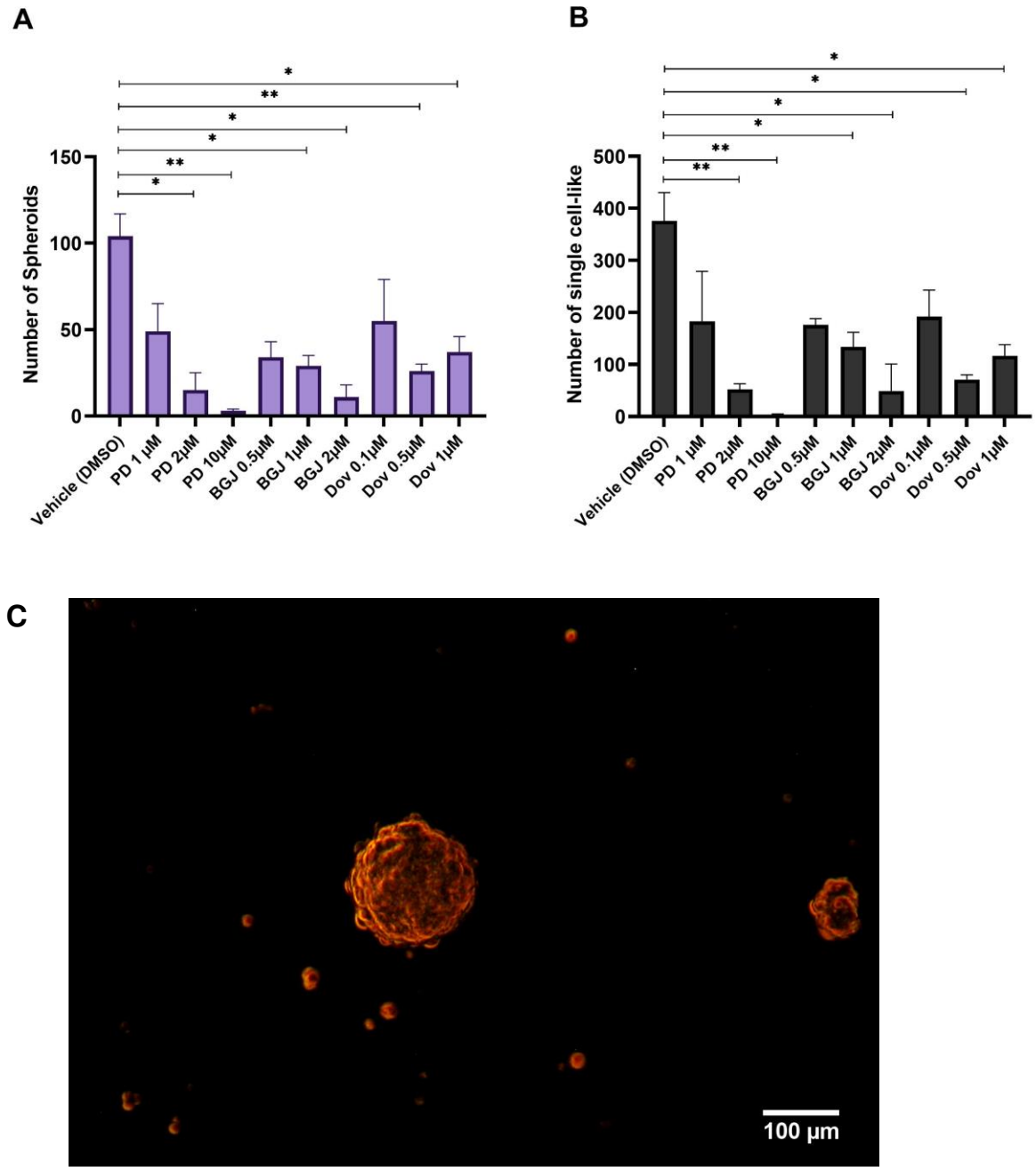

Figure 2.21. The effect of FGFR inhibitor treatment on the number of spheroids and the single cell-like of DU145.

(A) The number of spheroids (>500 µm^2) from total 6 random field views were counted using ImageJ software and the average number is shown. Error bars show the standard deviation. (B) The number of single cells were analyzed based on size of the spheroids measured and size of a single cell (approximately 490 µm^2) to estimate the number of single cells in the field view. Error bars show the standard deviation. *P* values are from two-tailed paired *t* tests. * = $P \leq 0.05$, ** = $P \leq 0.01$, *** = $P \leq 0.001$, **** = $P \leq 0.0001$. PD= PD166866, BGJ= BGJ398, Dov= Dovitinib. (C) The brightfield image of a DU145 spheroid.

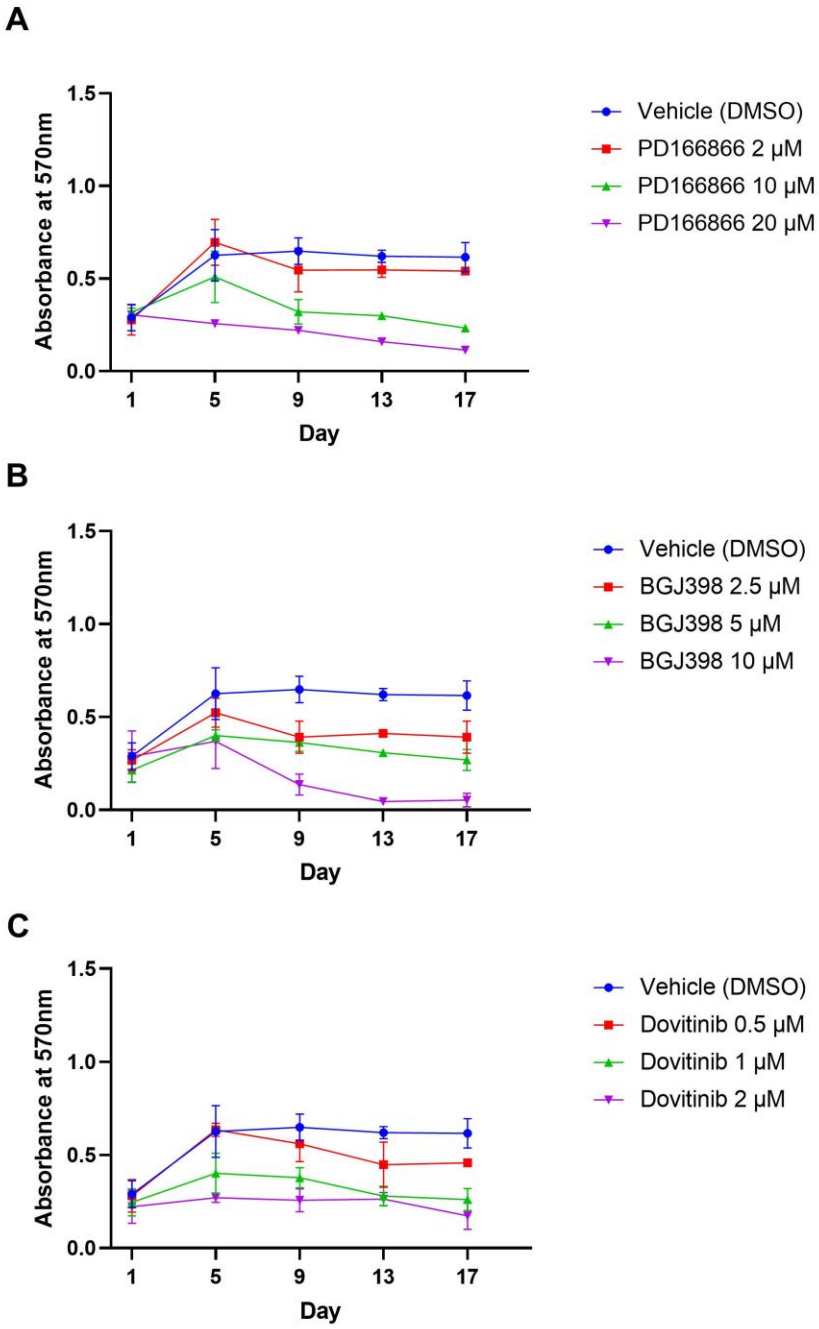

Figure 2.22. FGFR inhibition on LNCaP spheroids.
Triplicate cultures of LNCaP 3D spheroids were grown in RPMI 1640 with 10% SR on agarose-coated dishes. As described in the material and method, samples of cultures were taken and assayed by MTT metabolic assay indicating the number of viable cells on days 1, 5, 9, 13, and 17 to show the proliferation over time. (A) 2 µM -20µM of PD166866 was treated. (B) 2.5µM - 10µM of BGJ398 was treated. (C) 0.5µM -2µM of Dovitinib was treated. Error bars show the standard deviation.

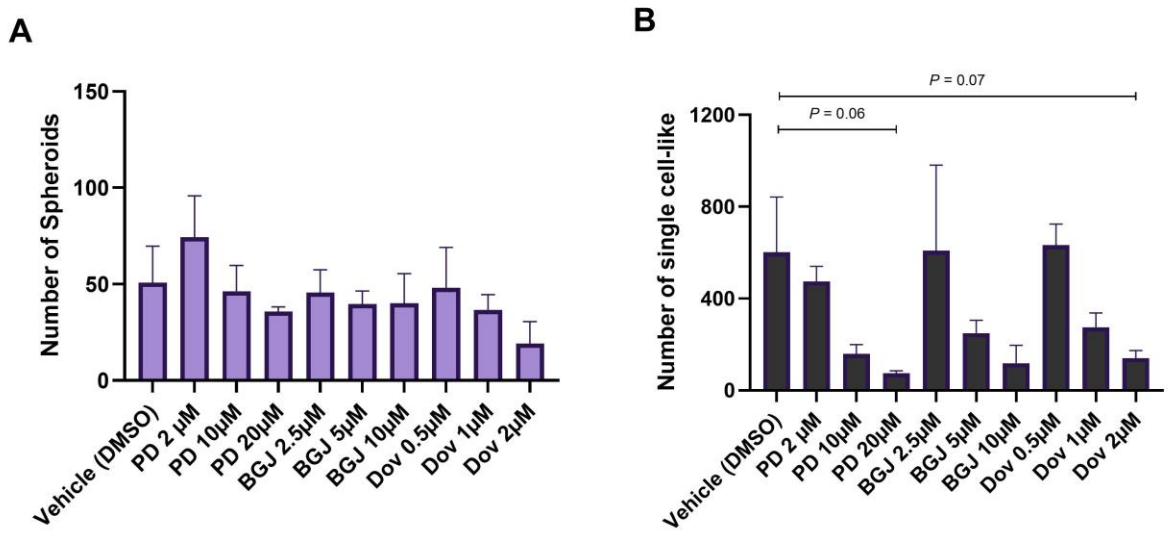

Figure 2.23. The effect of FGFR inhibitor treatment on the number of spheroids and the single cell-like of LNCaP.

(A) The number of spheroids (>500 μm^2) from total 3 random field views were counted using ImageJ software and the average number is shown. Error bars show the standard deviation. (B) The number of single cells were analyzed based on size of the spheroids measured and size of a single cell (approximately 440 μm^2) to estimate the number of single cells in the field view. Error bars show the standard deviation. T-test analysis showed that there are no significant differences between the samples. Two of the lowest *P* values are shown. PD= PD166866, BGJ= BGJ398, Dov= Dovitinib.

Effect of FGFR Inhibition on Signaling Pathways of 3D spheroids

FGFR1 has emerged as a promising target for prostate cancer therapeutics, due to a clinical trial involving Dovitinib treatment (29). However, the mechanism behind Dovitinib treatment has not been clearly elucidated in regard to the activation of FGFR downstream signaling pathways. Our findings suggest that Dovitinib treatment may result in different inhibitory effects depending on the cell line and cell culture conditions (i.e. 2D vs 3D). To better understand the involvement of FGFR and its downstream signaling at a molecular level, we have compared and evaluated the effects of three TKIs, PD166866, BGJ398, and Dovitinib, on the signaling pathways of PC3, LNCaP and DU145 spheroids. We additionally compared the effects of these 3 TKIs to their respective 2D monolayer cells. We performed westernblot analysis, examining receptor expression of FGFR1 and VEGFR2, examined activation of STAT5, AKT, and MAPK pathways, and expression of stemness markers ALDH7A1 and OCT4.

Figure 2. 24 A shows the effects of respective TKIs on PC3 spheroids. We observed that PC3 spheroids were not sensitive to PD166866 (lane 3 and 4), as the activation of downstream cell signaling is similar to that of the negative control (DMSO) in lane 2. Although addition of PD166866 decreased cell survival and proliferation at high concentrations, it is speculated that this effect was exerted through increased cellular toxicity based on the non-FGFR signaling specific inhibition (lane 3 and 4).

Next, FGFR-selective inhibitor, BGJ398, was shown to reduce the expression of VEGFR2 unexpectedly while not affecting the expression of FGFR1(Panel 1 & 2, lane 5 &6). It effectively reduced the kinase activity of FGFR shown via reduction of p-FGFR signal and consequent decrease in p-STAT5 and p-AKT signal (Panel 3, 4 &5, lane 5 &6). However, p-MAPK was shown up-regulated by high concentration treatment, possibly as compensation

mechanism for cell survival (Panel 6, lane 5 &6). The expression of ALDH7A1 was not affected by addition of BGJ398, suggesting there may not be a direct association of FGFR signaling and ALDH7A1 protein expression. However, the activity of ALDH7A1 may have been affected but this remains to be tested (Panel 7, lane 5 &6). OCT4 protein did not show changes in their expression (Panel 8, lane 5 &6).

Addition of Dovitinib, a multi-RTK inhibitor, was shown to decrease the expression of FGFR1 while not affecting VEGFR2 expression (Panel 1 & 2, lane 7 & 8). Although treatment with Dovitinib showed an inhibitory effect on cell survival and proliferation, this may have not been due to FGFR inhibition. We speculate that the this decrease in cell survival and proliferation was due to a global inhibitory effect on multiple RTKs as the kinase activity of FGFR is moderately reduced (Panel 3, lane 7 & 8) while downstream signaling of STAT5, AKT, and MAPK pathways is all effectively down-regulated (Panel 4 & 5 & 6, lane 7 & 8). ALDH7A1 expression was not affected (Panel 7, lane 7 & 8). Interestingly, OCT4 was shown ablated by Dovitinib treatment (Panel 8, lane 7 & 8). It is believed that Dovitinib induces further differentiation of PC3 cells and our previous observation of the morphology change with the treatment. This finding might explain why Dovitinib treatment could result in disease progression observed in the clinical trial (29) since differentiation into neuroendocrine phenotype is more aggressive. Beta-actin was used as a loading control for all samples (Panel 9, all lanes).

Figure 2. 24B shows the effect of TKIs on DU145 spheroids. This result shows that although DU145 spheroids were the most sensitive to FGFR inhibition by all three TKIs, there were no observed effects of TKI treatment on receptor expression (Panel 1 & 2 & 3, lanes 2-8) and little decrease in the activation of downstream signaling (Panel 5 & 6, lanes 2-8).

Of note, Dovitinib was shown to decrease ALDH7A1 expression, possibly suggesting

decreased metastatic potential *in vitro* (Panel 7, lane 7 & 8). It is not clear whether FGFR signaling is involved in this regulation since it is not the only targeted pathway by the inhibitor. Contrasting to the above result with PC3 spheroids that showed ablated OCT4 expression, Dovitinib treatment did not affect OCT4 expression, suggesting that DU145 spheroids may have not undergone differentiation and maintained similar level of stemness (Panel 8, lane 7 & 8).

Taken together, despite the prominent expression of FGFR1 and the sensitive inhibitory response by Dovitinib treatment observed as reduced cell survival and growth, there was no correlation to other markers such as ALDH7A1 and OCT4. These findings suggest that predicting the treatment outcome of FGFR inhibition based on the profile of FGFR1-overexpressing prostate cancer may not lead to the best treatment effect.

Figure 2. 24 C shows the effect of TKIs on LNCaP 3D spheroids. Similar to DU145 spheroids, p-FGFR signal was not detectable to show the direct effect of TKIs on the FGFR kinase activity. The result shows that there were no observed effects of TKI treatment on receptor expression (Panel 1 & 2, lanes 3-8). AKT activation did not seem to be affected by TKI treatments (Panel 3, lanes 3-8). MAPK signaling was only affected by high concentration treatments of BGJ398 and Dovitinib, 5 μM and1 μM treatment, respectively (Panel 4, lanes 6 & 8). Both ALDH7A1and OCT4 expression did not change with addition of TKIs (Panel 7 & 8, lanes 3-8).

Collectively, these findings support that in order to expect significant treatment outcome using TKIs, prostate cancer cells need to be characterized with multiple markers, in addition to FGFR1. ALDH7A1 and OCT4 expression were all different as a result of Dovitinib treatment among all cell lines tested even though they were all expressing FGFR1 prominently. We hypothesized that RTKs other than FGFR may be an important target by Dovitinib to result in

different outcome that we examined the kinase activity of VEGFR2. VEGFR2 expression was observed in PC3 and DU145 spheroids and not in LNCaP spheroids. We probed for the kinase activation of VEGFR2, however, neither cell lines showed detectable p-VEGFR2 signal although the total protein expression was prominent (Figure 2. 25). This suggests that although VEGFR2 expression was found to be significantly increasing in the anchorage independent subgroup of cells compared to the monolayer cells, however, the 3D cells might not be able to produce VEGF for autocrine/paracrine signaling for the receptor to be activated, and signal through VEGFR pathway. There may be other receptor signaling which is utilized by the cells in autocrine/paracrine manner that is targeted by Dovitinib that we have not shown.

Figure 2.24. The effect of FGFR TKI treatment on signaling pathways of 3D spheroids.
All inhibitor treatment was performed every 3-4 days during 2 weeks of culture in triplicate. (A) PD166866 was treated at (L) 2 μM, (H) 10 μM; BGJ398 at (L) 1 μM, (H) 3 μM; Dovitinib at (L) 0.5 μM, (H) 1 μM for PC3 spheroids. (Panel 1, 2) Total expression of FGFR1 and VEGFR2 were probed to show the different effect of BGJ398 and Dovitinib. (Panel 3) p-FGFR signal was detected using p-Y653/654 antibody. (Panel 4) p-STAT5 detected by p-Y694 antibody showed decreased FGFR kinase activity. (Panel 5) p-AKT was probed using p-S473 antibody and the signal was shown decreased by BGJ398 and Dovitinib treatment. (Panel 6) p-MAPK signal shown by phospho-p44/42 MAPK (Erk1/2) (T202/Y204) was largely blocked except in lane 6 with high concentration of BGJ398. (Panel 7) Total expression of ALDH7A1 expression was mostly maintained. (Panel 8) Total expression of OCT4 expression was shown ablated by Dovitinib treatment (lane 7,8) while it was not affected by other inhibitors. (Panel 9) Beta-actin was used as a loading control.
(B) PD166866 was treated at (L) 1 μM, (H) 2 μM; BGJ398 at (L) 0.5 μM, (H) 1 μM; Dovitinib at (L) 0.1 μM, (H) 0.3 μM for DU145 spheroids. (Panel 1, 2, and 3) Total expression of FGFR1 FGFR4 and VEGFR2 were probed and showed little change. (Panel 4) p-AKT was shown mostly decreased by all three inhibitors. (Panel 5) p-MAPK showed little change. (Panel 6) Total expression of ALDH7A1 expression was shown reduced by Dovitinib treatment (lane 7, 8). (Panel 7) OCT4 expression was not affected. (Panel 8) Beta-actin was used as a loading control.
(C) PD166866 was treated at (L) 2 μM, (H) 8 μM; BGJ398 at (L) 2.5 μM, (H) 5 μM; Dovitinib at (L) 0.5 μM, (H) 1 μM for LNCaP spheroids. (Panel 1, 2) Total expression of FGFR1 FGFR4 were probed and showed little change. (Panel 3) p-AKT showed little change. (Panel 4) p-MAPK signal was reduced by high concentration of BGJ398 and Dovitinib (lane 6, 8). (Panel 5, 6) Total expression of ALDH7A1 and OCT4 did not show any change. (Panel 7) Beta-actin was used as a loading control.

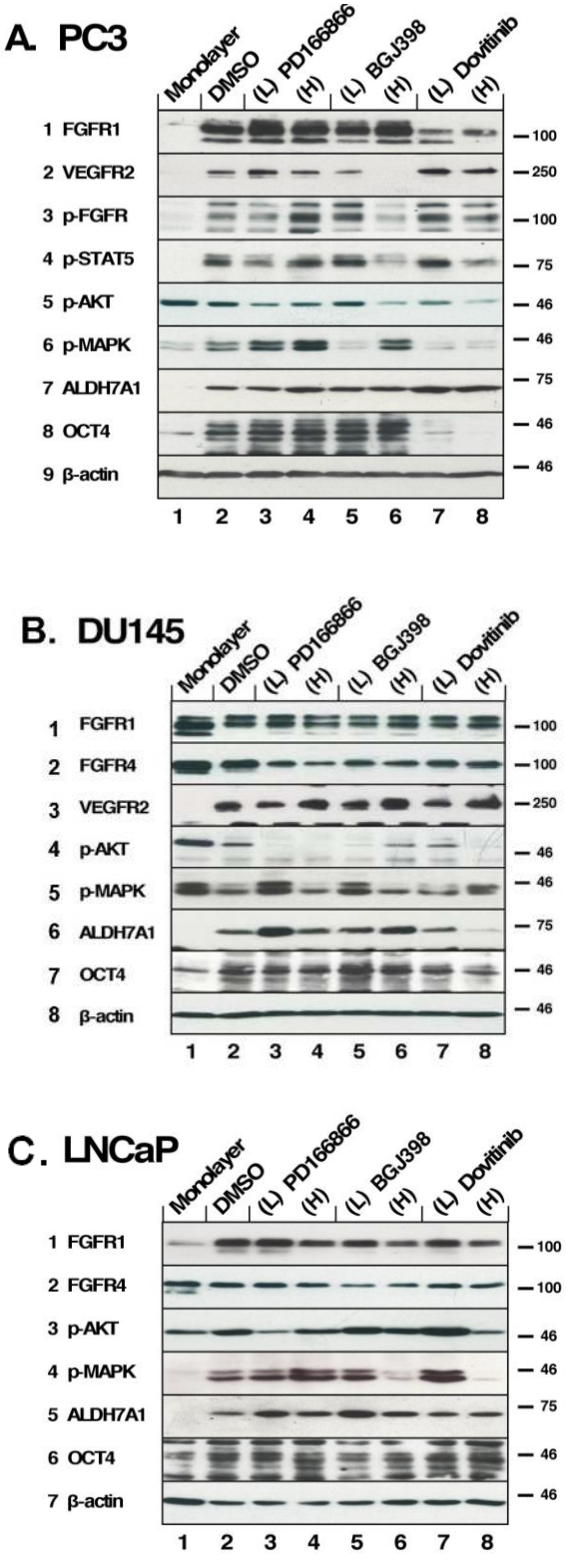
A. PC3
Monolayer
DMSO
(L) PD166866
(H)
(L) BGJ398
(H)
(L) Dovitinib
(H)
1 FGFR1
2 VEGFR2
3 p-FGFR
4 p-STAT5
5 p-AKT
6 p-MAPK
7 ALDH7A1
8 OCT4
9 β-actin
100
250
100
75
46
46
75
46
46
1 2 3 4 5 6 7 8
B. DU145
Monolayer
DMSO
(L) PD166866
(H)
(L) BGJ398
(H)
(L) Dovitinib
(H)
1 FGFR1
2 FGFR4
3 VEGFR2
4 p-AKT
5 p-MAPK
6 ALDH7A1
7 OCT4
8 β-actin
100
100
250
46
46
75
46
46
1 2 3 4 5 6 7 8
C. LNCaP
Monolayer
DMSO
(L) PD166866
(H)
(L) BGJ398
(H)
(L) Dovitinib
(H)
1 FGFR1
2 FGFR4
3 p-AKT
4 p-MAPK
5 ALDH7A1
6 OCT4
7 β-actin
100
100
46
46
75
46
46
1 2 3 4 5 6 7 8

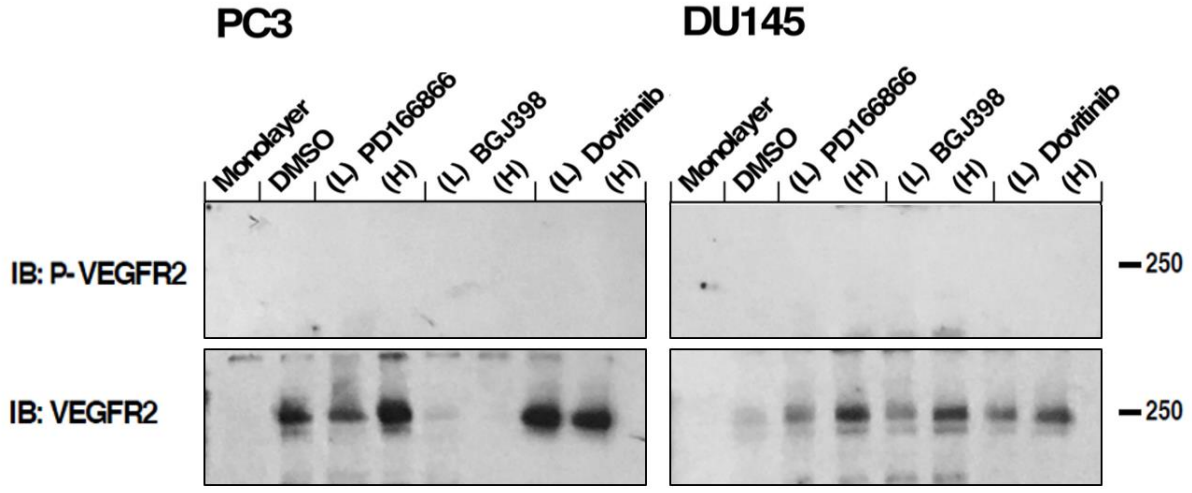

Figure 2.25. No phosphorylation of VEGFR2 was detected from PC3 and DU145 spheroids. Top panels show p-VEGFR signal probed using p-Y1175 antibody and no signal was detected. Bottom panels show the total expression of VEGFR2 by PC3 and DU145 spheroids. Monolayer cells of PC3 and DU145 in each panel were included as a negative control for VEGFR2 expression. PD166866 was treated at (L) 2 μM, (H) 10 μM; BGJ398 at (L) 1 μM, (H) 3 μM; Dovitinib at (L) 0.5 μM, (H) 1 μM for PC3 spheroids, DMSO as a negative control. PD166866 was treated at (L) 1 μM, (H) 2 μM; BGJ398 at (L) 0.5 μM, (H) 1 μM; Dovitinib at (L) 0.1 μM, (H) 0.3 μM for DU145 spheroids, DMSO as a negative control.

Effect of FGFR Inhibition on Gene Expression of 3D spheroids of AR-independent Prostate Cancer Cell Lines

We aimed to compare the gene expression of 2D monolayer cells and 3D spheroids of PC3 and DU145 and also the effect of BGJ398 and Dovitinib on the 3D spheroids. RT-qPCR was performed for the target genes of FGFR1, OCT4, ALDH7A1, E-cadherin, Vimentin, and Snail in PC3 cells and the relative mRNA expression was determined by normalizing against the housekeeping gene, beta-actin (**Figure 2.26**). First of all, FGFR1 mRNA was found increased about 3.8-fold in PC3 spheroids compared to 2D monolayer cells, supporting that FGFR1 supports the anchorage independent growth of PC3 spheroids. The treatment of BGJ398 and Dovitinib resulted in the up-regulation of FGFR1, possibly compensating for the inhibited activity. PC3 spheroids also up-regulated OCT4 about 11-fold, and ALDH7A1 about 7-fold,

showing that the PC3 spheroids are enriched for stemness property. The treatment of BGJ398 and Dovitinib resulted in the decrease of OCT4 to demonstrate that FGFR1 regulates stemness in PC3. ALDH7A1 was decreased only by BGJ398 and was not affected by Dovitinib, suggesting that it may regulated by FGFR1 but in combination with other kinases of Dovitinib. Taken together, inhibition of FGFR1 via TKI treatment may target the CSC population of PC3, suppressing the self-renewal ability of these tumorigenic cells.

We examined the mRNA levels of EMT markers of E-cadherin, Vimentin, and Snail to find that 3D spheroids of PC3 show increased metastatic potential than 2D monolayer cells, which is considered highly metastatic cell line among the common cell lines used in prostate cancer research (**Figure 2.26 D-F**). The result showed that PC3 spheroids up-regulate E-cadherin, vimentin, and Snail, which suggests that cells maintained its epithelial characteristics but possessed increased motility. Notably, PC3 spheroids showed about 69-fold increase in the level of vimentin. Vimentin is a type of intermediate filaments, regulated by transcription factors of Twist, Snail, Zeb1 and Slug, which promotes cell migration and invasion. It is considered a potential drug target for cancer treatment for its role in EMT and metastasis (126). BGJ398 and Dovitinib treatment reduced the level of E-cadherin and vimentin, but not of Snail, and notably as a response to Dovitinib treatment, the expression of Snail increased significantly compared to that of negative control treated with DMSO. Taken together, the specific inhibition of FGFR signaling by BGJ398 showed more favorable molecular level changes than the utilization of multi-RTK inhibitor Dovitinib as BGJ398 was shown to target the CSCs more effectively indicated by reduced ALDH7A1 regulation and with less predicted adverse effect indicated by marginal increase in level of Snail compared to Dovitinib. Exact values in the fold changes of mRNA expression for all the target genes are detailed in the **Table 2.3**.

In DU145 cells, RT-qPCR was performed for the same target genes of FGFR1, OCT4, ALDH7A1, E-cadherin, Vimentin, and Snail (**Figure 2.27**). In DU145 spheroids compared to 2D monolayer cells, FGFR1 mRNA level was found increased about 1.7-fold, which was increased by TKI treatment even further, and showed almost no changes in OCT4 expression, and ALDH7A1 mRNA level was increased about 1.5-fold. TKI treatment didn't seem to affect stemness of DU145 spheroids shown by the gene regulations.

Next, we examined the mRNA levels of EMT markers of E-cadherin, vimentin, and Snail (**Figure 2.27D-F**). Similar to PC3 spheroids, DU145 spheroids up-regulated E-cadherin, and Snail, however, the level of vimentin was found decreased about 0.6-fold. The results were not clear to assess any changes in the metastatic potential of the DU145 spheroids. There were no significant changes of the EMT markers by the TKI treatment. Although it was observed that DU145 spheroids respond to TKI treatment sensitively at a cellular level, TKI treatment did not lead to any significant changes in the gene regulation shown by the RT-qPCR results. Exact values in the fold changes of mRNA expression for all the target genes are detailed in the **Table 2.4**.

In a conclusion, higher fold changes were observed for both CSC markers and EMT markers in PC3 spheroids than in DU145 spheroids compared to their 2D monolayer cells, and the effect of TKIs were more prominent in PC3 spheroids. The data may suggest that CSCs exhibit more metastatic property than the bulk population. Both PC3 and DU145 cell lines are AR-negative but prostate cancer is very heterogeneous and thus it may be speculated that the difference in up-regulation of FGFR1 may play a role in the stemness and inclination for EMT process.

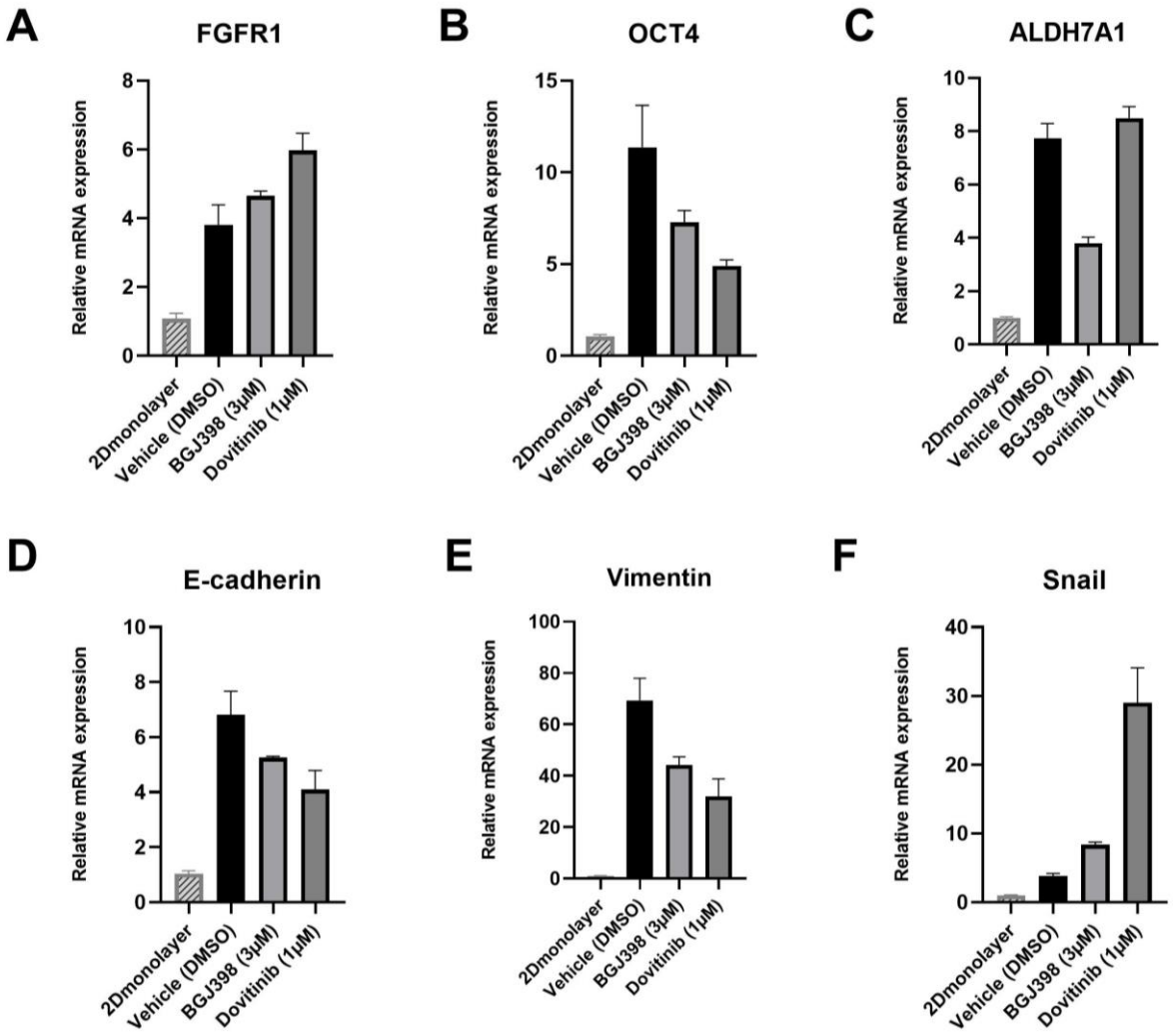

Figure 2.26. RT-qPCR of PC3 cells treated with TKIs.

Gene expression of PC3 2D monolayer and the spheroids cultured for 14 days and their response to TKI treatment of BGJ398 and Dovitinib was examined. RT-qPCR was performed for (A) FGFR1, (B) OCT4, a stem cell marker, (C) ALDH7A1, prostate specific CSC marker, and (D) the epithelial marker, E-cadherin, (E, F) the mesenchymal markers, vimentin and Snail. mRNA expression was normalized against beta-actin and the fold changes were evaluated. The data represent the average of three independent experiments and the error bars represent standard error of the means (mean ± SEM).

Table 2.3. Fold changes of the target genes in quantitative PCR of PC3 cells.
Fold change value and the standard error of mean of each data point from the graph above was provided in the table below.

Genes	Samples	Fold changes with SEM
FGFR1	2Dmonolayer	1.08 ± 0.18
	Vehicle (DMSO)	3.8 ± 0.7
	BGJ398 (3μM)	4.65 ± 0.16
	Dovitinib (1μM)	6.0 ± 0.6
OCT4a	2Dmonolayer	1.05 ± 0.13
	Vehicle (DMSO)	11.4 ± 2.7
	BGJ398 (3μM)	7.3 ± 0.8
	Dovitinib (1μM)	4.9 ± 0.4
ALDH7A1	2Dmonolayer	1.01 ± 0.05
	Vehicle (DMSO)	7.7 ± 0.6
	BGJ398 (3μM)	3.80 ± 0.27
	Dovitinib (1μM)	8.5 ± 0.5
E-cadherin	2Dmonolayer	1.04 ± 0.12
	Vehicle (DMSO)	6.8 ± 1.0
	BGJ398 (3μM)	5.26 ± 0.05
	Dovitinib (1μM)	4.1 ± 0.8
Vimentin	2Dmonolayer	1.03 ± 0.09
	Vehicle (DMSO)	69.3 ± 9.9
	BGJ398 (3μM)	44 ± 4
	Dovitinib (1μM)	32 ± 8
Snail	2Dmonolayer	1.02 ± 0.07
	Vehicle (DMSO)	3.9 ± 0.4
	BGJ398 (3μM)	8.4 ± 0.4
	Dovitinib (1μM)	29 ± 6

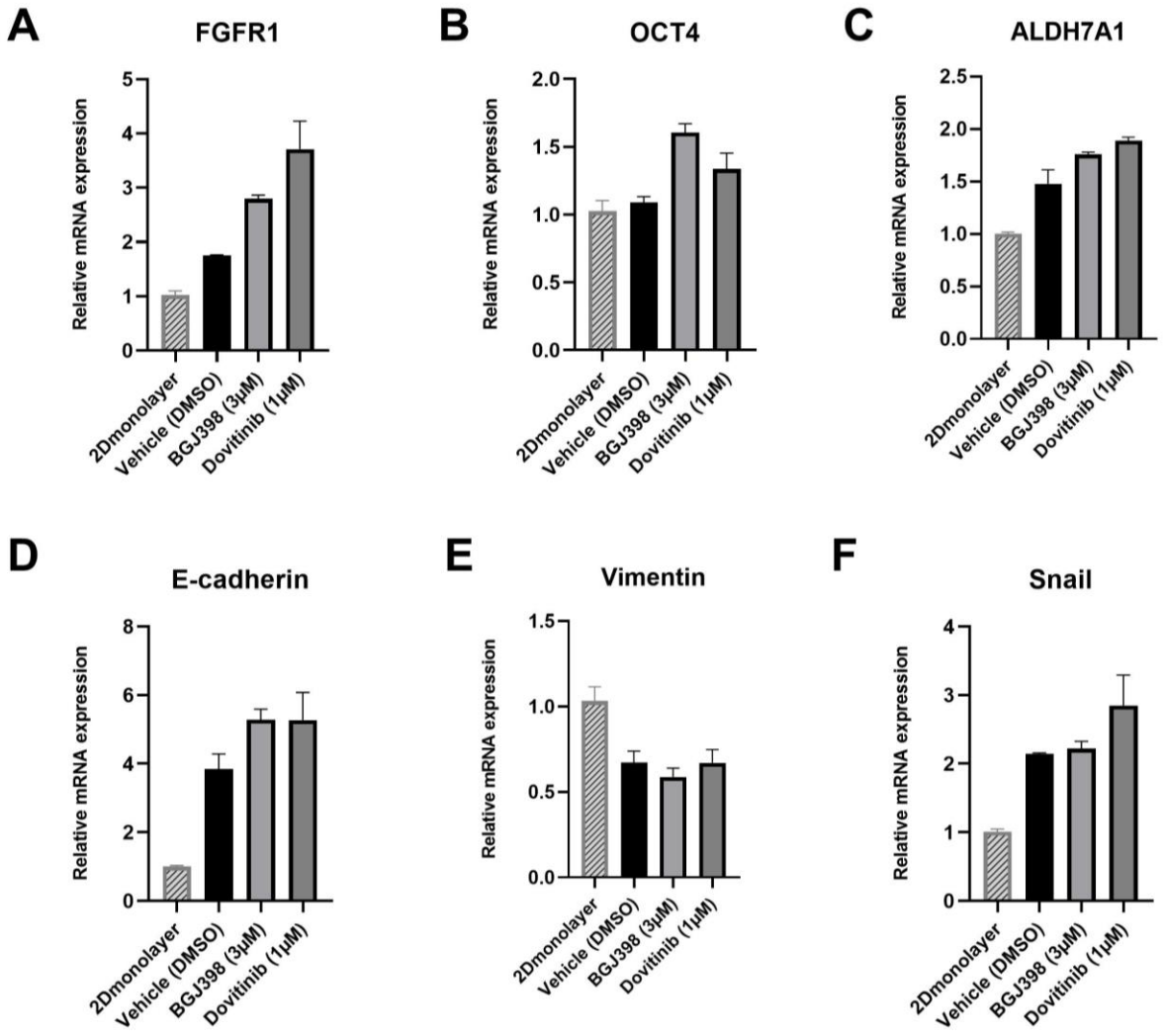

Figure 2.27. RT-qPCR of DU145 cells treated with TKIs.

Gene expression of DU145 2D monolayer and the spheroids cultured for 14 days and their response to TKI treatment of BGJ398 and Dovitinib was examined. RT-qPCR was performed for (A) FGFR1, (B) OCT4, a stem cell marker, (C) ALDH7A1, prostate specific CSC marker, and (D) the epithelial marker, E-cadherin, (E, F) the mesenchymal markers, vimentin and Snail. mRNA expression was normalized against beta-actin and the fold changes were evaluated. The data represent the average of three independent experiments and the error bars represent standard error of the means (mean ± SEM).

Table 2.4. Fold changes of the target genes in quantitative PCR of DU145 cells.

Fold change value and the standard error of mean of each data point from the graph above was provided in the table below.

Genes	Samples	Fold changes with SEM		
FGFR1	2Dmonolayer	1.02	±	0.09
	Vehicle (DMSO)	1.76	±	0.01
	BGJ398 (3μM)	2.80	±	0.08
	Dovitinib (1μM)	3.7	±	0.6
OCT4a	2Dmonolayer	1.03	±	0.09
	Vehicle (DMSO)	1.09	±	0.05
	BGJ398 (3μM)	1.61	±	0.07
	Dovitinib (1μM)	1.34	±	0.14
ALDH7A1	2Dmonolayer	1.00	±	0.02
	Vehicle (DMSO)	1.48	±	0.15
	BGJ398 (3μM)	1.76	±	0.03
	Dovitinib (1μM)	1.89	±	0.04
E-cadherin	2Dmonolayer	1.00	±	0.04
	Vehicle (DMSO)	3.8	±	0.5
	BGJ398 (3μM)	5.3	±	0.4
	Dovitinib (1μM)	5.3	±	0.9
Vimentin	2Dmonolayer	1.03	±	0.10
	Vehicle (DMSO)	0.67	±	0.08
	BGJ398 (3μM)	0.59	±	0.06
	Dovitinib (1μM)	0.67	±	0.09
Snail	2Dmonolayer	1.01	±	0.05
	Vehicle (DMSO)	2.146	±	0.015
	BGJ398 (3μM)	2.22	±	0.12
	Dovitinib (1μM)	2.85	±	0.51

Utilization of Induced Pluripotent Stem (iPS) 87 Cells

As we examined the prostate CSCs from the common cancer cell lines by selection and enrichment, we also aimed to investigate 3D culture of iPSC-derived cells from biopsy samples of prostate cancer patient (iPS87 cells). The iPS87 cell line was established recently, by reprogramming primary prostate tumor cells into iPSCs and was shown to possess tumor initiating ability *in vivo*. The iPS87 cells are grown as colonies on mouse embryonic fibroblast (MEF) feeder cell layer in ES+/+ medium (described in the Material and Method section), however, in the absence of the MEF layer they readily formed 3D spheroids in the same medium on a regular TC plate. As shown in the **Figure 2.28**., single cells detached from the MEF layer after a day were free-floating, and by 7 days, they were able to grow into a spheroid size of about 100 µm, and by 14 days they were fully grown, and no apparent size change was observed passed the time point but the cell culture media became acidic, turning yellow in color.

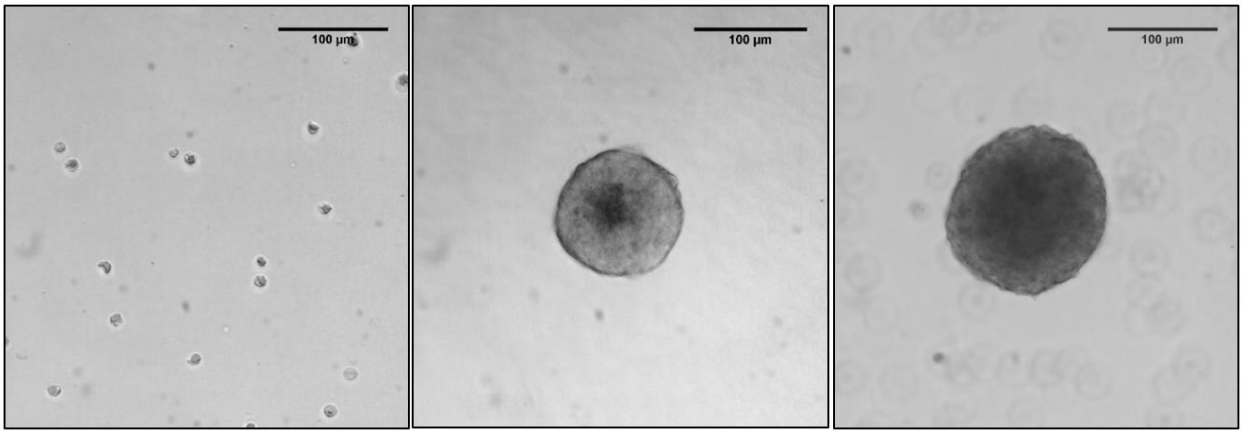

Figure 2.28. Brightfield microscope images of iPS87 cells and spheroids.
The left panel shows single cells of iPS87 in a TC plate after 24 hours of culturing on a TC plate in ES+/+ medium, and the middle panel shows growth of a spheroid at day 7, and the right panel shows a spheroid at day 14. The scale bars indicate 100 µm.

The protein expression of iPS87 single cells and the spheroids were examined via westernblot on days 1, 7, and 14 comparing the same amount of total protein lysates (**Figure**

2.29). It was found that the iPS87 cells initially express FGFR1, but the kinase activity is not detectable as shown in panels of 1 and 2. Interestingly, the spheroids express increased FGFR1 protein and the phospho-FGFR signal was detected, as well as increased downstream signaling of STAT3, STAT5, AKT, and MAPK pathways shown in panels of 3-6. The CSC markers of ALDH7A1 and OCT4 were found increased as shown in panels 7 and 8.

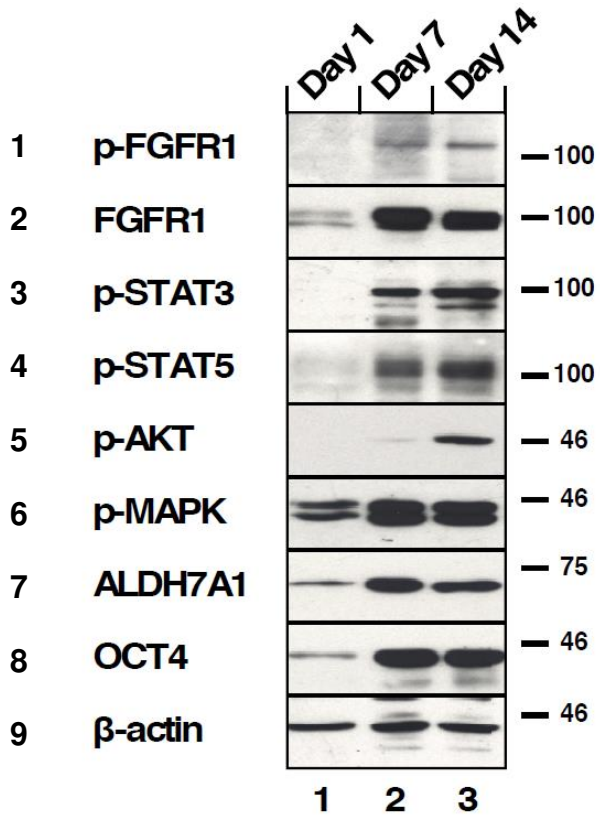

Figure 2.29. Expression and downstream cell signaling activation of FGFR of iPS87 cells. iPS87 cells on day 1 as single cells in lane 1, and 3D spheroids on day 7 in lane 2 and day 14 in lane 3 were subjected to westernblot analysis. (1st row) FGFR activation was shown by immunoblotting for phospho-Y653/654 FGFR antiserum and only PC3 spheroids showed positive signal. (2nd row) Total FGFR1 expression was shown increasing as cultured into spheroids. (3rd row) STAT3 activation was detected by immunoblotting for phospho-Y705-STAT3, and (4th row) STAT5 activation was detected by immunoblotting for phospho-Y694-STAT5. (5th row) AKT activation was detected by immunoblotting for phospho-S473-AKT. (6th row) MAPK activation was shown by immunoblotting for phospho-T202/Y204-MAPK. (7th row) Total ALDH7A1 expression and (8th row) OCT4 expression was shown increasing as cultured into spheroids. (9th row) Beta-actin was used as a loading control.

We then investigated if the 3D spheroids of iPS87 require FGF/FGFR signaling for cell survival and growth via MTT assay over the time-course of 11 days. As the cell line is maintained in the ES+/+culture with exogeneous bFGF added unlike the culture condition used for the cell lines of PC3, DU145, and LNCaP, it was hypothesized that bFGF is essential for the growth of iPS87 cells and the 3D spheroids. Indeed, it was observed that in the absence of bFGF the proliferation was hindered to approximately 30-40% (data not shown).

Next, to examine the effect of BGJ398 and Dovitinib, samples of cell culture were used for measuring metabolic activity by MTT assay on days 1, 4, 7 and 11, followed by the treatment with the TKIs every 3 days. Both BGJ398 (10nM-100nM) and Dovitinib (100nM-1μM) demonstrated their inhibitory effect reducing the metabolic activity in a dose dependent manner shown in F**igure 2.30 A, B**. The 3D spheroids of iPS87 responded to TKI treatment the most sensitively at nanomolar range, highlighting their dependency of FGFR signaling. The number of spheroids were found decreased as a result of the TKI treatment (**Figure 2.30 C**) and collectively the data support that FGFR inhibition results in the decrease of cell survival and proliferation combined with MTT assay.

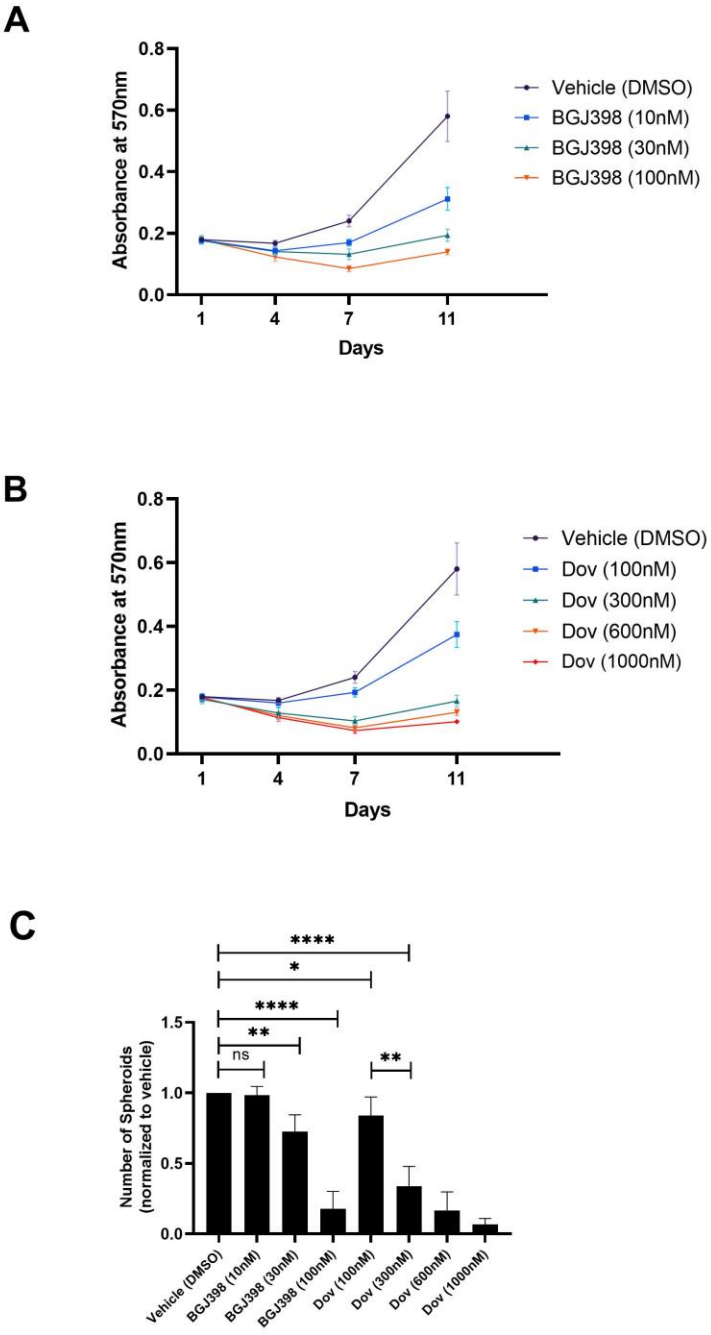

Figure 2.30. iPS87 MTT and number of spheroids.
Triplicate cultures of 3D spheroids of iPS87 were grown in ES+/+ on 12-well TC plates. Samples of cultures were assayed by MTT metabolic assay indicating the number of viable cells on days 1, 4, 7, and 11 to show the proliferation over time. (A) 10nM -100nM of BGJ398 was treated. (B) 100nM-1μM of Dovitinib was treated. Triplicate experiment was performed, and error bars show the standard deviation. (C) The number spheroids (>1,000 μm^2) from each well of 12-well plates were subjected to counting at day 11. Error bars show the standard deviation. *P* values are from two-tailed paired t tests. ns= not significant ($P>0.05$), * = $P \leq 0.05$, ** = $P \leq 0.01$, **** = $P \leq 0.0001$.

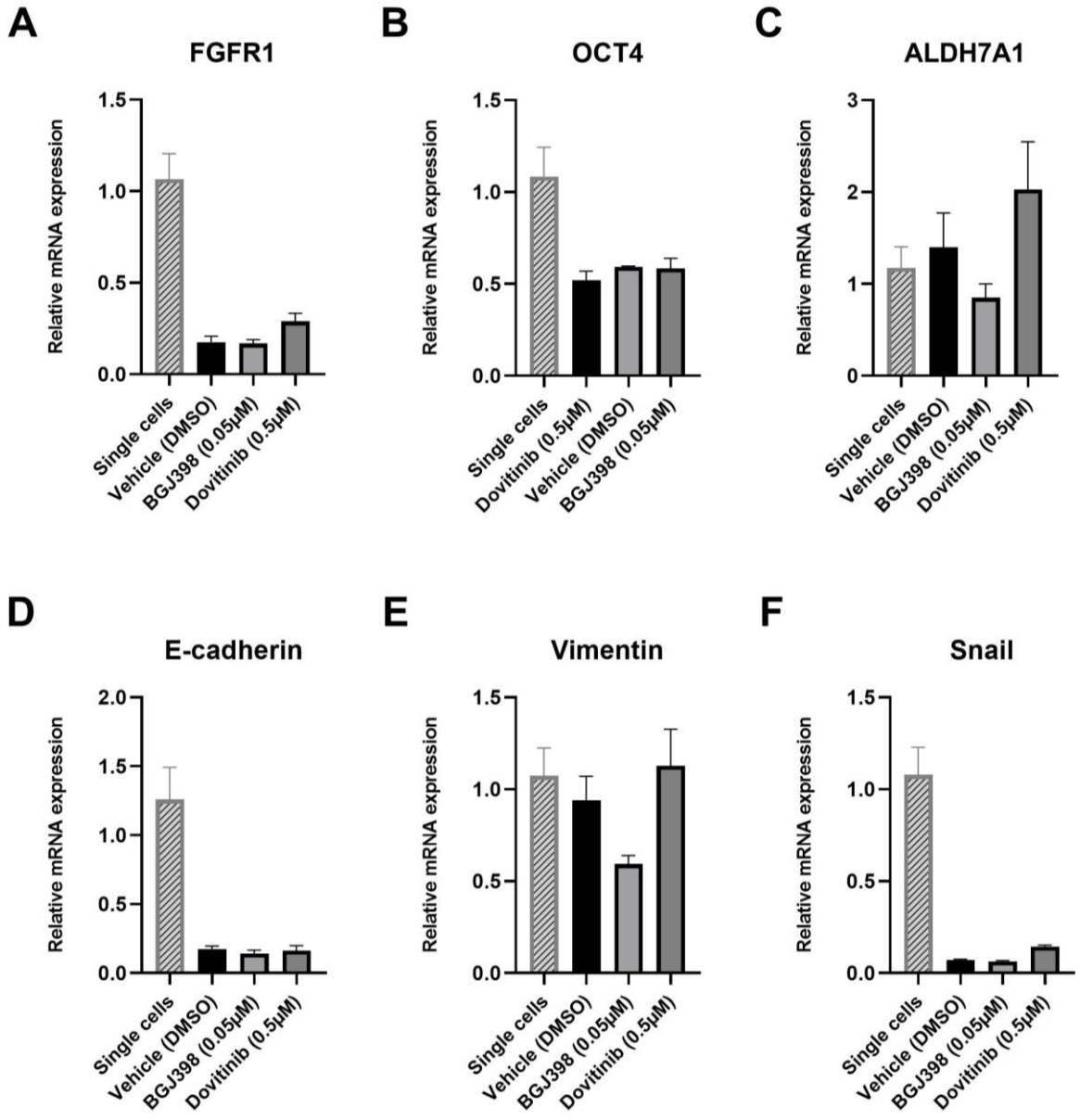

Figure 2.31. RT-qPCR of iPS87 cells treated with TKIs.

Gene expression of iPS87 single cells and the spheroids cultured for 11 days and their response to TKI treatment of BGJ398 and Dovitinib was examined. RT-qPCR was performed for (A) FGFR1, (B) OCT4, a stem cell marker, (C) ALDH7A1, prostate specific CSC marker, and (D) the epithelial marker, E-cadherin, (E, F) the mesenchymal markers, vimentin and Snail. mRNA expression was normalized against beta-actin and the fold changes were evaluated. The data represent the average of three independent experiments and the error bars represent standard error of the means (mean ± SEM).

Table 2.5. Fold changes of the target genes in quantitative PCR of iPS87 cells.
Fold change value and the standard error of mean of each data point from the graph above was provided in the table below.

Genes	Samples	Fold changes with SEM		
FGFR1	2Dmonolayer	1.07	±	0.16
	Vehicle (DMSO)	0.18	±	0.04
	BGJ398 (3μM)	0.17	±	0.02
	Dovitinib (1μM)	0.29	±	0.05
OCT4a	2Dmonolayer	1.08	±	0.18
	Vehicle (DMSO)	0.593	±	0.004
	BGJ398 (3μM)	0.58	±	0.06
	Dovitinib (1μM)	0.52	±	0.06
ALDH7A1	2Dmonolayer	1.18	±	0.26
	Vehicle (DMSO)	1.4	±	0.4
	BGJ398 (3μM)	0.85	±	0.17
	Dovitinib (1μM)	2.0	±	0.6
E-cadherin	2Dmonolayer	1.26	±	0.27
	Vehicle (DMSO)	0.17	±	0.03
	BGJ398 (3μM)	0.14	±	0.03
	Dovitinib (1μM)	0.16	±	0.04
Vimentin	2Dmonolayer	1.07	±	0.17
	Vehicle (DMSO)	0.94	±	0.15
	BGJ398 (3μM)	0.59	±	0.05
	Dovitinib (1μM)	1.13	±	0.23
Snail	2Dmonolayer	1.08	±	0.17
	Vehicle (DMSO)	0.071	±	0.005
	BGJ398 (3μM)	0.063	±	0.006
	Dovitinib (1μM)	0.144	±	0.009

Effect of FGFR Inhibition on Gene Expression of 3D spheroids of iPS87 cells

We aimed to compare the gene expression of single cells and 3D spheroids of iPS87 and also the effect of BGJ398 and Dovitinib on the 3D spheroids. RT-qPCR was performed for the target genes of FGFR1, OCT4, ALDH7A1, E-cadherin, Vimentin, and Snail. The relative mRNA expression was determined by normalizing against the housekeeping gene, beta-actin (**Figure 2.31**). Noticeably, FGFR1 mRNA was found decreased about 0.18-fold in the spheroids compared in single cells in contrast to up-regulating FGFR1 protein expression shown via westernblot. The spheroids also showed decrease in the level of OCT4 mRNA about 0.59-fold, in contrast to up-regulating OCT4 protein. We speculate that as the single cells of iPS87 proliferate without the MEF feeder layer which prevents differentiation and maintains the stemness characteristics of the iPSCs, the differentiated spheroids may not be able to express self-renewal genes as much as the iPSCs and so to compensate they up-regulate the protein expression. TKI treatment did not affect the gene expression of FGFR1 and OCT4. The level of ALDH7A1 mRNA expression showed no significant changes as the iPS87 cells grow into spheroids or when treated with TKIs.

We examined the mRNA levels of EMT markers of E-cadherin, vimentin, and Snail as before (**Figure 2.31 D-F**). The results showed that E-cadherin and Snail were significantly down-regulated in the spheroids but were not affected by TKI treatment. Vimentin level was not changed growing into spheroids and was only affected when treated with BGJ398, being decreased by about 0.59-fold. Overall, FGFR inhibition didn't seem to result in any significant changes of the EMT markers, and although FGFR inhibition reduces the survival and proliferation of the spheroids, no apparent molecular level changes occurred to indicate for favorable outcome caused by suppression of FGFR signaling.

DISCUSSION

Current prostate cancer therapies focus on the targeting of AR signaling. However, a majority of patients eventually develop progressive disease, eventually becoming AR-negative and castration independent. Thus, androgen deprivation therapy (ADT) is no longer a plausible treatment option for these patients. This highlights the need for the development of therapeutic options to treat CRPC patients. It has been particularly challenging to find a new target due to the overwhelming heterogeneity of prostate cancer in contrast to many other solid tumors. Efforts have been made to find non-AR related targets that can be clinically utilized for prognostic purposes, and FGFR1 has been shown to be a promising alternative target (26, 27, 28, 29).

In this study, it was hypothesized that there is a rare population of prostate CSCs with stemness properties that are AR-independent, and these cells may promote cancer progression to more aggressive phenotype via FGFR1 and its downstream signaling pathways. It was investigated if inhibition of FGFR signaling utilizing TKI treatment would lead to any changes at a molecular and cellular level that may be favorable for CRPC patients. Additionally, the study aimed to provide a comparison of utilizing FGFR specific inhibitor versus multi-RTK inhibitor as the multi-RTKs commonly show excellent efficacy but adverse off-target effects, by using 3D culture system of human cancer cell lines and of human iPSC-derived cells from biopsy samples of a prostate cancer patient (iPS87 cells) (126).

First of all, the study presented here reports for the first time that FGFR1 expression is up-regulated in PC3 and LNCaP spheroids and is maintained in DU145 spheroids in a culture condition supporting stem cell growth in the absence of serum and of exogeneous addition of bFGF, establishing a new 3D in vitro model to study the involvement of FGFR1 using the

common cell lines. Although FGFR1 has been shown to be overexpressed in prostate cancer patient samples through sequencing and FGFR1-overexpressing PDX models have been developed (29), prostate cancer cell lines used in pre-clinical research do not show sufficient detectable FGFR1 expression to be suitable for studying the role of FGFR signaling. This issue hinders efforts of researchers to examine endogenous FGFR signaling without exogenous DNA transfection. For example, previous research by Feng *et al*. (127) has examined the effect of AZ8010, an ATP-competitive FGFR tyrosine kinase inhibitor, on prostate cancer cells overexpressing FGFR1 or FGFR4 to suggest that targeting FGFR signaling inhibits prostate cancer progression. However, because FGFRs and its downstream pathways are artificially hyperactivated, the usage of FGFR-transfected cell lines stimulated with FGF may not provide an accurate understanding of the involvement of FGFRs, which limits clinical relevance unless supported by findings from mouse models. Thus, the in vitro model utilizing 3D spheroids is expected to provide significant values to other researchers who do not have access to suitable patient samples or PDX models for investigation of FGFR in prostate cancer.

As 3D culturing of cells select for the cells which possess anchorage-independent properties, it was hypothesized that 3D spheroids would be enriched for stem/progenitor like cells from the bulk population. This study demonstrates the role of FGFR signaling in prostate CSCs which require FGFR signaling for their survival and proliferation. Both FGFR specific inhibitor and multi-RTK inhibitor effectively suppressed the growth of prostate CSCs in PC3, DU145 and iPS87 cell lines that are AR-negative. FGFR1 has been shown to promote stemness in malignant subpopulations in lung cancer (71) and breast cancer (128), and here, this study provides evidence for the first time that FGFR1 supports the CSC population in prostate cancer not only at a cellular level but also at a molecular level.

The previous report by Wan *et al*. (29) has shown an antitumor effect of Dovitinib targeting FGFR1 in prostate cancer *in vivo*, however, the authors were not able to clarify the molecular mechanism as they were not able to observe any effects of Dovitinib on FGFR downstream signaling pathways of STAT, AKT, and MAPK. This study presented here provides the result of FGFR inhibition in prostate CSCs with up-regulated FGFR1 by both BGJ398 and Dovitinib. All three prostate cancer cell lines of PC3, Du145, and LNCaP showed different activation of the STAT, AKT, and MAPK pathways as they were selected for 3D spheroids, but consistently TKI treatment by both BGJ398 and Dovitinib decreased the activation of the downstream signaling.

Of note, the spheroids of LNCaP cells didn't seem to respond significantly to FGFR inhibitors at a cellular level despite the up-regulation of FGFR1, which may be due to the inefficient inhibition of Akt signaling shown by immunoblotting. Moreover, LNCaP cells are AR-positive which may activate an unidentified compensatory signaling mechanism. A study by Bluemn *et al.* (129) has shown that AR-null/NE-null LNCaP cells which survived AR antagonists exhibited increased FGF signaling and were more sensitive to FGFR inhibition than AR-positive LNCaP cells. They identified activation of the MAPK pathway as the main mechanism allowing AR-independent signaling pathway and which supports proliferation and survival of the double negative prostate cancer cells *in vitro* and *in vivo*. Taken together, the results from this study and of Bluemn and colleagues strongly support the concept that FGFR/MAPK inhibition may be a promising strategy for the treatment of AR-negative prostate cancer but less effective for AR-positive prostate cancer.

Furthermore, the differential activation of FGFR and its downstream signaling between

2D and 3D cell culture provide evidence that FGFR signaling is involved in maintenance of prostate cancer stem cells enriched by one of the characteristics of anchorage independence, and not of the bulk population. Numerous research articles have emphasized that cells grown in 2D conventional method may not recapitulate gene/protein expression and thus drug response in human tumor physiology (73-75, 110, 111). This study demonstrates that the 3D spheroids of PC3, DU145 and iPS87 show different activation of FGFR as well as up-regulation of OCT4, a stem cell marker, and ALDH7A1, a CSC marker in prostate cancer examined via RT-qPCR. ALDH7A1 has been shown by other studies (66, 116) to be utilized as a CSC marker in prostate cancer that progresses to metastasis.

As CSCs are considered to be responsible for drug resistance in many cancer types including prostate cancer, this study aimed to examine if TKI treatment targeting FGFR would show signs of drug resistance suggested via ALDH7A1 expression. This study demonstrated that both gene and protein expression of ALDH7A1 in the 3D spheroids of PC3, DU145 and iPS87 increased when treated with Dovitinib. The result suggests that Dovitinib treatment may have an adverse effect and that utilizing TKIs with greater specificity for FGFR may have more favorable outcomes in clinical setting. Further investigation is needed to assess the direct correlation of ALDH7A1 levels to TKI treatment as FGFR-specific TKI treatment using BGJ398 decreased its expression in 3D spheroids of PC3 and iPS87 cells. Interestingly, a study by Yadav *et al.* (130) has provided findings regarding the effect of Dovitinib in prostate cancer treatment; they found that PC3 cells and LNCaP cells differentiated into a neuroendocrine phenotype, which is a more aggressive prostate cancer. The authors examined 2D cell culture which certainly affected their outcome; nevertheless, the negative off-target effect of Dovitinib in promoting neuroendocrine differentiation was observed. With its greater specificity, it may be predicted that BGJ398 will

likely have more beneficial effects based on the findings from PC3 and iPS87 spheroids that ALDH7A1 was decreased.

Nevertheless, long-term assays taking about 3-18 months are required to accurately assess the drug resistance of cells *in vitro* (131). Further assessment is required to utilize ALDH7A1 as a prognostic marker as it remains unclear if FGFR1 regulates ALDH7A1 activity in prostate cancer, and the extent to which other kinase receptors that are targeted by Dovitinib are involved in modulation of ALDH7A1 activity. In fact, it was examined in this study if VEGFR2 is involved since it is one of the main targets of Dovitinib and it plays an important role in angiogenesis and cancer progression. However, kinase activation of VEGFR2 was not detected, although we found increased expression of VEGFR2 in PC3 and DU145 spheroids. It would be worth investigating if the specific inhibition of FGFR signaling would benefit prostate cancer patients regardless of their response to ADT therapy, decreasing the probability of cancer metastasis and drug resistance through regulation of ALDH7A1.

This study also examined whether prostate CSCs would possess increased metastatic potential as CSCs are considered to be responsible for cancer metastasis in numerous cancer types (61, 63). It effects of TKI treatment on EMT markers was examined via RT-qPCR to provide information at a molecular level.

The results show that the spheroids of PC3 cells significantly up-regulate Vimentin and Snail, which are critical mesenchymal markers in the EMT process indicating increased metastatic potential of the cells enriched for their stemness property via 3D culture. The epithelial–mesenchymal transition (EMT) refers to the developmental process whereby epithelial cells acquire mesenchymal features. In cancer biology, EMT is correlated with tumor initiation,

invasion, and metastasis. Interestingly, the spheroids of PC3 cells show increased level of E-cadherin, which may seem to contradict the typical EMT process, where the loss of the cell adhesion molecule, E-cadherin, occurs as the initiation of EMT process prior to acquisition of enhanced cell mobility. The result from this study is in line with findings by De Marzo *et al.* (132), describing re-expression of previously downregulated E-cadherin in tumor samples of advanced prostate cancer patients, showing its potential to be used as a biomarker of disease progression. Another study by Bae *et al.* (133) showed that the E-cadherin-positive subpopulation in PC3 and DU145 cell lines compared to E-cadherin-negative cells exhibited highly invasive properties, significant tumor formation in mouse models, and higher expression of stem cell markers. Taken together, the results support that the 3D culture system may select for prostate CSCs that possess increased metastatic potential and ultimately support the notion that CSCs are responsible for cancer re-occurrence and metastasis suggested by many researchers and reviewed here (61).

3D spheroids of DU145 showed increased E-cadherin and Snail, suggesting a similar trend in PC3 spheroids; however, the level of vimentin decreased, displaying the heterogeneous characteristics of prostate cancer cell lines. Further examination of mesenchymal markers such as ZEB, Twist, and N-cadherin may provide a more complete understanding of EMT and metastasis for this cell line. As for iPS87, the gene expression of single cells of iPS87 (126), which as an induced pluripotent cell line with stem cell-like properties exhibit greater stemness and self-renewal properties in comparison with 3D spheroids, which consist of a necrotic core, proliferating zone, and the outer layer, which requires cellular differentiation. Interestingly, not only did iPS87 cells exhibit a decrease in stemness markers such as OCT4 and ALDH7A1, but E-cadherin and Snail were also observed to decrease. Although the 3D spheroids of iPS87 may

appear to have decreased stemness property compared to the single cells based on the reduced gene expression of OCT4 and ALDH7A1, the protein expression of these markers were significantly elevated. Therefore, despite the decreased gene expression of E-cadherin and Snail, further examination of these markers would provide us with a more complete understanding of their metastatic potential of the spheroids.

Collectively, FGFR inhibition by BGJ398 and Dovitinib did not induce any significant changes of EMT marker expression of the 3D spheroids of PC3, Du145, and iPS87, but it is clear that they compensated for the decrease in FGFR activity by up-regulating FGFR1 expression when treated with Dovitinib more than BGJ398. It is speculated that long term assays may be needed to accurately assess the effect of FGFR inhibition on the gene expression of the 3D spheroids and to assess the benefit of BGJ398 as it seems to result in less compensatory mechanism in the prostate cancer cells.

It has been addressed by many researchers that the lack of patient-specific in vitro prostate cancer models that accurately reflect the diversity of human prostate cancer has hampered the development of effective treatment. Thus, utilizing patient-derived organoids (PDOs) and iPSC-derived organoids (iDOs) has been emerging as a promising strategy in a disease modeling and drug development.

This study investigated if 3D culture of iPSC-derived cells from biopsy samples of prostate cancer patient (iPS87 cells) may provide a useful platform for other researchers to study prostate cancer stem cells with restored tumor initiating property *in vivo* (126). It was hypothesized that iPS87 spheroids may be utilized as iDOs for their characteristics of self-organizing free-floating cell aggregates with higher order tissue complexity. To begin with, the

term organoids in prostate cancer study is not well defined in literature as there hasn't been any successful generation of a fully mature organoid that truly recapitulating the human prostate tissue until July 2020 by Hepburn and colleagues (134). These authors demonstrated that human iPSC-derived cells that are co-cultured with rodent urogenital sinus mesenchyme for 12 weeks can comprehensively generate prostate tissue with epithelial architecture, containing cells at different differentiation stages of basal and luminal cells as well as neuroendocrine cells (134).

The iPS87 spheroids in this study were not cultured embedded within extracellular matrix (ECM) such as Matrigel nor co-cultured with other cells; they were also not examined for their composition of cells at different stages similarly to primary tissue. Yet, these spheroids are not generated merely from tumor biopsies but from iPSCs to be categorized as organoids, and the images of these iPS87 spheroids shown here resemble organoids more than spheroids. Moreover, when the spheroids were compared to the single cells of iPS87 for their gene expression via RT-qPCR, the stem cell marker OCT4 was down-regulated, suggesting cell differentiation of iPSCs into mature epithelial cells. Further studies such as frozen sectioning of the aggregates and staining with prostate epithelial markers would be required to examine the aggregates and determine if they are comprised of cells at different stages of cellular differentiation, similar to early stages of organoids, and whether they can grow into mature organoids that can accurately recapitulate human prostate tissue. If experimentally demonstrated, such findings would allow iPS87 cells to function as a valuable in vitro model that might become more generally utilized.

Whether these iPS87 spheroids are termed iDOs or not in this study, utilizing iPS87 spheroids has significant practical implications for drug testing for prostate cancer treatment, not only investigating FGFR1 as a molecular target. High-throughput screening utilizing organoids is shown to be more successful with greater physiological and clinical relevance (135). Evaluation

of thousands of compounds/drugs can be done more efficiently using iDOs than using primary tumor cells which are difficult to maintain or propagate when propagated as conventional 2D cultures that may have lost the parental tumor's characteristics as reflected by significant changes gene/protein expression (73-75, 110, 111).

Other researchers have utilized different approaches to isolate and investigate the rare prostate CSCs. For example, Bhatt *et al.* (136) isolated putative prostate CSCs using a modified Hoechst 33342 dye efflux assay to isolate what they referred to as side-populations from human prostatic epithelial cells. They demonstrated that approximately 1.4% of epithelial cells were identifiable as the side-population. This approach offered the advantage of allowing further examination of the selected cells by flow cytometry, examining cell surface marker expression and cell cycle status, given that stem cells are mostly quiescent, residing predominantly in the G0 phase of the cell cycle (137). Furthermore, the side-population cells were examined by xenograft tumor assay and shown to possess significantly increased tumor-initiating ability (138, 139, 140). Mice injected with side-population cells developed tumors more effectively, and required the injection of a lower number of cells, compared to control mice injected with the non-side-population cells. This clearly demonstrated the increased tumorigenic ability of the CSCs isolated in this manner (141, 142).

Other studies have reported that prostate CSCs may be identified and isolated using cell surface markers such as $CD44^{+}/\alpha2\beta1$ integrin^{+}/$CD133^{+}$ (118), or $ALDH^{high}$ /$CD44^{+}/\alpha2\beta1^{+}$ (143) when using primary tumor samples from patients, based on the exhibited self-renewal ability of these cells. However, the reliability of these cell surface markers remains unclear when using cell lines. A study examining prostate CSCs have reported that expression of CD133 was not observed in DU145 cells (77), and another study examining PC3 cells suggested

FAM65B^{high}/MFI2^{low}/LEF1^{low} cells represent the relevant CSC population rather than CD44^{+}/α2β1^{+} cells (144).

Another strategy to examine the prostate CSCs is through the forced expression of human telomerase reverse transcriptase (hTERT), which has the ability to induce immortalization in primary tumor cells (145, 146). Immortalization represents an important property of tumor cells, and refers to the ability of these cells to replicate indefinitely as a result of acquired mutations; this in in contrast to normal, noncancerous cell lines, which undergo cellular senescence after a fixed number of divisions, after which they are incapable of further propagation. These hTERT transformed cells were shown to express embryonic stem markers of Oct4, Nanog, and Sox2 and early progenitor cell markers of CD44 and Nestin, as well as display acquired anchorage-independence and unlimited lifespan. However, the tumorigenicity of these immortalized, putative CSCs will require further study as Gu *et al.* (145) demonstrated tumor formation by these cells when grafted under the renal capsule of male SCID mice, while, in contrast, Yasunaga *et al.* (146) failed to observe tumor formation after injection of telomerase-immortalized cells subcutaneously into the mid-dorsal interscapular region of SCID mice.

CSCs play important roles in cancer progression, metastasis and tumor recurrence, and in the development of drug resistance (61). Although conventional chemotherapeutics can eliminate the bulk of a tumor, they frequently fail to eliminate CSCs. This represents a major challenge in cancer treatment whereby cancer re-emerges sometimes long after treatment, due to the presence of latent CSCs which are resistant to various chemotherapeutics by virtue of their different biological properties. Thus, understanding the properties of CSCs and the relevant signaling pathways that are involved in maintaining self-renewal ability and increased tumorigenicity may provide valuable findings in advancing cancer treatment.

In fact, FGFR signaling pathway is not the sole signaling axis reported as promoting stemness of CSCs in various cancers including breast cancer, non-small cell lung cancer, and esophageal squamous cell carcinoma (70,71,72); Wnt/β-catenin pathway has been reported to play a significant role in the maintenance of CSCs in hepatocellular carcinoma and breast cancer. Pandit *et al.* (159) demonstrated that CSCs enriched by 3D spheroid culture exhibited up-regulated β-catenin and these spheroid cells yielded tumors in immunocompetent mice unlike the control cells. Silencing β-catenin reversed the spheroid phenotype, suggesting that β-catenin conferred the tumorigenic ability of the CSCs. Along with the aberrant expression, mutations in the β-catenin gene are frequently observed in hepatocellular carcinoma (160), and it has been suggested that the Wnt/β-catenin pathway represents a promising target for developing novel therapies for hepatocellular carcinoma (161). Similarly, blockade of Wnt/β-catenin signaling via small-molecule inhibitor treatment or shRNA-mediated Wnt knockdown was shown to suppress breast cancer metastasis by inhibiting CSC-like phenotype (162).

The PTEN/mTOR/STAT3 pathway has also been reported as critical for CSCs in breast cancer. Zhou *et al.* (163) showed that CSCs enriched as side-populations had higher in vivo tumorigenicity in NOD/SCID mice, and inhibition of STAT3 or knockdown of the STAT3 gene led to the loss of the side-populations and thus, tumorigenicity as demonstrated *in vivo*. Similarly, JAK/STAT signaling was found to be constitutively activated in CSCs isolated from patients with acute myeloid leukemia, and the inhibition of STAT signaling via treatment with a JAK inhibitor resulted in the loss of the tumorigenicity, demonstrated *in vivo* (164).

Hedgehog signaling is yet another pathway reported to promote self-renewal properties in CSCs in multiple myeloma through ligand-driven constitutive activation, leading to the suggestion that inhibition of Hedgehog signaling may reduce proliferation of multiple myeloma

cells (165). Moreover, Hedgehog signaling is reported to up-regulate the stem cell marker and EMT markers in colon cancer CSCs, and inhibition of the signaling via cyclopamine treatment resulted in decreased expression of the stem cell markers and EMT markers, and thus, it was suggested that targeting the Hedgehog signaling in CSCs may be a novel approach for colon cancer therapy (166). Hedgehog signaling is heavily involved in cellular differentiation, embryonic development, regulation of pluripotency genes including Nanog, Sox2 and Bmi1, EMT process protein trafficking, and post-translational modifications of a protein among other functions (167, 168). Nanog plays a major role in Hedgehog signaling by promoting proliferative potential and self-renewal in embryonic stem cells and re-programming of differentiated mature, somatic cells to pluripotency (169). Thus, it is not surprising that inappropriate activation of Hedgehog signaling in mature cells may contribute to initiation of cancer.

Lastly, NF-κB signaling has been reported to be increased in CSCs in prostate cancer (170), and has also been described to promote breast CSCs to metastasize to lungs (171). It has been reported that NF-κB signaling regulates stem cell markers of Nanog and Sox2 to expand CSC population as well as EMT markers in a Her2 mouse model in breast cancer (172). Another study found that NF-κB activity caused expansion of cancer stem cell populations via Notch signaling and conferred tumorigenicity of CSCs in triple-negative breast cancer (173). The NF-κB transcription factor pathway is a key regulator in inflammation, cytokine production, immune responses, cell survival, and growth, which is heavily associated with CSC function and cancer progression (174).

Collectively, there is abundant evidence from multiple convergent approaches suggesting that the targeting of signaling pathways exploited by CSCs will prove to be a promising strategy in finding alternative therapeutic options (175, 176). In conclusion, the study presented here

shows that targeting FGFR by TKI treatment represents a promising strategy for AR-independent CRPC patients, utilizing iDOs/3D spheroids established from iPS87 cell line and prostate CSCs enriched by 3D in vitro system. Establishing proper *in vitro* models to study the CSC population is critical in order to properly assess the biological properties of CSCs; results from in vitro studies would then allow subsequent examination in animal models. This study provides evidence for the first time that signaling dependent upon FGFR1 plays a fundamental role in supporting the maintenance and proliferation of prostate CSCs, which are believed to underlie prostate cancer progression and metastasis at a molecular and cellular level.

MATERIALS AND METHODS

Cell Lines and Culture

DU145 cells and LNCaP cells were obtained from American Type Culture Collection and PC3 were obtained from Leonard Deftos at UCSD, and were maintained in RPMI 1640 media supplemented with 10% fetal bovine serum and 1x pen/strep and in 5% CO2 at 37°C. For spheroids assay, cells were maintained in RPMI 1640 media supplemented with 10% Gibco™ KnockOut™ Serum Replacement (KnockOut™ SR) from ThermoFisher Scientific. For the comparison of basal media for culturing PC3 spheroids, DMEM-F12 (Gibco) was used, and either DMEM-F12 or RPMI 1640 media cultures were supplemented with 40 ng/µl EGF (R&D), and/or 50 ng/µl bFGF (R&D).

Induced pluripotent stem (iPS) 87 cells (iPSC87) were generated as previously described (126, 177). Briefly, prostatectomy samples were collected from patients at Stage I and II prostate cancers, and iPS 87 cells were generated by using the retroviral vector plasmids pMXs-hOCT4, pMXs-hSOX2, pMXs-hKlf4, pMXs-hc-Myc (Yamanaka factors). The iPS87 cells were grown on Mitomycin-C inactivated MEF feeder cells and maintained in KnockOut DMEM (Gibco) supplemented with 0.125% Bovine Serum Albumin (Sigma), 2% L-glutamine, 1% non-essential amino acids, 1% Fungizone/0.5% gentamycin, 10% serum replacement (Gibco), 6.25 ng/mL bFGF (Peprotech), referred to as "ES++," 5% CO2, 37°C.

Flow cytometric analysis

PC3 cells were harvested and dissociated into single cells using versine/EDTA treatment and washed with 2%BSA/PBS. Samples were prepared with 1 X 10^7 cells, and were incubated with anti-CD133-phycoerythrin (PE) (Miltenyi Biotec Ltd., Surrey, UK) in 0.1%

NaN_3/2%BSA/PBS for 30 min on ice, and washed and resuspended to be the final concentration of cells at 1 X 10^6 cells/ml with 0.5 µg/ml final concentration of propidium iodide (Thermo Fisher Scientific) to analyze live cells. PC3 cell samples were subjected to flow cytometry analysis at the Flow Cytometry Shared Resource at UC San Diego Moores Cancer Center.

Soft agar colony formation assay

Experiments were carried out in 60 mm plates coated with 3ml volume of a base layer of RPMI 1640 containing 0.6% agar, and single cells of PC3, DU145 and LNCaP were seeded at densities indicated per plate with 3ml volume in RPMI 1640 supplemented with 10% SR containing 0.3 % agar. 1ml of media was added on top to prevent dehydration, and plates were placed in 5% CO2 at 37°C for about 4-6 weeks. Colonies were stained with 0.005% crystal violet (Sigma)/10%EtOH/1XPBS overnight and were de-stained with 1XPBS and plates were scanned or photographed, and the number of colonies were analyzed using ImageJ software.

Spheroids Assay and Images of Spheroids

Single cells of PC3, DU145 and LNCaP were obtained by dissociating them with VE incubation and seeded onto 1% agarose-coated TC plates in 10% SR/RPMI 1640 media with 1X pen/strep with following densities: PC3 at an initial density of ~6.6 x 10^3 cells/ml, DU145 at ~3.3x 10^4 cells/ml, and LNCaP at ~3.3 x 10^4 cells/ml. iPS87 spheroids were cultured in ES++ media as mentioned above without MEF feeder cells to readily grow into spheroids from single cells in 12-well TC plates a density of 8.0 x 10^4 cells/ml.

Images of spheroids (and monolayer cells) were acquired using an inverted microscope (Carl Zeiss Microscopy GmbH, Germany) with a 20x objective. Image processing was done in Fiji/ImageJ.

MTT Metabolic Assays and Addition of Inhibitors

From the initial plating of single cells onto the non-adherent substrates, measurements were taken after 1, 4, 7, 11, and 14 days for PC3 cells or after 1, 5, 9, 13, and 17 days for DU145 and LNCaP. PC3 cells were plated on 60mm plates with total 3ml volume of media, at each time point 300 µl of cell cultures were transferred to a 24-well TC plate with additional 200 µl of media and incubated with 50µl of 5 mg/mL of thiazolyl blue tetrazolium bromide (MTT) (Sigma) at 37°C in 5% CO2 for 4 h, after which 500 µl of 0.04 M HCl in isopropanol was added and incubated again for at least 30 min. Absorbance was measured at 570 nm. The protocol (103) was generally followed. DU145 and LNCaP cells were plated on 10cm plates with total 10ml volume of media, at each time point 1ml of cultures were transferred to a 24-well TC plate and incubated with 100µl of 5 mg/mL of thiazolyl blue tetrazolium bromide (MTT) at 37°C in 5% CO2 for 4 h, and cells were concentrated by centrifuging and removing 770 µl of the supernatant, after which 300µl of 0.04 M HCl in isopropanol was added and incubated again for at least 30 min. Absorbance was measured at 570 nm. Inhibitors (Dovitinib, BGJ398, PD166866) were added to the cell culture with 300µl (for PC3) and 1ml (for DU145 and LNCaP) of same media to maintain the total volume consistent. Experiments were performed in triplicate.

From the initial plating of single cells iPS87 onto 12-well TC plates, measurements were taken on days 1, 4, 7, and 11 and the inhibitors (BGJ398, and Dovitinib) were added to the cell

cultures every 3 days (on days 1, 4, and 7). Experiments were performed in triplicate with technical duplicate.

Immunoblotting, antibodies and additional reagents

Lysates were collected in RIPA lysis buffer containing inhibitors 10 ng/ml Aprotinin, 1 mM PMSF, and 1 mM Na3VO4, and 25μg or 30μg of total proteins were separated by 10% or 12.5% SDS-PAGE followed by transfer to Immobilon-P membrane. Immunoblotting reagents were from the following sources: antibodies against p-FGFR (Tyr653/654), FGFR1 (D8E4), FGFR4 (D3B12), p-VEGFR (19A10), VEGFR2 (55B11), p-AKT (D9E), AKT (9272), p-MAPK (D13.14.4E), p44/42 MAPK (Erk1/2), OCT4 (2750), CD133 (D2V8Q), Androgen Receptor (D6F11), and β-actin (4967) antibodies from Cell Signaling Technology; FGFR2 (C-8), FGFR3 (B-9) and STAT5 (C-17) from Santa Cruz Biotechnology; ALDH7A1 (CAT:ABO11656) from Abgent; HRP anti-mouse, HRP anti-rabbit, and Enhanced Chemiluminescence (ECL) reagents from GE Healthcare. Other reagents included: Dovitinib, BGJ398, PD166866 from Selleckchem.

RT-qPCR reagents and primers

Cells were collected and washed with 1x PBS (chilled) and then RNA was extracted using Trizol reagent (Invitrogen) according to the manufacturer's protocol. Total RNA concentration was measured using nanodrop. 100 ng of total RNA was used to prepare cDNA using ProtoScript II Reverse Transcriptase (NEB #M0368) with oligo(dT) primers (Cat# 51-01-15-01, IDT) following the manufacturer's protocol. qPCR was performed using a SYBR green assay system with Phusion® High-Fidelity DNA Polymerase on Stratagene Mx3000 qPCR

machine (Agilent Technologies, CA, USA). The mRNA levels were normalized to beta-actin abundance, and the fold change between samples was calculated by a standard ΔΔCt analysis.

Following primers were used; FGFR1; forward 5'-TAATGGACTCTGTGGTGCCCTC-3', reverse 5'-ATGTGTGGTTGATGCTGCCG-3' (71), OCT4; forward 5'-GCAATTTGCCAAGCTCCTGAA-3', reverse 5'-GCAGATGGTCGTTTGGCTGA-3' (178), ALDH7A1; forward 5′-CAACGAGCCAATAGCAAGAG-3′, reverse 5′-GCATCGCCAATCTGTCTTAC-3′ (116), E-cadherin; forward 5′-CGGGAATGCAGTTGAGGATC-3′, reverse 5′-AGGATGGTGTAAGCGATGGC-3′ (179), vimentin; forward 5′-AGATGGCCCTTGACATTGAG-3′, reverse 5′-TGGAAGAGGCAGAGAAATCC-3′ (180), Snail; forward 5′-GAAAGGCCTTCAACTGCAAA-3′, reverse 5′-TGACATCTGAGTGGGTCTGG-3′ (179), beta-actin; forward 5'-AGAGCTACGAGCTGCCTGAC-3', reverse 5'-AGCACTGTGTTGGCGTACAG-3' (181).

ACKNOWLEDGEMENTS

Chapter 2, in part, contains material published in the following. Ko J., Meyer A. N., Haas M., Donoghue D. J. Characterization of FGFR signaling in prostate cancer stem cells and inhibition via TKI treatment. Oncotarget. 2021; 12: 22-36. The dissertation author was the primary investigator and first author of this material, being responsible for designing and performing entire experiments and the manuscript writing.

REFERENCES

1. American Cancer Society: Cancer Facts & Statistics. (2019). Retrieved from https://cancerstatisticscenter.cancer.org/#!/

2. Bray, F., Ferlay, J., Soerjomataram, I., Siegel, R. L., Torre, L. A., & Jemal, A. (2018). Global cancer statistics 2018: GLOBOCAN estimates of incidence and mortality worldwide for 36 cancers in 185 countries. *CA: A Cancer Journal for Clinicians*, *68*(6), 394–424. https://doi.org/10.3322/caac.21492

3. Toivanen, R., & Shen, M. M. (2017). Prostate organogenesis: tissue induction, hormonal regulation and cell type specification. *Development (Cambridge, England)*, *144*(8), 1382–1398. doi:10.1242/dev.148270

4. Rojas-Jiménez, A., Otero-Garcia, M., & Mateos-Martin, A. (2013). Stromal prostatic sarcoma: a rare tumor with rare clinical and imaging presentation. *Journal of Radiology Case Reports*, *7*(7), 24—31. https://doi.org/10.3941/jrcr.v7i7.1177

5. Deantoni, E. P., Crawford, E. D., Oesterling, J. E., Ross, C. A., Berger, E. R., McLeod, D. G., … Stone, N. N. (1996). Age- and race-specific reference ranges for prostate-specific antigen from a large community-based study. *Urology*, *48*(2), 234–239. https://doi.org/10.1016/S0090-4295(96)00091-X

6. Brawer M. K. (2005). Prostatic intraepithelial neoplasia: an overview. *Reviews in urology*, *7 Suppl 3*(Suppl 3), S11–S18.

7. Rybak, A. P., Bristow, R. G., & Kapoor, A. (2015). Prostate cancer stem cells: deciphering the origins and pathways involved in prostate tumorigenesis and aggression. *Oncotarget*, *6*(4), 1900–1919. doi:10.18632/oncotarget.2953

8. Pourmand, G., Ziaee, A. A., Abedi, A. R., Mehrsai, A., Alavi, H. A., Ahmadi, A., & Saa dati, H. R. (2007). Role of PTEN gene in progression of prostate cancer. *Urology Journa l*, *4*(2), 95–100. https://doi.org/10.22037/uj.v4i2.138

9. Wedge, D. C., Gundem, G., Mitchell, T., Woodcock, D. J., Martincorena, I., Ghori, M., Zamora, J., Butler, A., Whitaker, H., Kote-Jarai, Z., Alexandrov, L. B., Van Loo, P., Massie, C. E., Dentro, S., Warren, A. Y., Verrill, C., Berney, D. M., Dennis, N., Merson, S., Hawkins, S., … Eeles, R. A. (2018). Sequencing of prostate cancers identifies new cancer genes, routes of progression and drug targets. *Nature genetics*, 50(5), 682–692. https://doi.org/10.1038/s41588-018-0086-z

10. Lonergan, P. E., & Tindall, D. J. (2011). Androgen receptor signaling in prostate cancer development and progression. *Journal of carcinogenesis*, *10*, 20. doi:10.4103/1477-3163.83937

11. Cassinelli, G., Zuco, V., Gatti, L., Lanzi, C., Zaffaroni, N., Colombo, D., & Perego, P. (2013). Targeting the Akt kinase to modulate survival, invasiveness and drug resistance of cancer cells. *Current medicinal chemistry*, *20*(15), 1923–1945. https://doi.org/10.2174/09298673113209990106

12. Robinson, D., Van Allen, E. M., Wu, Y. M., Schultz, N., Lonigro, R. J., Mosquera, J. M., Montgomery, B., Taplin, M. E., Pritchard, C. C., Attard, G., Beltran, H., Abida, W., Bradley, R. K., Vinson, J., Cao, X., Vats, P., Kunju, L. P., Hussain, M., Feng, F. Y., Tomlins, S. A., … Chinnaiyan, A. M. (2015). Integrative clinical genomics of advanced prostate cancer. *Cell*, *161*(5), 1215–1228. https://doi.org/10.1016/j.cell.2015.05.001

13. Hamid, A. A., Gray, K. P., Shaw, G., MacConaill, L. E., Evan, C., Bernard, B., Loda, M., Corcoran, N. M., Van Allen, E. M., Choudhury, A. D., & Sweeney, C. J. (2019). Compound Genomic Alterations of TP53, PTEN, and RB1 Tumor Suppressors in Localized and Metastatic Prostate Cancer. *European urology*, *76*(1), 89–97. https://doi.org/10.1016/j.eururo.2018.11.045

14. Navarro, G., Xu, W., Jacobson, D. A., Wicksteed, B., Allard, C., Zhang, G., … Mauvais-Jarvis, F. (2016). Extranuclear Actions of the Androgen Receptor Enhance Glucose-Stimulated Insulin Secretion in the Male. *Cell metabolism*, *23*(5), 837–851. doi:10.1016/j.cmet.2016.03.015

15. Askew, E. B., Gampe, R. T., Jr, Stanley, T. B., Faggart, J. L., & Wilson, E. M. (2007). Modulation of androgen receptor activation function 2 by testosterone and dihydrotestosterone. *The Journal of biological chemistry*, *282*(35), 25801–25816. doi:10.1074/jbc.M703268200

16. Lonergan, P. E., & Tindall, D. J. (2011). Androgen receptor signaling in prostate cancer development and progression. *Journal of carcinogenesis*, *10*, 20. doi:10.4103/1477-3163.83937

17. Huggins, C., & Hodges, C. V. (1941). Studies on Prostatic Cancer. I. The Effect of Castration, of Estrogen and of Androgen Injection on Serum Phosphatases in Metastatic Carcinoma of the Prostate. *Cancer Research*, *1*(4), 293 LP – 297. Retrieved from http://cancerres.aacrjournals.org/content/1/4/293.abstract

18. Scher, H. I., Fizazi, K., Saad, F., Taplin, M. E., Sternberg, C. N., Miller, K., … De Bono, J. S. (2012). Increased survival with enzalutamide in prostate cancer after chemotherapy. *New England Journal of Medicine*, *367*(13), 1187–1197. https://doi.org/10.1056/NEJMoa1207506

19. Saad F. (2013). Evidence for the efficacy of enzalutamide in postchemotherapy metastatic castrate-resistant prostate cancer. *Therapeutic advances in urology*, *5*(4), 201–210. doi:10.1177/1756287213490054

20. Smith, M. R., Saad, F., Chowdhury, S., Oudard, S., Hadaschik, B. A., Graff, J. N., … S mall, E. J. (2018). Apalutamide treatment and metastasis-free survival in prostate cancer. *New England Journal of Medicine*, *378*(15), 1408–1418. https://doi.org/10.1056/NEJM oa1715546

21. Bryce, A., & Ryan, C. J. (2012). Development and clinical utility of abiraterone acetate a s an androgen synthesis inhibitor. *Clinical Pharmacology and Therapeutics*, *91*(1), 101–108. https://doi.org/10.1038/clpt.2011.275

22. Hu, R., Dunn, T. A., Wei, S., Isharwal, S., Veltri, R. W., Humphreys, E., … Luo, J. (2009). Ligand-independent androgen receptor variants derived from splicing of cryptic exons signify hormone-refractory prostate cancer. *Cancer research*, *69*(1), 16–22. doi:10.1158/0008-5472.CAN-08-2764

23. Kregel, S., Chen, J. L., Tom, W., Krishnan, V., Kach, J., Brechka, H., … Vander Griend, D. J. (2016). Acquired resistance to the second-generation androgen receptor antagonist enzalutamide in castration-resistant prostate cancer. *Oncotarget*, *7*(18), 26259–26274. doi:10.18632/oncotarget.8456

24. Tucci, M., Zichi, C., Buttigliero, C., Vignani, F., Scagliotti, G. V., & Di Maio, M. (2018). Enzalutamide-resistant castration-resistant prostate cancer: challenges and solutions. *OncoTargets and therapy*, 11, 7353–7368. https://doi.org/10.2147/OTT.S153764

25. Ware, J. L. (1993). Growth factors and their receptors as determinants in the proliferatio n and metastasis of human prostate cancer. *Cancer and Metastasis Reviews*, *12*(3), 287–301. https://doi.org/10.1007/BF00665959

26. Armstrong, K., Ahmad, I., Kalna, G., Tan, S. S., Edwards, J., Robson, C. N., & Leung, H. Y. (2011). Upregulated FGFR1 expression is associated with the transition of hormone-naive to castrate-resistant prostate cancer. *British journal of cancer,* 105(9), 1362–1369. doi:10.1038/bjc.2011.367

27. Acevedo, V. D., Gangula, R. D., Freeman, K. W., Li, R., Zhang, Y., Wang, F., Ayala, G. E., Peterson, L. E., Ittmann, M., & Spencer, D. M. (2007). Inducible FGFR-1 activation leads to irreversible prostate adenocarcinoma and an epithelial-to-mesenchymal transition. *Cancer cell*, *12*(6), 559–571. https://doi.org/10.1016/j.ccr.2007.11.004

28. Sahadevan, K., Darby, S., Leung, H. Y., Mathers, M. E., Robson, C., & Gnanapragasam, V. (2007). Selective over-expression of fibroblast growth factor receptors 1 and 4 in clinical prostate cancer. *The Journal of Pathology*, *213*, 82–90.

29. Wan, X., Corn, P. G., Yang, J., Palanisamy, N., Starbuck, M. W., Efstathiou, E., … Navone, N. M. (2014). Prostate cancer cell-stromal cell crosstalk via FGFR1 mediates antitumor activity of Dovitinib in bone metastases. *Science translational medicine*, *6*(252), 252ra122. doi:10.1126/scitranslmed.3009332

30. Lemmon, M. A., & Schlessinger, J. (2010). Cell signaling by receptor tyrosine kinases. *Cell*, *141*(7), 1117–1134. doi:10.1016/j.cell.2010.06.011

31. Ornitz, D. M., & Itoh, N. (2015). The Fibroblast Growth Factor signaling pathway. *Wiley interdisciplinary reviews. Developmental biology*, *4*(3), 215–266. doi:10.1002/wdev.176

32. Gallo, L. H., Nelson, K. N., Meyer, A. N., & Donoghue, D. J. (2015). Functions of Fibro blast Growth Factor Receptors in cancer defined by novel translocations and mutations. *Cytokine and Growth Factor Reviews*, *26*(4), 425–449. https://doi.org/10.1016/j.cytogfr. 2015.03.003

33. Levy, D. E., & Darnell, J. E. (2002). STATs: transcriptional control and biological impa ct. *Nature Reviews Molecular Cell Biology*, *3*(9), 651–662. https://doi.org/10.1038/nrm9 09

34. Santarpia, L., Lippman, S. M., & El-Naggar, A. K. (2012). Targeting the MAPK-RAS-RAF signaling pathway in cancer therapy. *Expert opinion on therapeutic targets*, *16*(1), 103–119. doi:10.1517/14728222.2011.645805

35. Mukherjee, R., McGuinness, D. H., McCall, P., Underwood, M. A., Seywright, M., Orange, C., & Edwards, J. (2011). Upregulation of MAPK pathway is associated with survival in castrate-resistant prostate cancer. *British journal of cancer*, *104*(12), 1920–1928. doi:10.1038/bjc.2011.163

36. Fresno Vara, J. Á., Casado, E., de Castro, J., Cejas, P., Belda-Iniesta, C., & González-Ba rón, M. (2004). P13K/Akt signalling pathway and cancer. *Cancer Treatment Reviews*, *30* (2), 193–204. https://doi.org/10.1016/j.ctrv.2003.07.007

37. Cassinelli, G., Zuco, V., Gatti, L., Lanzi, C., Zaffaroni, N., Colombo, D., & Perego, P. (2013). Targeting the Akt Kinase to Modulate Survival, Invasiveness and Drug Resistance of Cancer Cells. *Current Medicinal Chemistry*, *20*(15), 1923–1945. https://doi.org/10.2174/09298673113209990106

38. Turner, T., Epps-Fung, M. V., Kassis, J., & Wells, A. (1997). Molecular inhibition of phospholipase c gamma signaling abrogates DU-145 prostate tumor cell invasion. *Clinical cancer research : an official journal of the American Association for Cancer Research*, *3*(12 Pt 1), 2275–2282.

39. Kassis, J., Moellinger, J., Lo, H., Greenberg, N. M., Kim, H. G., & Wells, A. (1999). A role for phospholipase C-γ-mediated signaling in tumor cell invasion. *Clinical Cancer Research*, *5*(8), 2251–2260.

40. Desai, A., & Adjei, A. A. (2016). FGFR signaling as a target for Lung cancer therapy. *Jo urnal of Thoracic Oncology*, *11*(1), 9–20. https://doi.org/10.1016/j.jtho.2015.08.003

41. Perez-Garcia, J., Muñoz-Couselo, E., Soberino, J., Racca, F., & Cortes, J. (2018). Target ing FGFR pathway in breast cancer. *Breast*, *37*, 126–133. https://doi.org/10.1016/j.breast .2017.10.014

42. Gowardhan, B., Douglas, D. A., Mathers, M. E., McKie, A. B., McCracken, S. R., Robson, C. N., & Leung, H. Y. (2005). Evaluation of the fibroblast growth factor system as a potential target for therapy in human prostate cancer. *British journal of cancer*, *92*(2), 320–327. doi:10.1038/sj.bjc.6602274

43. Roskoski, R. (2016). Classification of small molecule protein kinase inhibitors based upon the structures of their drug-enzyme complexes. *Pharmacological Research*, *103*, 26–48. https://doi.org/10.1016/j.phrs.2015.10.021

44. Trudel, S., Li, Z. H., Wei, E., Wiesmann, M., Chang, H., Chen, C., … Stewart, A. K. (2005). CHIR-258, a novel, multitargeted tyrosine kinase inhibitor for the potential treatment of t(4;14) multiple myeloma. *Blood*, *105*(7), 2941–2948. https://doi.org/10.1182/blood-2004-10-3913

45. Guagnano, V., Furet, P., Spanka, C., Bordas, V., Le Douget, M., Stamm, C., … Graus P orta, D. (2011). Discovery of 3-(2,6-Dichloro-3,5-dimethoxy-phenyl)-1-{6-[4-(4-ethyl- p iperazin-1-yl)-phenylamino]-pyrimidin-4-yl}-1-methyl-urea (NVP-BGJ398), A potent a nd selective inhibitor of the fibroblast growth factor receptor family of receptor tyrosine kinase. *Journal of Medicinal Chemistry*, *54*(20), 7066–7083. https://doi.org/10.1021/jm2 006222

46. Panek, R & Lu, G & Dahring, T & Batley, B & Connolly, C & Hamby, James & Brown, K. (1998). In vitro biological characterization and antiangiogenic effects of PD 166866, a selective inhibitor of the FGF-1 receptor tyrosine kinase. *The Journal of pharmacology and experimental therapeutics*. 286. 569-77.

47. Bussard, K. M., Gay, C. V, & Mastro, A. M. (2008). The bone microenvironment in metastasis; what is special about bone? *Cancer and Metastasis Reviews*, *27*(1), 41–55. https://doi.org/10.1007/s10555-007-9109-4

48. Nishida, N., Yano, H., Nishida, T., Kamura, T., & Kojiro, M. (2006). Angiogenesis in cancer. *Vascular health and risk management*, *2*(3), 213–219. doi:10.2147/vhrm.2006.2.3.213

49. Bielenberg, D. R., & Zetter, B. R. (2015). The Contribution of Angiogenesis to the Process of Metastasis. *Cancer journal (Sudbury, Mass.)*, *21*(4), 267–273. doi:10.1097/PPO.0000000000000138

50. Micalizzi, D. S., Farabaugh, S. M., & Ford, H. L. (2010). Epithelial-mesenchymal transition in cancer: parallels between normal development and tumor progression. *Journal of mammary gland biology and neoplasia*, *15*(2), 117–134. doi:10.1007/s10911-010-9178-9

51. Zeisberg, M., & Neilson, E. G. (2009). Biomarkers for epithelial-mesenchymal transitions. *The Journal of clinical investigation*, *119*(6), 1429–1437. https://doi.org/10.1172/JCI36183

52. Kim, Y. N., Koo, K. H., Sung, J. Y., Yun, U. J., & Kim, H. (2012). Anoikis resistance: an essential prerequisite for tumor metastasis. *International journal of cell biology*, *2012*, 306879. doi:10.1155/2012/306879

53. Yu, M., Bardia, A., Wittner, B. S., Stott, S. L., Smas, M. E., Ting, D. T., … Maheswaran, S. (2013). Circulating breast tumor cells exhibit dynamic changes in epithelial and mesenchymal composition. *Science (New York, N.Y.)*, *339*(6119), 580–584. doi:10.1126/science.1228522

54. Cheung, K. J., & Ewald, A. J. (2016). A collective route to metastasis: Seeding by tumor cell clusters. *Science*, *352*(6282), 167 LP – 169. https://doi.org/10.1126/science.aaf6546

55. Brook, N., Brook, E., Dharmarajan, A., Dass, C. R., & Chan, A. (2018). Breast cancer bone metastases: pathogenesis and therapeutic targets. *International Journal of Biochemistry and Cell Biology*, *96*(January), 63–78. https://doi.org/10.1016/j.biocel.2018.01.003

56. Jin, J. K., Dayyani, F., & Gallick, G. E. (2011). Steps in prostate cancer progression that lead to bone metastasis. *International journal of cancer*, *128*(11), 2545–2561. doi:10.1002/ijc.26024

57. Vatandoust, S., Price, T. J., & Karapetis, C. S. (2015). Colorectal cancer: Metastases to a single organ. *World journal of gastroenterology*, *21*(45), 11767–11776. doi:10.3748/wjg.v21.i41.11767

58. Milovanovic, I. S., Stjepanovic, M., & Mitrovic, D. (2017). Distribution patterns of the metastases of the lung carcinoma in relation to histological type of the primary tumor: An autopsy study. *Annals of thoracic medicine*, *12*(3), 191–198. doi:10.4103/atm.ATM_276_16

59. Shiozawa, Y., Nie, B., Pienta, K. J., Morgan, T. M., & Taichman, R. S. (2013). Cancer stem cells and their role in metastasis. *Pharmacology & therapeutics*, *138*(2), 285–293. doi:10.1016/j.pharmthera.2013.01.014

60. Neuzil, J., Stantic, M., Zobalova, R., Chladova, J., Wang, X., Prochazka, L., … Ralph, S. J. (2007). Tumour-initiating cells vs. cancer "stem" cells and CD133: What's in the name? *Biochemical and Biophysical Research Communications*, *355*(4), 855–859. https://doi.org/10.1016/j.bbrc.2007.01.159

61. Reya, T., Morrison, S. J., Clarke, M. F., & Weissman, I. L. (2001). Stem cells, cancer, and cancer stem cells. *Nature*, *414*(6859), 105–111. https://doi.org/10.1038/35102167

62. Harris, K. S., & Kerr, B. A. (2017). Prostate Cancer Stem Cell Markers Drive Progression, Therapeutic Resistance, and Bone Metastasis. *Stem cells international*, *2017*, 8629234. doi:10.1155/2017/8629234

63. Liao, W. T., Ye, Y. P., Deng, Y. J., Bian, X. W., & Ding, Y. Q. (2014). Metastatic cancer stem cells: from the concept to therapeutics. *American journal of stem cells*, *3*(2), 46–62.

64. Moserle, L., Ghisi, M., Amadori, A., & Indraccolo, S. (2010). Side population and cancer stem cells: Therapeutic implications. *Cancer Letters*, *288*(1), 1–9. https://doi.org/10.1016/j.canlet.2009.05.020

65. Medema, J. P. (2013). Cancer stem cells: The challenges ahead. *Nature Cell Biology*, *15*(4), 338–344. https://doi.org/10.1038/ncb2717

66. van den Hoogen, C., van der Horst, G., Cheung, H., Buijs, J. T., Lippitt, J. M., Guzmán-Ramírez, N., Hamdy, F. C., Eaton, C. L., Thalmann, G. N., Cecchini, M. G., Pelger, R. C., & van der Pluijm, G. (2010). High aldehyde dehydrogenase activity identifies tumor-initiating and metastasis-initiating cells in human prostate cancer. *Cancer research*, *70*(12), 5163–5173. https://doi.org/10.1158/0008-5472.CAN-09-3806

67. Ishiguro, T., Ohata, H., Sato, A., Yamawaki, K., Enomoto, T., & Okamoto, K. (2017). Tumor-derived spheroids: Relevance to cancer stem cells and clinical applications. *Cancer science*, *108*(3), 283–289. doi:10.1111/cas.13155

68. Marsden, C. G., Wright, M. J., Pochampally, R., & Rowan, B. G. (2009). Breast Tumor-Initiating Cells Isolated from Patient Core Biopsies for Study of Hormone Action. In O.-K. Park-Sarge & T. E. Curry (Eds.), *Molecular Endocrinology: Methods and Protocols* (pp. 363–375). Totowa, NJ: Humana Press. https://doi.org/10.1007/978-1-60327-378-7_23

69. Suvà, M. L., Riggi, N., Janiszewska, M., Radovanovic, I., Provero, P., Stehle, J. C., … Stamenkovic, I. (2009). EZH2 is essential for glioblastoma cancer stem cell maintenance. *Cancer Research*, *69*(24), 9211–9218. https://doi.org/10.1158/0008-5472.CAN-09-1622

70. Reis-Filho, J. S., Simpson, P. T., Turner, N. C., Lambros, M. B., Jones, C., Mackay, A., … Ashworth, A. (2006). FGFR1 emerges as a potential therapeutic target for lobular breast carcinomas. *Clinical Cancer Research*, *12*(22), 6652–6662. https://doi.org/10.1158/1078-0432.CCR-06-1164

71. Ji, W., Yu, Y., Li, Z., Wang, G., Li, F., Xia, W., & Lu, S. (2016). FGFR1 promotes the stem cell-like phenotype of FGFR1-amplified non-small cell lung cancer cells through the Hedgehog pathway. *Oncotarget*, *7*(12), 15118–15134. doi:10.18632/oncotarget.7701

72. Maehara, O., Suda, G., Natsuizaka, M., Ohnishi, S., Komatsu, Y., Sato, F., … Sakamoto, N. (2017). Fibroblast growth factor-2-mediated FGFR/Erk signaling supports maintenance of cancer stem-like cells in esophageal squamous cell carcinoma. *Carcinogenesis*, *38*(11), 1073–1083. doi:10.1093/carcin/bgx095

73. Kapałczyńska, M., Kolenda, T., Przybyła, W., Zajączkowska, M., Teresiak, A., Filas, V., … Lamperska, K. (2018). 2D and 3D cell cultures - a comparison of different types of cancer cell cultures. *Archives of medical science : AMS*, *14*(4), 910–919. doi:10.5114/aoms.2016.63743

74. Jong, B. K. (2005). Three-dimensional tissue culture models in cancer biology. *Seminars in Cancer Biology*, *15*(5 SPEC. ISS.), 365–377. https://doi.org/10.1016/j.semcancer.2005.05.002

75. Portillo-Lara, R., & Alvarez, M. M. (2015). Enrichment of the Cancer Stem Phenotype in Sphere Cultures of Prostate Cancer Cell Lines Occurs through Activation of Developmental Pathways Mediated by the Transcriptional Regulator ΔNp63α. *PloS one*, *10*(6), e0130118. doi:10.1371/journal.pone.0130118

76. Martine, L. C., Holzapfel, B. M., McGovern, J. A., Wagner, F., Quent, V. M., Hesami, P., … Hutmacher, D. W. (2017). Engineering a humanized bone organ model in mice to study bone metastases. *Nature Protocols*, *12*(4), 639–663. https://doi.org/10.1038/nprot.2017.002

77. Rybak, A. P., He, L., Kapoor, A., Cutz, J. C., & Tang, D. (2011). Characterization of sphere-propagating cells with stem-like properties from DU145 prostate cancer cells. *Biochimica et Biophysica Acta - Molecular Cell Research*, *1813*(5), 683–694. https://doi.org/10.1016/j.bbamcr.2011.01.018

78. Lee, J. W., Sung, J. S., Park, Y. S., Chung, S., & Kim, Y. H. (2018). Isolation of spheroid-forming single cells from gastric cancer cell lines: enrichment of cancer stem-like cells. *BioTechniques*, *65*(4), 197–203. https://doi.org/10.2144/btn-2018-0046

79. Wu, X., Gong, S., Roy-Burman, P., Lee, P., & Culig, Z. (2013). Current mouse and cell models in prostate cancer research. *Endocrine-related cancer*, *20*(4), R155–R170. doi:10.1530/ERC-12-0285

80. Kaighn, M & Narayan, K. & Ohnuki, Y & Lechner, J & Jones, L. (1979). Establishment of a human prostate cancer cell line (PC-3). *Investigative urology.* 17. 16-23.

81. Stone, Kenneth & Mickey, Don & Wunderli, Heidi & Mickey, George & Paulson, David. (1978). Isolation of a human prostate carcinoma cell line (DU 145). International journal of cancer. *Journal international du cancer*. 21. 274-81. 10.1002/ijc.2910210305.

82. Veldscholte, Jos & Berrevoets, C.A. & Ris-Stalpers, Carrie & Kuiper, G.G.J.M. & Jenster, Guido & Trapman, J & Brinkmann, A.O. & Mulder, Elizah. (1992). A Mutation in the ligand binding domain of the androgen receptor of human LNCaP cells affects steroid binding characteristics and response to anti-androgens. *The Journal of steroid biochemistry and molecular biology*. 41. 665-9. 10.1016/0960-0760(92)90401-4.

83. Zhau, H. Y., Chang, S. M., Chen, B. Q., Wang, Y., Zhang, H., Kao, C., Sang, Q. A., Pathak, S. J., & Chung, L. W. (1996). Androgen-repressed phenotype in human prostate cancer. *Proceedings of the National Academy of Sciences of the United States of America*, *93*(26), 15152–15157. https://doi.org/10.1073/pnas.93.26.15152

84. Navone, N. M., Olive, M., Ozen, M., Davis, R., Troncoso, P., Tu, S. M., Johnston, D., Pollack, A., Pathak, S., von Eschenbach, A. C., & Logothetis, C. J. (1997). Establishment of two human prostate cancer cell lines derived from a single bone metastasis. *Clinical cancer research : an official journal of the American Association for Cancer Research*, *3*(12 Pt 1), 2493–2500.

85. Sramkoski, R. M., Pretlow, T. G., 2nd, Giaconia, J. M., Pretlow, T. P., Schwartz, S., Sy, M. S., Marengo, S. R., Rhim, J. S., Zhang, D., & Jacobberger, J. W. (1999). A new human prostate carcinoma cell line, 22Rv1. *In vitro cellular & developmental biology. Animal*, *35*(7), 403–409. https://doi.org/10.1007/s11626-999-0115-4

86. Korenchuk, S., Lehr, J. E., MClean, L., Lee, Y. G., Whitney, S., Vessella, R., Lin, D. L., & Pienta, K. J. (2001). VCaP, a cell-based model system of human prostate cancer. *In vivo (Athens, Greece)*, *15*(2), 163–168.

87. Yoshida, T., Kinoshita, H., Segawa, T., Nakamura, E., Inoue, T., Shimizu, Y., Kamoto, T., & Ogawa, O. (2005). Antiandrogen bicalutamide promotes tumor growth in a novel androgen-dependent prostate cancer xenograft model derived from a bicalutamide-treated patient. *Cancer research*, *65*(21), 9611–9616. https://doi.org/10.1158/0008-5472.CAN-05-0817

88. Mertz, K. D., Setlur, S. R., Dhanasekaran, S. M., Demichelis, F., Perner, S., Tomlins, S., Tchinda, J., Laxman, B., Vessella, R. L., Beroukhim, R., Lee, C., Chinnaiyan, A. M., & Rubin, M. A. (2007). Molecular characterization of TMPRSS2-ERG gene fusion in the NCI-H660 prostate cancer cell line: a new perspective for an old model. *Neoplasia (New York, N.Y.)*, *9*(3), 200–206. https://doi.org/10.1593/neo.07103

89. Gao, D., Vela, I., Sboner, A., Iaquinta, P. J., Karthaus, W. R., Gopalan, A., Dowling, C., Wanjala, J. N., Undvall, E. A., Arora, V. K., Wongvipat, J., Kossai, M., Ramazanoglu, S., Barboza, L. P., Di, W., Cao, Z., Zhang, Q. F., Sirota, I., Ran, L., MacDonald, T. Y., … Chen, Y. (2014). Organoid cultures derived from patients with advanced prostate cancer. *Cell*, *159*(1), 176–187. https://doi.org/10.1016/j.cell.2014.08.016

90. Hepburn, A. C., Curry, E. L., Moad, M., Steele, R. E., Franco, O. E., Wilson, L., Singh, P., Buskin, A., Crawford, S. E., Gaughan, L., Mills, I. G., Hayward, S. W., Robson, C. N., & Heer, R. (2020). Propagation of human prostate tissue from induced pluripotent stem cells. *Stem cells translational medicine*, *9*(7), 734–745. https://doi.org/10.1002/sctm.19-0286

91. Hedlund, T. E., Duke, R. C., & Miller, G. J. (1999). Three-dimensional spheroid cultures of human prostate cancer cell lines. *The Prostate*, *41*(3), 154–165. https://doi.org/10.1002/(sici)1097-0045(19991101)41:3<154::aid-pros2>3.0.co;2-m

92. Bahmad, H. F., Cheaito, K., Chalhoub, R. M., Hadadeh, O., Monzer, A., Ballout, F., El-Hajj, A., Mukherji, D., Liu, Y. N., Daoud, G., & Abou-Kheir, W. (2018). Sphere-Formation Assay: Three-Dimensional *in vitro* Culturing of Prostate Cancer Stem/Progenitor Sphere-Forming Cells. *Frontiers in oncology*, *8*, 347. https://doi.org/10.3389/fonc.2018.00347

93. Wu, X., Gong, S., Roy-Burman, P., Lee, P., & Culig, Z. (2013). Current mouse and cell models in prostate cancer research. *Endocrine-related cancer*, *20*(4), R155–R170. https://doi.org/10.1530/ERC-12-0285

94. Masumori, N., Tsuchiya, K., Tu, W. H., Lee, C., Kasper, S., Tsukamoto, T., Shappell, S. B., & Matusik, R. J. (2004). An allograft model of androgen independent prostatic neuroendocrine carcinoma derived from a large probasin promoter-T antigen transgenic mouse line. *The Journal of urology*, *171*(1), 439–442. https://doi.org/10.1097/01.ju.0000099826.63103.94

95. Haughey, Charles & Mukherjee, Debayan & Steele, Rebecca & Popple, Amy & Dura-Perez, Lara & Pickard, Adam & Jain, Suneil & Mullan, Paul & Williams, Rich & Oliveira, Pedro & Buckley, Niamh & Honeychurch, Jamie & Mcdade, Simon & Illidge, Tim & Mills, Ian & Eddie, Sharon. (2020). Development of a novel allograft model of prostate cancer: a new tool to inform clinical translation. 10.1101/2020.02.16.942789.

96. Parisotto, M., & Metzger, D. (2013). Genetically engineered mouse models of prostate cancer. *Molecular oncology*, *7*(2), 190–205. https://doi.org/10.1016/j.molonc.2013.02.005

97. Greenberg, N. M., DeMayo, F., Finegold, M. J., Medina, D., Tilley, W. D., Aspinall, J. O., Cunha, G. R., Donjacour, A. A., Matusik, R. J., & Rosen, J. M. (1995). Prostate cancer in a transgenic mouse. *Proceedings of the National Academy of Sciences of the United States of America*, *92*(8), 3439–3443. https://doi.org/10.1073/pnas.92.8.3439

98. Elbadawy, M., Abugomaa, A., Yamawaki, H., Usui, T., & Sasaki, K. (2020). Development of Prostate Cancer Organoid Culture Models in Basic Medicine and Translational Research. *Cancers*, *12*(4), 777. https://doi.org/10.3390/cancers12040777

99. Gao, D., Vela, I., Sboner, A., Iaquinta, P. J., Karthaus, W. R., Gopalan, A., Dowling, C., Wanjala, J. N., Undvall, E. A., Arora, V. K., Wongvipat, J., Kossai, M., Ramazanoglu, S., Barboza, L. P., Di, W., Cao, Z., Zhang, Q. F., Sirota, I., Ran, L., MacDonald, T. Y., … Chen, Y. (2014). Organoid cultures derived from patients with advanced prostate cancer. *Cell*, *159*(1), 176–187. https://doi.org/10.1016/j.cell.2014.08.016

100. Hepburn, A. C., Sims, C., Buskin, A., & Heer, R. (2020). Engineering Prostate Cancer from Induced Pluripotent Stem Cells-New Opportunities to Develop Preclinical Tools in Prostate and Prostate Cancer Studies. *International journal of molecular sciences*, *21*(3), 905. https://doi.org/10.3390/ijms21030905

101. Namekawa, T., Ikeda, K., Horie-Inoue, K., & Inoue, S. (2019). Application of Prostate Cancer Models for Preclinical Study: Advantages and Limitations of Cell Lines, Patient-Derived Xenografts, and Three-Dimensional Culture of Patient-Derived Cells. *Cells*, *8*(1), 74. https://doi.org/10.3390/cells8010074

102. Lin, D., Wyatt, A. W., Xue, H., Wang, Y., Dong, X., Haegert, A., Wu, R., Brahmbhatt, S., Mo, F., Jong, L., Bell, R. H., Anderson, S., Hurtado-Coll, A., Fazli, L., Sharma, M., Beltran, H., Rubin, M., Cox, M., Gout, P. W., Morris, J., … Wang, Y. (2014). High fidelity patient-derived xenografts for accelerating prostate cancer discovery and drug development. *Cancer research*, *74*(4), 1272–1283. https://doi.org/10.1158/0008-5472.CAN-13-2921-T

103. Mossman, T. (1983). Rapid colorimetric assay for cellular growth and survival: application to proliferation and cytotoxicity assays. *J. Immunol. Methods.* 65. 55-61.

104. Oerlemans, R., Franke, N. E., Assaraf, Y. G., Cloos, J., van Zantwijk, I., Berkers, C. R., … Jansen, G. (2008). Molecular basis of bortezomib resistance: proteasome subunit β5 (PSMB5) gene mutation and overexpression of PSMB5 protein. *Blood*, *112*(6), 2489–2499. https://doi.org/10.1182/blood-2007-08-104950

105. Van Meerloo, J., Kaspers, G. J. L., & Cloos, J. (2011). Cell Sensitivity Assays: The MTT Assay. In I. A. Cree (Ed.), *Cancer Cell Culture: Methods and Protocols* (pp. 237–245). Totowa, NJ: Humana Press. https://doi.org/10.1007/978-1-61779-080-5_20

106. Rai, Y., Pathak, R., Kumari, N., Sah, D. K., Pandey, S., Kalra, N., … Bhatt, A. N. (2018). Mitochondrial biogenesis and metabolic hyperactivation limits the application of MTT assay in the estimation of radiation induced growth inhibition. *Scientific reports*, *8*(1), 1531. doi:10.1038/s41598-018-19930-w

107. Yu, S. Q., Lai, K. P., Xia, S. J., Chang, H. C., Chang, C., & Yeh, S. (2009). The diverse and contrasting effects of using human prostate cancer cell lines to study androgen receptor roles in prostate cancer. *Asian journal of andrology*, *11*(1), 39–48. doi:10.1038/aja.2008.44

108. Roberts, E., Cossigny, D. A., & Quan, G. M. (2013). The role of vascular endothelial growth factor in metastatic prostate cancer to the skeleton. *Prostate cancer*, *2013*, 418340. doi:10.1155/2013/418340

109. Edmondson, R., Broglie, J. J., Adcock, A. F., & Yang, L. (2014). Three-dimensional cell culture systems and their applications in drug discovery and cell-based biosensors. *Assay and drug development technologies*, *12*(4), 207–218. doi:10.1089/adt.2014.573

110. Hirschhaeuser, F., Menne, H., Dittfeld, C., West, J., Mueller-Klieser, W., & Kunz-Schughart, L. A. (2010). Multicellular tumor spheroids: An underestimated tool is catching up again. *Journal of Biotechnology*, *148*(1), 3–15. https://doi.org/10.1016/j.jbiotec.2010.01.012

111. Shi, Xudong & Gipp, Jerry & Bushman, Wade. (2008). Anchorage-independent c ulture maintains prostate stem cells. Developmental biology. 312. 396-406. 10.1016/j.yd bio.2007.09.042.

112. Mori, S., Chang, J. T., Andrechek, E. R., Matsumura, N., Baba, T., Yao, G., … Nevins, J. R. (2009). Anchorage-independent cell growth signature identifies tumors with metastatic potential. *Oncogene*, *28*(31), 2796–2805. doi:10.1038/onc.2009.139

113. Wagner, K., & Welch, D. (2010). Cryopreserving and recovering of human iPS ce lls using complete Knockout Serum Replacement feeder-free medium. *Journal of visuali zed experiments : JoVE*, (45), 2237. doi:10.3791/2237

114. Toren, P., Kim, S., Johnson, F., & Zoubeidi, A. (2016). Combined AKT and MEK pathway blockade in pre-clinical models of enzalutamide-resistant prostate cancer. *PLoS ONE*, *11*(4), 1–16. https://doi.org/10.1371/journal.pone.0152861

115. Van Den Hoogen, van der Horst, G., Cheung, H., Buijs, J. T., Pelger, R. C., & van der Pluijm, G. (2011). The aldehyde dehydrogenase enzyme 7A1 is functionally involved in prostate cancer bone metastasis. *Clinical & experimental metastasis*, *28*(7), 615–625. https://doi.org/10.1007/s10585-011-9395-7

116. Vaddi, P. K., Stamnes, M. A., Cao, H., & Chen, S. (2019). Elimination of SOX2/OCT4-Associated Prostate Cancer Stem Cells Blocks Tumor Development and Enhances Therapeutic Response. *Cancers*, 11(9), 1331. https://doi.org/10.3390/cancers11091331

117. Collins, A. T., Berry, P. A., Hyde, C., Stower, M. J., & Maitland, N. J. (2005). Pr ospective identification of tumorigenic prostate cancer stem cells. *Cancer Research*, *65*(23), 10946–10951. https://doi.org/10.1158/0008-5472.CAN-05-2018

118. Patrawala, L., Calhoun, T., Schneider-Broussard, R., Li, H., Bhatia, B., Tang, S., … Tang, D. G. (2006). Highly purified CD44+ prostate cancer cells from xenograft human tumors are enriched in tumorigenic and metastatic progenitor cells. *Oncogene*, *25*(12), 1696–1708. https://doi.org/10.1038/sj.onc.1209327

119. Patrawala, L., Calhoun-Davis, T., Schneider-Broussard, R., & Tang, D. G. (2007). Hierarchical organization of prostate cancer cells in xenograft tumors: The CD44+α2β1+ cell population is enriched in tumor-initiating cells. *Cancer Research*, *67*(14), 6796–6805. https://doi.org/10.1158/0008-5472.CAN-07-0490

120. Fan, X., Liu, S., Su, F., Pan, Q., & Lin, T. (2012). Effective enrichment of prostate cancer stem cells from spheres in a suspension culture system. *Urologic Oncology: Seminars and Original Investigations*, *30*(3), 314–318. https://doi.org/10.1016/j.urolonc.2010.03.019

121. Pfeiffer, M. J., & Schalken, J. A. (2010). Stem Cell Characteristics in Prostate Cancer Cell Lines. *European Urology*, *57*(2), 246–255. https://doi.org/10.1016/j.eururo.2009.01.015

122. Borowicz, S., Van Scoyk, M., Avasarala, S., Karuppusamy Rathinam, M. K., Tauler, J., Bikkavilli, R. K., & Winn, R. A. (2014). The soft agar colony formation assay. *Journal of visualized experiments : JoVE*, (92), e51998. doi:10.3791/51998

123. Rajendran, V., & Jain, M. V. (2018). In Vitro Tumorigenic Assay: Colony Forming Assay for Cancer Stem Cells. *Methods in molecular biology (Clifton, N.J.)*, *1692*, 89–95. https://doi.org/10.1007/978-1-4939-7401-6_8

124. Zhao, Q., Parris, A. B., Howard, E. W., Zhao, M., Ma, Z., Guo, Z., Xing, Y., & Yang, X. (2017). FGFR inhibitor, AZD4547, impedes the stemness of mammary epithelial cells in the premalignant tissues of MMTV-ErbB2 transgenic mice. *Scientific reports*, *7*(1), 11306. https://doi.org/10.1038/s41598-017-11751-7

125. Strouhalova, K., Přechová, M., Gandalovičová, A., Brábek, J., Gregor, M., & Rosel, D. (2020). Vimentin Intermediate Filaments as Potential Target for Cancer Treatment. *Cancers*, *12*(1), 184. https://doi.org/10.3390/cancers12010184

126. Assoun, E. N., Meyer, A. N., Jiang, M. Y., Baird, S. M., Haas, M., & Donoghue, D. J. (2020). Characterization of iPS87, a prostate cancer stem cell-like cell line. *Oncotarget*, *11*(12), 1075–1084. https://doi.org/10.18632/oncotarget.27524

127. Feng, S., Shao, L., Yu, W., Gavine, P., & Ittmann, M. (2012). Targeting fibroblast growth factor receptor signaling inhibits prostate cancer progression. *Clinical cancer research : an official journal of the American Association for Cancer Research*, *18*(14), 3880–3888. doi:10.1158/1078-0432.CCR-11-3214

128. Zhao, Q., Parris, A. B., Howard, E. W., Zhao, M., Ma, Z., Guo, Z., Xing, Y., & Yang, X. (2017). FGFR inhibitor, AZD4547, impedes the stemness of mammary epithelial cells in the premalignant tissues of MMTV-ErbB2 transgenic mice. *Scientific reports*, *7*(1), 11306. https://doi.org/10.1038/s41598-017-11751-7

129. Bluemn, E. G., Coleman, I. M., Lucas, J. M., Coleman, R. T., Hernandez-Lopez, S., Tharakan, R., … Nelson, P. S. (2017). Androgen Receptor Pathway-Independent Prostate Cancer Is Sustained through FGF Signaling. *Cancer cell*, *32*(4), 474–489.e6. doi:10.1016/j.ccell.2017.09.003

130. Yadav, S. S., Li, J., Stockert, J. A., Herzog, B., O'Connor, J., Garzon-Manco, L., … Yadav, K. K. (2017). Induction of Neuroendocrine Differentiation in Prostate Cancer Cells by Dovitinib (TKI-258) and its Therapeutic Implications. *Translational oncology*, *10*(3), 357–366. doi:10.1016/j.tranon.2017.01.011

131. McDermott, M., Eustace, A. J., Busschots, S., Breen, L., Crown, J., Clynes, M., O'Donovan, N., & Stordal, B. (2014). In vitro Development of Chemotherapy and Targeted Therapy Drug-Resistant Cancer Cell Lines: A Practical Guide with Case Studies. *Frontiers in oncology*, *4*, 40. https://doi.org/10.3389/fonc.2014.00040

132. De Marzo, A. M., Knudsen, B., Chan-Tack, K., & Epstein, J. I. (1999). E-cadherin expression as a marker of tumor aggressiveness in routinely processed radical prostatectomy specimens. *Urology*, *53*(4), 707–713. https://doi.org/10.1016/s0090-4295(98)00577-9

133. Bae, K. M., Su, Z., Frye, C., McClellan, S., Allan, R. W., Andrejewski, J. T., Kelley, V., Jorgensen, M., Steindler, D. A., Vieweg, J., & Siemann, D. W. (2010). Expression of pluripotent stem cell reprogramming factors by prostate tumor initiating cells. *The Journal of urology*, *183*(5), 2045–2053. https://doi.org/10.1016/j.juro.2009.12.092

134. Hepburn, A. C., Curry, E. L., Moad, M., Steele, R. E., Franco, O. E., Wilson, L., Singh, P., Buskin, A., Crawford, S. E., Gaughan, L., Mills, I. G., Hayward, S. W., Robson, C. N., & Heer, R. (2020). Propagation of human prostate tissue from induced pluripotent stem cells. *Stem cells translational medicine*, *9*(7), 734–745. https://doi.org/10.1002/sctm.19-0286

135. Kondo, J., & Inoue, M. (2019). Application of Cancer Organoid Model for Drug Screening and Personalized Therapy. *Cells*, *8*(5), 470. https://doi.org/10.3390/cells8050470

136. Bhatt, R. I., Brown, M. D., Hart, C. A., Gilmore, P., Ramani, V. A., George, N. J., & Clarke, N. W. (2003). Novel method for the isolation and characterisation of the putative prostatic stem cell. *Cytometry. Part A : the journal of the International Society for Analytical Cytology*, 54(2), 89–99. https://doi.org/10.1002/cyto.a.10058

137. Cheung, T. H., & Rando, T. A. (2013). Molecular regulation of stem cell quiescence. *Nature reviews. Molecular cell biology*, *14*(6), 329–340. https://doi.org/10.1038/nrm3591

138. Hu, J., Mirshahidi, S., Simental, A., Lee, S. C., De Andrade Filho, P. A., Peterson, N. R., Duerksen-Hughes, P., & Yuan, X. (2019). Cancer stem cell self-renewal as a therapeutic target in human oral cancer. *Oncogene*, *38*(27), 5440–5456. https://doi.org/10.1038/s41388-019-0800-z

139. Quintana, E., Shackleton, M., Sabel, M. S., Fullen, D. R., Johnson, T. M., & Morrison, S. J. (2008). Efficient tumour formation by single human melanoma cells. *Nature*, *456*(7222), 593–598. https://doi.org/10.1038/nature07567

140. Schatton, T., Murphy, G. F., Frank, N. Y., Yamaura, K., Waaga-Gasser, A. M., Gasser, M., Zhan, Q., Jordan, S., Duncan, L. M., Weishaupt, C., Fuhlbrigge, R. C., Kupper, T. S., Sayegh, M. H., & Frank, M. H. (2008). Identification of cells initiating human melanomas. *Nature*, *451*(7176), 345–349. https://doi.org/10.1038/nature06489

141. Chen, Y., Zhao, J., Luo, Y., Wang, Y., Wei, N., & Jiang, Y. (2012). Isolation and identification of cancer stem-like cells from side population of human prostate cancer cells. *Journal of Huazhong University of Science and Technology. Medical sciences = Hua zhong ke ji da xue xue bao. Yi xue Ying De wen ban = Huazhong keji daxue xuebao. Yixue Yingdewen ban*, 32(5), 697–703. https://doi.org/10.1007/s11596-012-1020-8

142. Wei, Z., Lv, S., Wang, Y., Sun, M., Chi, G., Guo, J., Song, P., Fu, X., Zhang, S., & Li, Y. (2016). Biological characteristics of side population cells in a self-established human ovarian cancer cell line. *Oncology letters*, 12(1), 41–48. https://doi.org/10.3892/ol.2016.4565

143. Chen, X., Li, Q., Liu, X., Liu, C., Liu, R., Rycaj, K., Zhang, D., Liu, B., Jeter, C., Calhoun-Davis, T., Lin, K., Lu, Y., Chao, H. P., Shen, J., & Tang, D. G. (2016). Defining a Population of Stem-like Human Prostate Cancer Cells That Can Generate and Propagate Castration-Resistant Prostate Cancer. *Clinical cancer research : an official journal of the American Association for Cancer Research*, *22*(17), 4505–4516. https://doi.org/10.1158/1078-0432.CCR-15-2956

144. Zhang, K., & Waxman, D. J. (2010). PC3 prostate tumor-initiating cells with molecular profile FAM65Bhigh/MFI2low/LEF1low increase tumor angiogenesis. *Molecular cancer*, *9*, 319. https://doi.org/10.1186/1476-4598-9-319

145. Uchida, N., Buck, D. W., He, D., Reitsma, M. J., Masek, M., Phan, T. V., Tsukamoto, A. S., Gage, F. H., & Weissman, I. L. (2000). Direct isolation of human central nervous system stem cells. *Proceedings of the National Academy of Sciences of the United States of America*, *97*(26), 14720–14725. https://doi.org/10.1073/pnas.97.26.14720

146. Singh, S. K., Hawkins, C., Clarke, I. D., Squire, J. A., Bayani, J., Hide, T., Henkelman, R. M., Cusimano, M. D., & Dirks, P. B. (2004). Identification of human brain tumour initiating cells. *Nature*, *432*(7015), 396–401. https://doi.org/10.1038/nature03128

147. Feng, H. L., Liu, Y. Q., Yang, L. J., Bian, X. C., Yang, Z. L., Gu, B., Zhang, H., Wang, C. J., Su, X. L., & Zhao, X. M. (2010). Expression of CD133 correlates with differentiation of human colon cancer cells. *Cancer biology & therapy*, *9*(3), 216–223. https://doi.org/10.4161/cbt.9.3.10664

148. Immervoll, H., Hoem, D., Sakariassen, P. Ø., Steffensen, O. J., & Molven, A. (2008). Expression of the "stem cell marker" CD133 in pancreas and pancreatic ductal adenocarcinomas. *BMC cancer*, *8*, 48. https://doi.org/10.1186/1471-2407-8-48

149. Lardon, J., Corbeil, D., Huttner, W. B., Ling, Z., & Bouwens, L. (2008). Stem cell marker prominin-1/AC133 is expressed in duct cells of the adult human pancreas. *Pancreas*, *36*(1), e1–e6. https://doi.org/10.1097/mpa.0b013e318149f2dc

150. Schmelzer, E., Zhang, L., Bruce, A., Wauthier, E., Ludlow, J., Yao, H. L., Moss, N., Melhem, A., McClelland, R., Turner, W., Kulik, M., Sherwood, S., Tallheden, T., Cheng, N., Furth, M. E., & Reid, L. M. (2007). Human hepatic stem cells from fetal and postnatal donors. *The Journal of experimental medicine*, *204*(8), 1973–1987. https://doi.org/10.1084/jem.20061603

151. Rountree, C. B., Ding, W., Dang, H., Vankirk, C., & Crooks, G. M. (2011). Isolation of CD133+ liver stem cells for clonal expansion. *Journal of visualized experiments : JoVE*, (56), 3183. https://doi.org/10.3791/3183

152. Shmelkov, S. V., Butler, J. M., Hooper, A. T., Hormigo, A., Kushner, J., Milde, T., St Clair, R., Baljevic, M., White, I., Jin, D. K., Chadburn, A., Murphy, A. J., Valenzuela, D. M., Gale, N. W., Thurston, G., Yancopoulos, G. D., D'Angelica, M., Kemeny, N., Lyden, D., & Rafii, S. (2008). CD133 expression is not restricted to stem

cells, and both CD133+ and CD133- metastatic colon cancer cells initiate tumors. *The Journal of clinical investigation*, *118*(6), 2111–2120. https://doi.org/10.1172/JCI34401

153. Eramo, A., Lotti, F., Sette, G., Pilozzi, E., Biffoni, M., Di Virgilio, A., Conticello, C., Ruco, L., Peschle, C., & De Maria, R. (2008). Identification and expansion of the tumorigenic lung cancer stem cell population. *Cell death and differentiation*, *15*(3), 504–514. https://doi.org/10.1038/sj.cdd.4402283

154. Glumac, P. M., & LeBeau, A. M. (2018). The role of CD133 in cancer: a concise review. *Clinical and translational medicine*, *7*(1), 18. https://doi.org/10.1186/s40169-018-0198-1

155. Gu, G., Yuan, J., Wills, M., & Kasper, S. (2007). Prostate cancer cells with stem cell characteristics reconstitute the original human tumor in vivo. *Cancer research*, *67*(10), 4807–4815. https://doi.org/10.1158/0008-5472.CAN-06-4608

156. Yasunaga, Y., Nakamura, K., Ko, D., Srivastava, S., Moul, J. W., Sesterhenn, I. A., McLeod, D. G., & Rhim, J. S. (2001). A novel human cancer culture model for the study of prostate cancer. *Oncogene*, *20*(55), 8036–8041. https://doi.org/10.1038/sj.onc.1205002

157. Palapattu, G. S., Wu, C., Silvers, C. R., Martin, H. B., Williams, K., Salamone, L., Bushnell, T., Huang, L. S., Yang, Q., & Huang, J. (2009). Selective expression of CD44, a putative prostate cancer stem cell marker, in neuroendocrine tumor cells of human prostate cancer. *The Prostate*, *69*(7), 787–798. https://doi.org/10.1002/pros.20928

158. Bernal, A., & Arranz, L. (2018). Nestin-expressing progenitor cells: function, identity and therapeutic implications. *Cellular and molecular life sciences : CMLS*, *75*(12), 2177–2195. https://doi.org/10.1007/s00018-018-2794-z

159. Pandit, H., Li, Y., Li, X., Zhang, W., Li, S., & Martin, R. (2018). Enrichment of cancer stem cells via β-catenin contributing to the tumorigenesis of hepatocellular carcinoma. *BMC cancer*, *18*(1), 783. https://doi.org/10.1186/s12885-018-4683-0

160. Audard, V., Grimber, G., Elie, C., Radenen, B., Audebourg, A., Letourneur, F., Soubrane, O., Vacher-Lavenu, M. C., Perret, C., Cavard, C., & Terris, B. (2007). Cholestasis is a marker for hepatocellular carcinomas displaying beta-catenin mutations. *The Journal of pathology*, *212*(3), 345–352. https://doi.org/10.1002/path.2169

161. Takigawa, Y., & Brown, A. M. (2008). Wnt signaling in liver cancer. *Current drug targets*, *9*(11), 1013–1024. https://doi.org/10.2174/138945008786786127

162. Jang, G. B., Kim, J. Y., Cho, S. D., Park, K. S., Jung, J. Y., Lee, H. Y., Hong, I. S., & Nam, J. S. (2015). Blockade of Wnt/β-catenin signaling suppresses breast cancer metastasis by inhibiting CSC-like phenotype. *Scientific reports*, *5*, 12465. https://doi.org/10.1038/srep12465

163. Zhou, J., Wulfkuhle, J., Zhang, H., Gu, P., Yang, Y., Deng, J., Margolick, J. B., Liotta, L. A., Petricoin, E., 3rd, & Zhang, Y. (2007). Activation of the PTEN/mTOR/STAT3 pathway in breast cancer stem-like cells is required for viability and maintenance. *Proceedings of the National Academy of Sciences of the United States of America*, *104*(41), 16158–16163. https://doi.org/10.1073/pnas.0702596104

164. Cook, A. M., Li, L., Ho, Y., Lin, A., Li, L., Stein, A., Forman, S., Perrotti, D., Jove, R., & Bhatia, R. (2014). Role of altered growth factor receptor-mediated JAK2 signaling in growth and maintenance of human acute myeloid leukemia stem cells. *Blood*, *123*(18), 2826–2837. https://doi.org/10.1182/blood-2013-05-505735

165. Peacock, C. D., Wang, Q., Gesell, G. S., Corcoran-Schwartz, I. M., Jones, E., Kim, J., Devereux, W. L., Rhodes, J. T., Huff, C. A., Beachy, P. A., Watkins, D. N., & Matsui, W. (2007). Hedgehog signaling maintains a tumor stem cell compartment in multiple myeloma. *Proceedings of the National Academy of Sciences of the United States of America*, *104*(10), 4048–4053. https://doi.org/10.1073/pnas.0611682104

166. Batsaikhan, B. E., Yoshikawa, K., Kurita, N., Iwata, T., Takasu, C., Kashihara, H., & Shimada, M. (2014). Cyclopamine decreased the expression of Sonic Hedgehog and its downstream genes in colon cancer stem cells. *Anticancer research*, *34*(11), 6339–6344.

167. Cochrane, C. R., Szczepny, A., Watkins, D. N., & Cain, J. E. (2015). Hedgehog Signaling in the Maintenance of Cancer Stem Cells. *Cancers*, *7*(3), 1554–1585. https://doi.org/10.3390/cancers7030851

168. Armas-López, L., Zúñiga, J., Arrieta, O., & Ávila-Moreno, F. (2017). The Hedgehog-GLI pathway in embryonic development and cancer: implications for pulmonary oncology therapy. *Oncotarget*, *8*(36), 60684–60703. https://doi.org/10.18632/oncotarget.19527

169. Po, A., Ferretti, E., Miele, E., De Smaele, E., Paganelli, A., Canettieri, G., Coni, S., Di Marcotullio, L., Biffoni, M., Massimi, L., Di Rocco, C., Screpanti, I., & Gulino, A. (2010). Hedgehog controls neural stem cells through p53-independent regulation of Nanog. *The EMBO journal*, *29*(15), 2646–2658. https://doi.org/10.1038/emboj.2010.131

170. Rajasekhar, V. K., Studer, L., Gerald, W., Socci, N. D., & Scher, H. I. (2011). Tumour-initiating stem-like cells in human prostate cancer exhibit increased NF-κB signalling. *Nature communications*, *2*, 162. https://doi.org/10.1038/ncomms1159

171. Chen, C., Cao, F., Bai, L., Liu, Y., Xie, J., Wang, W., Si, Q., Yang, J., Chang, A., Liu, D., Liu, D., Chuang, T. H., Xiang, R., & Luo, Y. (2015). IKKβ Enforces a LIN28B/TCF7L2 Positive Feedback Loop That Promotes Cancer Cell Stemness and Metastasis. *Cancer research*, *75*(8), 1725–1735. https://doi.org/10.1158/0008-5472.CAN-14-2111

172. Liu, M., Sakamaki, T., Casimiro, M. C., Willmarth, N. E., Quong, A. A., Ju, X., Ojeifo, J., Jiao, X., Yeow, W. S., Katiyar, S., Shirley, L. A., Joyce, D., Lisanti, M. P., Albanese, C., & Pestell, R. G. (2010). The canonical NF-kappaB pathway governs mammary tumorigenesis in transgenic mice and tumor stem cell expansion. *Cancer research*, *70*(24), 10464–10473. https://doi.org/10.1158/0008-5472.CAN-10-0732

173. Yamamoto, M., Taguchi, Y., Ito-Kureha, T., Semba, K., Yamaguchi, N., & Inoue, J. (2013). NF-κB non-cell-autonomously regulates cancer stem cell populations in the basal-like breast cancer subtype. *Nature communications*, *4*, 2299. https://doi.org/10.1038/ncomms3299

174. Baldwin A. S. (2012). Regulation of cell death and autophagy by IKK and NF-κB: critical mechanisms in immune function and cancer. *Immunological reviews*, *246*(1), 327–345. https://doi.org/10.1111/j.1600-065X.2012.01095.x

175. Matsui W. H. (2016). Cancer stem cell signaling pathways. *Medicine*, *95*(1 Suppl 1), S8–S19. https://doi.org/10.1097/MD.0000000000004765

176. Dreesen, O., & Brivanlou, A. H. (2007). Signaling pathways in cancer and embryonic stem cells. *Stem cell reviews*, *3*(1), 7–17. https://doi.org/10.1007/s12015-007-0004-8

177. Fiñones, R. R., Yeargin, J., Lee, M., Kaur, A. P., Cheng, C., Sun, P., Wu, C., Nguyen, C., Wang-Rodriguez, J., Meyer, A. N., Baird, S. M., Donoghue, D. J., & Haas, M. (2013). Early human prostate adenocarcinomas harbor androgen-independent cancer cells. *PloS one*, *8*(9), e74438. https://doi.org/10.1371/journal.pone.0074438

178. Bae, W. J., Lee, S. H., Rho, Y. S., Koo, B. S., & Lim, Y. C. (2016). Transforming growth factor β1 enhances stemness of head and neck squamous cell carcinoma cells through activation of Wnt signaling. *Oncology letters*, *12*(6), 5315–5320. https://doi.org/10.3892/ol.2016.5336

179. Wang, W., Wang, L., Mizokami, A., Shi, J., Zou, C., Dai, J., Keller, E. T., Lu, Y., & Zhang, J. (2017). Down-regulation of E-cadherin enhances prostate cancer chemoresistance via Notch signaling. *Chinese journal of cancer*, *36*(1), 35. https://doi.org/10.1186/s40880-017-0203-x

180. Avtanski, D., Garcia, A., Caraballo, B., Thangeswaran, P., Marin, S., Bianco, J., Lavi, A., & Poretsky, L. (2019). *In vitro* effects of resistin on epithelial to mesenchymal transition (EMT) in MCF-7 and MDA-MB-231 breast cancer cells - qRT-PCR and Westen blot analyses data. *Data in brief*, *25*, 104118. https://doi.org/10.1016/j.dib.2019.104118

181. Chen, F., Zhang, G., Yu, L., Feng, Y., Li, X., Zhang, Z., Wang, Y., Sun, D., & Pradhan, S. (2016). High-efficiency generation of induced pluripotent mesenchymal stem cells from human dermal fibroblasts using recombinant proteins. *Stem cell research & therapy*, *7*(1), 99. https://doi.org/10.1186/s13287-016-0358-4